

Aalto University
School of Chemical
Technology

School of Chemical Technology
Degree Programme of Bioproduct Technology

Katja Kortelainen

AN INVESTIGATION INTO THE SURFACE TEMPERATURE CHANGES IN SOLID WOOD DURING SORPTION

**Master's thesis for the degree of Master of Science in Technology
submitted for inspection, Espoo, 19 May, 2015.**

Supervisor

Professor Mark Hughes

Instructors

M.Sc. Katja Vahtikari
M.Sc. Tuula Noponen



Tekijä Katja Kortelainen

Työn nimi Tutkimus puun pinnan lämpötilan mittaamisesta sorption aikana

Laitos Biotuotetekniikka

Professuuri Kuitutuotetekniikka

Professuurikoodi KM3003

Työn valvoja Mark Hughes

Työn ohjaajat/Työn tarkastajat DI Katja Vahtikari ja DI Tuula Noponen

Päivämäärä 19.05.2015

Sivumäärä 90+48

Kieli Englanti

Tiivistelmä

Suurin osa rakennusten energiankulutuksesta koostuu lämmityksestä, ilmanvaihdosta, ilmastoinnista ja jäähdytyksestä. Tätä kulutusta voi vähentää laskeamalla sisäilman lämpötilaa, mutta se vaikuttaa rakennusten lämpöviihtyvyyteen. Kuitenkin, lämpöviihtyvyyttä voidaan ylläpitää hyödyntämällä puisten pintojen lämmön ja kosteuden siirtoa.

Tämän diplomityön tavoitteena oli määrittää sorption aiheuttamaa lämpötilan muutosta massiivipuun pinnalla. Sorptio tarkoittaa vuorovaikutusta ympäröivän kosteuden ja puun välillä. Kun suhteellinen kosteus sisätiloissa kasvaa, niin puu sitoo kosteutta ja kun suhteellinen kosteus laskee, niin puu vapauttaa kosteutta. Sorption yhteydessä myös lämpöä sitoutuu ja vapautuu puussa. Tätä kutsutaan lämpösorptioksi. Kirjallisuusosassa käsiteltiin puun kosteuden- ja lämmönsiirtoa.

Kokeellisessa osassa kuvattiin lämpökameralla puun pinnan lämpötilavaihteluita sorption aikana. Kokeessa tutkittiin koivun, männyn pinta- ja sydänpuun, uuni-kuivan männyn sydänpuun ja betonin eroja. Lisäksi jokaisesta puusta vertailtiin sen kolmea syysuuntaa: poikittaista, pitkittäistä ja tangentiaalista. Suhteellinen kosteus adsorption aikana oli 80,5 % ja lämpötila 23,4 °C ja desorption aikana 33,5 % ja 23,0 °C. Tulokset viittaavat, että lämpötilan muutos puun pinnassa johtuu ainoastaan kosteuden vaihtelusta. Kaikista suurin muutos havaittiin puun poikittaispinnalla, n. 2,6 °C lajista ja kosteuspitoisuudesta riippuen. Pitkittäis- ja tangentiaalipinnalla muutos oli samankaltainen, n. 1,5 °C taas lajista ja kosteuspitoisuudesta riippuen. Näytteiden lähtökosteus vaikutti lämpötilan vaihteluun. Mitä kuivempi näyte oli, sitä suurempi lämpötilan vaihtelu. Männyn pinta- ja sydänpuun välillä ei ollut huomattavaa eroa. Koivulla oli suurempi kosteudesta aiheutuva lämmönmuutos kuin männyllä. Lisäksi, lämpötilan nousu adsorption aikana oli suurempaa, kuin lämpötilan lasku desorption aikana.

Avainsanat Puu, sorptio, kosteuden puskurointi, lämmönsiirto, lämpösorptio, lämpökuvaus, lämpökamera, lämpöviihtyvyys, energiatehokkuus

Author Katja Kortelainen

Title of thesis An investigation into the surface temperature changes of solid wood during sorption

Department Bioproduct Technology

Professorship Fibre Products Technology **Code of professorship** KM3003

Thesis supervisor Mark Hughes

Thesis advisors / Thesis examiners M.Sc. Katja Vahtikari and M.Sc. Tuula Noponen

Date 19.05.2015

Number of pages 90+48

Language English

Abstract

Energy consumption of buildings consists mainly of the heating, ventilation, air-conditioning, and cooling (HVAC) systems, which could be reduced by decreasing the indoor temperature, but this usually decreases also the perceived thermal comfort. However, the thermal comfort could be maintained by utilising the moisture and heat transfer of wooden interior surfaces.

The objective of the thesis was to determine the temperature changes on solid wood surface due to the moisture sorption. The temperature change is due to heat of sorption, which describes the heat released or adsorbed in wood subjected to moisture sorption. The moisture and heat transfer of wood were discussed in the literature review.

Thermography was used as a method to record the temperature changes on wood surface during adsorption and desorption. The differences between birch, pine sapwood, pine heartwood, oven dry pine heartwood, and concrete were investigated. Also, the three grain orientations (transverse, radial, tangential) of wood were compared. The relative humidity (RH) during adsorption was 80.5% and temperature 23.4°C, and during desorption RH was 33.5% and temperature 23.0°C. The results imply that the temperature varied only due to the moisture sorption. The temperature of transverse surface changed the most, approximately 2.6°C depending on species and moisture content (MC). The radial and tangential surfaces had similar temperature changes, approximately 1.5°C. Initial MC affected the temperature changes: the lower the initial MC the greater the change in temperature. Differences between pine sapwood and heartwood were not significant. The temperature variation of birch samples was greater than that of pine samples. Also, the temperature increased more during adsorption than it decreased during desorption.

Keywords Wood, sorption, moisture buffering, heat transfer, heat of sorption, thermography, thermal camera, thermal comfort, energy efficiency

Acknowledgements

This Master's Thesis has been conducted in the Department of Forest Products Technology in Aalto University in the frame of Wood Life project between November 2014 and April 2015.

First thanks go naturally to my supervisor, Mark Hughes, and instructors, Katja Vahtikari and also Tuula Noponen. You have been an irreplaceable support for me during this process and also my studies. I could have not wished better advisors for my thesis. I am truly honored that I have gotten the possibility to work with you and explore the Wood Life project. Especially Katja, my namesake, who instructed also my Bachelor's Thesis, has had an unwavering confidence on me the whole time. Thank you!

I want to thank all my friends and family. I'm super grateful for your individual loving support and encouragement during this project. I literally couldn't have made it without you. My power-women have been an irreplaceable support and you made my student life unforgettable. Also, my family, especially my brilliant brothers and sister-in-law, have been a huge inspiration for me and guided me during my thesis. Thank you!

But the gratitude I feel for my boyfriend cannot be easily described with words. You have always had faith in me and have encouraged me during the toughest times. You are my, well not the first, but my last and my everything. I love you Mika!

Don't dream it, be it.

-Frank-N-Furter

19.5.2015 Espoo, Katja Kortelainen

Table of Contents

Abstracts

Acknowledgements

Abbreviations

1	Introduction.....	1
2	Moisture Transfer in Wood.....	3
2.1	Moisture Properties of Wood.....	3
2.2	Moisture Sorption.....	5
2.3	Moisture Buffering.....	8
3	Heat Transfer in Wood	10
3.1	Heat Transfer by Conduction.....	10
3.2	Heat Transfer by Radiation and Convection.....	11
3.3	Thermal Properties of Wood.....	12
3.3.1	Thermal diffusivity	13
4	Heat of sorption in Wood.....	14
4.1	Definition of Latent Heat Exchange and Heat of Sorption.....	14
4.2	Determining Heat of Sorption using the Clausius-Clapeyron Equation	15
4.3	Previous Research on Heat of Sorption	17
4.3.1	Heat of Sorption in Foodstuff.....	17
4.3.2	Heat of Sorption in Fabrics.....	18
4.3.3	Heat of Sorption in Wood.....	20
4.4	Problems with Numerical Methods and Modelling	23
5	Experimental Techniques	24
5.1	Moisture Sorption and Permeability Testing	24
5.1.1	Water Vapour Permeability	24
5.1.2	Water Sorption.....	25
5.2	Thermal Analysis	26
5.2.1	Temperature Measurement	26
5.2.2	Heat Measurement	26

5.2.3	Measuring Weight Change Subjected to Heat Exchange	27
5.3	Thermal Imaging.....	27
5.3.1	Challenges in Thermal Imaging.....	28
6	Materials and Methods.....	30
6.1	Materials.....	30
6.1.1	Birch (<i>Betula pendula</i>).....	30
6.1.2	Pine (<i>Pinus sylvestris</i>).....	31
6.1.3	Birch and concrete	32
6.2	Instruments	32
6.3	Determining the Emissivity and Transmission	33
6.4	The Experimental Method.....	35
7	Results and Discussion	40
7.1	Analysing the Methodology	43
7.2	Analysing the samples.....	45
7.3	Birch.....	47
7.4	Pine Sapwood.....	53
7.5	Pine Heartwood.....	58
7.6	Dry Pine Heartwood.....	63
7.7	Birch and Concrete.....	67
7.8	Transverse Grain Orientation.....	72
7.9	Radial Grain Orientation	74
7.10	Tangential Grain Orientation.....	76
7.11	Reference and Concrete.....	77
8	Conclusions.....	79

References

Appendices

Abbreviations

a_w	Water activity describes how many mass units of water there is in a substance of one mass unit
DSC	Differential scanning calorimetry
DVS	Dynamic vapour sorption
HVAC	Heating, ventilation, air-conditioning and cooling
PTFE	Polytetrafluoroethylene
Q_{st}	Isosteric Heat of sorption
R	Universal gas constant
TG	Thermogravimetry
VHC	Volumetric heat capacity, $\rho c_p = [\text{kJ}/\text{m}^3\text{K}]$

1 Introduction

The construction of the energy-efficient houses and facilities has been the focus of intensive research recently. Energy-efficiency can be improved indirectly by using wood as a construction and interior material (Kalamees et al., 2009). Wood has been used in building design not only due to its aesthetics, but also due to its impact on the perception of thermal comfort and indoor air quality (Simonson et al., 2002; Yang et al., 2007). In addition, recent studies have demonstrated that the heat and moisture transfer in wood could have a positive impact on the energy efficiency of buildings (Hameury, 2005).

The energy consumption of buildings accounted for 37% of the total energy consumption of the world in 2010 (Swedish Energy Agency, 2010). A significant amount of this energy consumption consists of maintaining a desired indoor climate. Heating and cooling respectively accounted for 48.8% and 24.8% of the total energy usage in residential and commercial buildings in the United States in 2010 (Ham & Golparvar-Fard, 2014). In Finland the amount of energy used for heating was 86.9% of the total energy used in residential buildings in 2013 (Tilastokeskus, 2015). Furthermore, the load of a heating, ventilation, air-conditioning, and cooling (HVAC) system can be directly influenced by the poor thermal behaviour of the building elements, such as heat loss through air leakages, and consequently increase the total building energy consumption by more than 10% (Roth et al., 2005; Golparvar-Fard et al., 2013). The energy consumption caused by HVAC systems could be decreased by decreasing the indoor temperature, but this could reduce the thermal comfort.

Aalto University has established the Aalto Energy Efficiency Programme where one of the projects “Wood Life” concentrates on finding energy-efficient living spaces through the use of wooden interior elements. One of the aims of the project is to decrease the indoor temperature in certain spaces without decreasing the perception of comfort of the residents. This comfort is achieved by utilising the

moisture and thermal properties in wooden interior surfaces (Kwiatkowski et al., 2009; Hameury, 2005).

This thesis was conducted within the frame of the Wood Life project, and also in collaboration with the Wood2New project, a European multidisciplinary collaboration project aiming to improve the competitiveness of wood-based interior products and systems. The objective of the thesis was to investigate the heat of sorption effect of wood, which is the phenomenon responsible of the perceived thermal comfort. Heat of sorption is the heat released or absorbed due to moisture sorption. In the experiment the temperature change, which was caused by heat of sorption, was detected with an infrared camera in a climate chamber, in which humidity conditions could be adjusted.

The structure of the thesis is divided in two parts: the literature review and the experimental part. First, the literature review comprising of chapters 2, 3, 4 and 5 concerns the moisture and heat transfer in wood, heat of sorption, and measurement methods of moisture and heat transfer. This is followed by an experimental investigation into the temperature change on the surface of wood due to the increase and decrease of humidity. The investigation also includes an examination of the effect of species, surface grain orientation and surface treatment.

2 Moisture Transfer in Wood

Wood is a hygroscopic material having the ability to attract and hold water molecules from the surrounding environment. The hygroscopicity results from the mostly hydrophilic composition of wood. The moisture properties of wood are further explained in this chapter.

2.1 Moisture Properties of Wood

Wood fibres consist of cellulose (35-50%), hemicellulose (20-35%), lignin (10-25%) and extractives (2-4%) of which the two first mentioned are hydrophilic polymers and the two latter are more hydrophobic. The composition is different between hardwood and softwood species. The hydroxyl groups of the hydrophilic parts of the fibre are responsible for forming hydrogen bonds with water molecules. This phenomenon permits the interaction between wood and water. (Sjöström, 1993)

Moisture content (MC), relative humidity (RH), and fibre saturation point (FSP) are factors describing wood-water relations. MC indicates the weight of water in wood and is frequently expressed as percentage of the weight of oven dry wood (Eq. 1).

$$MC \% = \frac{M_{init} - M_{od}}{M_{od}} \times 100\% \quad (1)$$

In the equation, MC is the moisture content expressed as a percentage, M_{init} is the initial mass of the sample, and M_{od} is the oven dry mass of the sample. (Wood Handbook, 2000)

The mass, dimensions, and strength of wood depend on its moisture content. According to the Wood Handbook (2000) the moisture content range in wood varies between 30 and 200%, and usually the MC in the sapwood of softwood species is higher than that of the heartwood and varies between wood species.

Furthermore, the equilibrium moisture content (EMC) describes the moisture content at which wood neither gains nor loses any moisture at a certain RH. (Wood Handbook, 2000)

Relative humidity is the ratio of the partial pressure of water vapour in the air to the saturated vapour pressure and is expressed as a percentage (Dinwoodie, 2000). When the RH reaches 100% water will condense, thus reaching the dew point. However, the temperature will define the amount of moisture in the air. As the temperature indoors decreases the RH increases although the absolute moisture remains the same, and vice versa. Regulating the indoor temperature can control relative humidity. (Simonson et al., 2001)

Moisture can exist in wood as free and bound water, and water can appear in three forms: as liquid, liquid-vapour mixture or vapour. The free water is located in the cell lumen as liquid water or water vapour, and the bound water is attached to the hydroxyl groups of the cell wall polymers by hydrogen bonds. Fibre saturation point (FSP) is the state when only the cell walls are saturated with bound water, the cell walls begin to dry and strength properties begin to increase. However, it is documented that these three phenomena cannot occur at the same MC, and liquid water may still be present in cell lumens during drying (Engelund et al., 2013). It was long believed that FSP appeared at a MC of 30% (Dinwoodie, 2000), but according to Engelund et al. (2013) and Hill et al. (2005) FSP is around 38-42% for a range of softwood species. When the moisture content decreases below the fibre saturation point, physical and mechanical changes occur, and the wood begins to shrink (Figure 1). In addition, the FSP decreases while temperature increases. (Skaar, 1988; Dinwoodie, 2000; Siikanen, 2008; Wood Handbook, 2000)

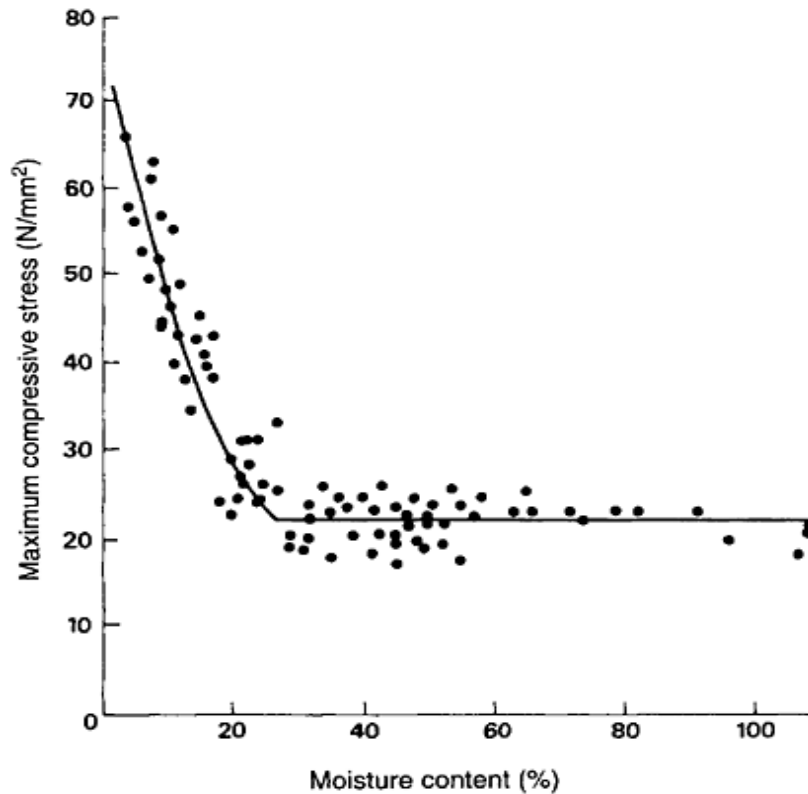


Figure 1 Compressive stress as a function of moisture content. The fibre saturation point can be observed at 27% (Dinwoodie, 2000).

2.2 Moisture Sorption

The sorption behaviour of wood is explained by the hygroscopicity of wood. As the relative humidity of the surroundings increase wood strives for the same moisture content until it reaches equilibrium with the surrounding moisture, thus generating an adsorption isotherm where the EMC is expressed as a function of RH (Figure 2). Commonly, as the RH of the surrounding environment decreases the water molecules are released from the wood, which creates a desorption isotherm. Together the adsorption and desorption isotherms form a hysteresis (Figure 2), where the desorption isotherm is located above the adsorption isotherm. Many studies have indicated that the phenomenon can be explained by the second law of thermodynamics, which states that the process of water sorption is irreversible, because entropy is produced during the process (Koumoutsakos et al., 1999; Mohamed et al., 2005). However, subsequent investigations suggest that thermodynamic principles cannot be applied to explain hysteresis (Hill et al., 2010).

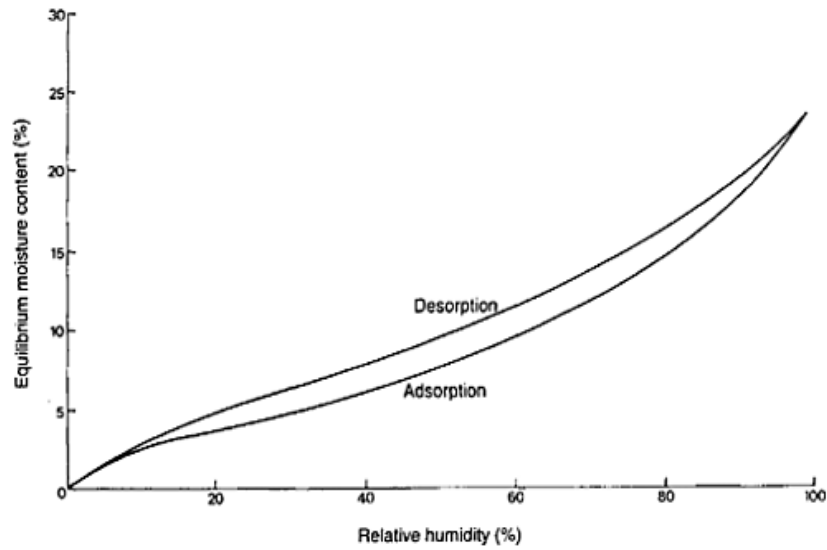


Figure 2 Hysteresis presenting the adsorption and desorption isotherms for six wood species at 40°C temperature (Dinwoodie, 2000).

For comparative purposes, the sorption behaviour of concrete, brick and wood are shown in Figure 3. The sorption of wood reaches its peak at 30% MC or 0.3 kg/kg. The figure shows that MC of brick or concrete does not increase significantly; in other words they do not adsorb moisture extensively (Kwiatkowski, 2009).

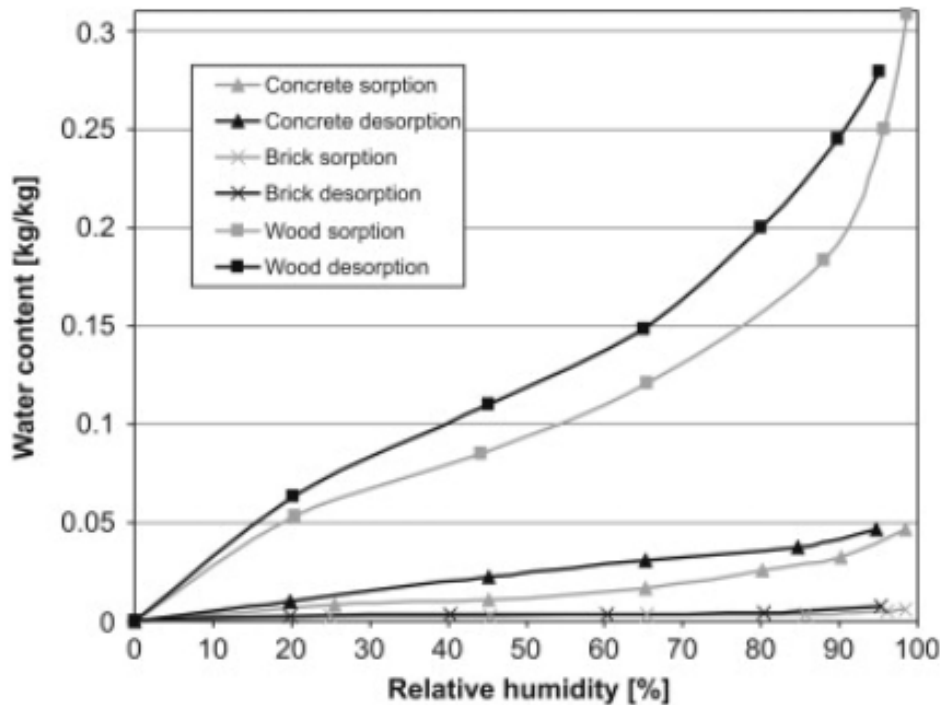


Figure 3 General shapes of the sorption/desorption isotherms for concrete, brick and wood (Kwiatkowski, 2009).

A universal explanation does not exist for the hysteresis, but commonly this is attributed to the chemical behaviour and complex structure of wood. Many of factors affect the hysteresis phenomenon such as temperature, chemical composition of wood, time in storage, and the number of previous sorption cycles. During adsorption wood begins to swell which causes the breakage of hydrogen bonds thus more sorption sites are created. (Frandsen, 2007) Sorption sites are the hydroxyl groups in the cell wall that are not participating in the formation of the cell wall polymers, but are responsible for producing hydrogen bonds with water molecules and cause water sorption due to their great affinity for water molecules (Avramidis, 1987; Dinwoodie, 2000). According to Al Hodali (1997) the explanation for hysteresis lies in the porous structure of wood where the structure can be pictured as a capillary surrounded by pores.

The rate of sorption is faster in the beginning and decelerates as the water adsorption or desorption proceeds. At lower moisture contents, water can be adsorbed only on to the hydroxyl groups in the surface of crystalline sugar, proteins and polysaccharides. (Yazdani et al., 2006) According to Hill et al. (2010) there are three hydroxyl groups per monomeric unit of cellulose or hemicellulose, but only the amorphous part of the cellulose in the microfibrils is accessible, although it is usually assumed that the hemicellulosic components are completely accessible to water molecules.

More chemical and molecular level explanations for moisture sorption have also been described in literature. According to Brunauer et al. (1938) sorption isotherms are believed to indicate the formation of multi-molecular adsorbed layers. They explained the adsorption of non-polar molecules on ionic adsorbents by assuming that the uppermost layer of the adsorbent induces dipoles in the first layer of adsorbed molecules, which in turn induce dipoles in the next layer and so on until several layers are built up.

2.3 Moisture Buffering

Wood strives for equilibrium with its surroundings and simultaneously balances the fluctuations of RH indoors. This effect is known as moisture buffering. As the relative humidity of the environment increases, the moisture content in wood increases as well. This leads to a reduction in RH and a decrease in the MC of the wood, which again results in a rise in indoor RH. When RH remains constant and the temperature increases, wood releases moisture and will dry. (Siikanen, 2008) Using hygroscopic materials, such as wood, can control the indoor relative humidity (Yang et al., 2007; Hameury, 2005). The interaction between the hygroscopic material and moisture balances the moisture variations, thus improving the comfort of the residents and the indoor air quality (Simonson et al., 2002).

The factors affecting moisture buffering and sorption are density, porosity, moisture and heat transfer, diffusion coefficient, and permeability (Rode & Grau, 2008). Also, the geometry and the grain orientation affect the moisture and heat transfer in wood. The proportions of the hydrophilic cellulose and hemicellulose and hydrophobic lignin and extractives have to be taken into consideration in terms of moisture buffering (Kärkkäinen, 2007). The thickness of wood has to be considered in moisture buffering and the storage of moisture. Ojanen & Salonvaara (2004) investigated moisture buffering by numerical methods, and according to the model only 1-2 mm of wood surface is actively buffering moisture. Moreover, the moisture transfer inside the wood is rather slow, and the moisture also equilibrates within the wood.

Kalamees et al. (2009) investigated the effect of ventilation and hygroscopic materials on the stability of indoor temperature and humidity in 170 detached houses in Finland. The duration of the test was one year and the measurements were conducted continuously at one-hour intervals. It was discovered that the ventilation had a greater impact on the indoor climate than the interior material, and the damping effect of the hygroscopic materials was remarkably less in the experimental measurements than in simulations in various studies. Furthermore,

the furniture, textiles, and other furnishings seemed to have a greater impact on indoor humidity than the building fabric. The hygroscopic materials in this case were logs, wooden boarding, and wallpaper on wood chipboard or plasterboard. (Kalamees et al., 2009) However, it has to be taken into consideration that the research did not include buildings with highly hygroscopic or vapour permeable materials since they were not available at that time. The hygroscopic materials in the buildings were mainly coated with impermeable surfacing.

3 Heat Transfer in Wood

Heat can be transferred in three different ways: by conduction, convection and radiation (Figure 4) (Wood Handbook, 2000; Siikanen, 2008; Fagerholm, 1986; Karlsson, 2000). These forms of heat transfer are discussed in more detail in this chapter. The thermodynamic properties of wood are also presented.

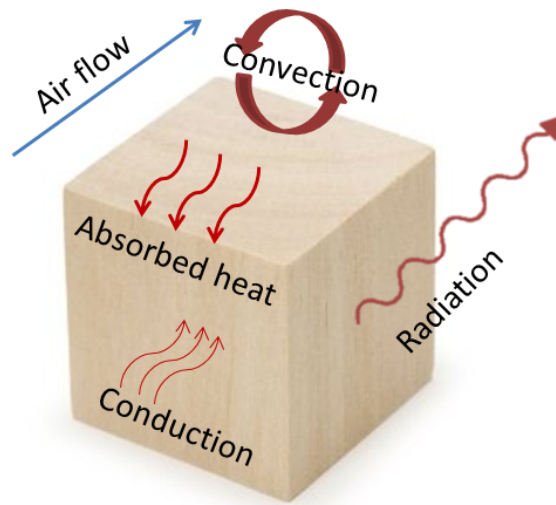


Figure 4 Heat transfer in wood.

3.1 Heat Transfer by Conduction

Thermal conductivity describes a material's ability to conduct heat and is presented as a function of temperature and location. It occurs inside of the system or from one system to another without material transfer, but by collisions between molecules. It also varies in different parts of the system. (Fagerholm, 1986) Conductivity is the dominant form of heat transfer within wood (Absetz, 1999).

Wood has low thermal conductivity due to its porous structure, because the air in the cavities conducts heat poorly. According to Siau (1984) the thermal conductivity of Scots pine is 0.119 W/mK against the grain and 0.297 W/mK along the grain, and of European beech 0.171 W/mK against the grain and 0.428 W/mK along the grain. Kärkkäinen (2007) presents similar results for the values against the grain. Thermal conductivity of pine and spruce is three times that of

mineral wool and approximately 1/10 that of concrete or cellular concrete. However, wood will not create cold bridges nor cause extra risk of moisture condensation in buildings. (Siikanen, 2008)

Thermal conductivity is related to wood density and moisture content. As the density of wood decreases the thermal conductivity approaches the value of air, which is 0.024 W/mK. With a 1% increase in moisture content thermal conductivity increases by 2.7% because water has higher thermal conductivity than wood. High-density species are better thermal conductors than low-density species. This is one reason why low-density wood species are used for instance in saunas. (Siikanen, 2008)

Also, the grain orientation has an impact on the thermal conductivity of wood. Siau (1984) suggested that the thermal conductivity in wood along the grain should be 2.5 times higher than across the grain. The values of thermal conductivity across the grain are of great importance when calculating the conductance values of massive timber walls and wooden thermal bridges in insulated wooden structures (Absetz, 1999).

3.2 Heat Transfer by Radiation and Convection

Radiation is the emission of electromagnetic waves generated by the thermal motion of charged particles in matter. Emissivity is the factor that defines the material surface and determines its ability to radiate energy (López et al., 2013). Materials that emit radiant energy well are also very good at absorbing it. Wood also radiates heat to some extent.

Thermal convection is the transfer of heat from one place to another in liquids and gases by the movement of the fluids (Fagerholm, 1986). If a material creates heat the convection can transfer the heat from the material surface as an effect of airflow.

3.3 Thermal Properties of Wood

This section describes thermal properties of wood. These properties are specific heat capacity, heat capacity and thermal expansion.

Heat capacity describes the amount of heat required to raise the temperature of a certain mass 1°C. The value of heat capacity depends on density, moisture, temperature and the grain orientation. (Wood Handbook, 2000) Structures with high heat capacity have the ability to store heat from the radiation of the sun or created by the appliances that produce heat thus decreasing the rise in temperature indoors (Siikanen, 2008). The volumetric heat capacity (VHC) is more generally used in the modelling of buildings (Kanda et al., 2005), and it describes the ability of a substance of certain volume to store internal energy as the temperature varies without undergoing a phase transition (Fagerholm, 1986). The VHC of softwood, which has a density of 500 kg/m³, is 1150 kJ/m³K, which is comparable with that of brick (1260 kJ/m³K). Also the heat capacity of water is quadruple to that of wood indicating that with increasing moisture content the specific heat of wood increases. (Siikanen, 2008)

Specific heat capacity describes the heat capacity per unit mass of a material. It depends on the temperature and MC of wood, but according to the Wood Handbook (2000) is practically independent of density or species. The specific heat capacity of water is very high, 4.18 kJ/kgK, thus, the greater the moisture content in wood the more heat is required to increase the temperature. In a research collected by Olek (2003) the specific heat of European beech is 1566 J/kgK when the MC is 8% and the specific heat of Scots pine is 1551 J/kgK at a MC of 7.36%. The additional specific heat capacity is due to the thermal energy absorbed by the wood-water bonds. Also as the temperature increases the apparent specific heat also increases due to the energy of absorption of wood, which increases with temperature. (Wood Handbook, 2000)

Wood expands with rising temperature, which can accelerate sorption. This effect is known as thermal expansion. As the wood cell wall swells either due to

moisture adsorption or to thermal expansion, the sorption sites become more accessible due to the increase in volume. The expansion also occurs in the lignin-hemicellulose matrix in which the microfibrils are embedded. (Hill et al., 2010)

3.3.1 Thermal diffusivity

Thermal diffusivity is the thermal conductivity divided by density and specific heat capacity at constant pressure (Eq. 2). This measures the ability of a material to conduct thermal energy relative to its ability to store thermal energy.

$$\alpha = \frac{k}{\rho c_p} \quad (2)$$

where k is thermal conductivity (W/mK), ρ is density (kg/m³) and c_p is the specific heat capacity (J/kgK). Density and specific heat capacity combined, ρc_p , indicates volumetric heat capacity (J/m³K).

The thermal diffusivity of wood decreases as the moisture content increases. This is due to the fact that water's diffusivity is lower than that of air. Also temperature and density affect thermal diffusivity. (Wood Handbook, 2000)

Due to its low thermal diffusivity wood does not feel extremely hot or cold to the touch as other materials with larger thermal diffusivity. Also, heat does not penetrate deeply in to the wood due to low thermal diffusivity of wood. (Wood Handbook, 2000)

4 Heat of sorption in Wood

Crank (1975) stated that when we discuss the transfer of moisture we must not forget to also mention the transfer of heat and vice versa. These are coupled together and one process cannot be considered without simultaneously taking the other into consideration. Thus when speaking of moisture buffering or sorption properties of wood we also need to consider the heat of sorption and latent heat exchange.

4.1 Definition of Latent Heat Exchange and Heat of Sorption

Latent heat is the energy released or absorbed by a material during a process at constant temperature, e.g. the melting of ice or boiling of water. When wood is dried, water in the wood changes its state from liquid into vapour. There is no temperature change during the phase change in an open system, thus there is no change in the kinetic energy of the particles in the material. The energy released comes from the potential energy stored in the bonds between the particles. (Hellier, 2001).

The heat of sorption is the energy required to vaporise the moisture from a biological material, which is higher than the energy required for vaporising moisture from the free water surface. (Ghodake et al., 2007) When a hygroscopic material adsorbs water vapour a large amount of heat is evolved. In contrast to latent heat, the heat of sorption can be observed by a temperature change in an open system (Hellier, 2001; Crank, 1975). As a body adsorbs moisture, heat is released and during desorption heat is absorbed (Figure 5).

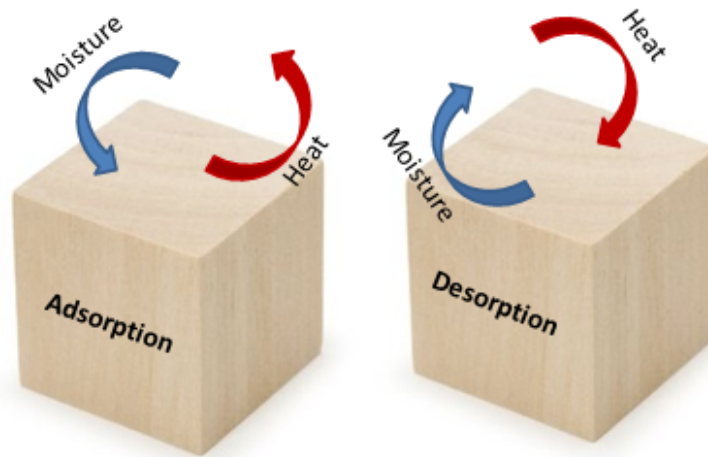


Figure 5 Simplified figure of heat and moisture transfer during adsorption and desorption.

The amount of heat of sorption increases rapidly at low moisture content because of the creation of a monomolecular layer. The layer is formed by water molecules, which are attached to the sorption sites. Also, at high moisture content, which is 8 % for pistachio powder, the values of heat of sorption are negative due to the endothermic reaction of sugar in sorbed water (Yazdani et al., 2006). To achieve reliable heat of sorption results the sorption experiments should be conducted at several temperatures (Chirife & Iglesias, 1992).

4.2 Determining Heat of Sorption using the Clausius-Clapeyron Equation

Numerical methods are a convenient and fast method to predict different behaviour of materials. For instance, models have been created for the sorption and thermal properties of wood, but the problem is the unpredictability and irregularity of wood. Models describing the heat and moisture transfer in materials are mostly based on the heat of sorption isosteres determined by means of the Clausius-Clapeyron technique, where the values are attained from the moisture sorption isotherms.

The heat of sorption can be defined through deviation of the sorption isotherm according to the Clausius-Clapeyron law. Stamm and Loughborough (1934)

presented the use of the Clausius-Clapeyron equation to establish thermodynamic parameters for the sorption of wood. They wanted to show that the oscillating isotherm is reversible. However, the characteristic irreversibility demonstrated by the presence of hysteresis stands strongly against the use of the Clausius-Clapeyron equation to determine the heat of sorption (Hill et al., 2010). More reliable technique employs experimental calorimetric measurements (Karlsson, 2000).

The heat of sorption can be expressed as a function of temperature and moisture content that is derived from the water activity model directly as shown in Equations 3 and 4. (Chen, 2006) Water activity describes the ratio of water vapour pressure of water in a material to the vapour pressure of pure water at the same temperature, and when multiplied by 100 it gives the equilibrium relative humidity (ERH) in percent (Water Activity, 2013).

$$q_{st} = -R \frac{\partial \ln a_w}{\partial \left(\frac{1}{T}\right)} \quad (3)$$

and

$$q_{st} = Q_{st} - \Delta H_{vap} \quad (4)$$

where a_w is the water activity, q_{st} the net isosteric heat of sorption (kJ/mol), Q_{st} the isosteric heat of sorption (kJ/mol), ΔH_{vap} the heat of vaporization (kJ/mol water), R the universal gas constant (kJ/mol K) and T is the absolute temperature (K).

The isosteric heat of sorption represents the energies for water molecules binding at a particular hydration level (Sinija & Mishra, 2008). It can be calculated from Equation 3 by plotting the sorption isostere line as $\ln a_w$ against $1/T$ for a specific moisture content of the material and determining the slope which equals $-q_{st}/R$ (Mulet et al. 1999). The heat of vaporisation is the enthalpy change of vaporization when heat is absorbed by the substance. The procedure is repeated for each moisture content in order to determine the dependence of q_{st} on the moisture content. The technique expresses a general error, which results from plotting and leads to graphical differentiation.

4.3 Previous Research on Heat of Sorption

This section discusses the heat of sorption and latent heat exchange in more depth and presents a few studies on the subject. Most of the studies on heat of sorption have been conducted for the food and fabric industries. Only a few studies about wood-based products were discovered.

4.3.1 Heat of Sorption in Foodstuff

Several experiments have shown that the heat of sorption decreases regularly as the moisture content increases approaching the heat of vaporisation of free water at higher moisture content (Sinija et al., 2008; Mohamed et al., 2005; Yazdani et al., 2006; Ghodake et al., 2007). This effect has been verified in many food experiments. Akanbi et al. (2006) experimented with the drying characteristics of tomato slices, Mohamed et al. (2005) concentrated on the heat of sorption of bitter orange leaves, Yazdani et al. (2006) measured the isosteric heat of pistachio, Garcíá-Perez et al. (2008) experimented with lemon peel, and Ghodake et al. (2007) and Sinija et al. (2008) tested the heat of sorption of different kinds of teas.

The experiments have included the measurement of moisture sorption isotherms in three to four different temperatures ranging from 15 to 40°C. The water activity ranged from 0.05 to 0.984. The heat of sorption was measured by modelling and the most applied methods were Guggenheim-Anderson-De Boer (GAB), Halsey, Brunauer-Emmett-Teller (BET), and Peleg models. The Clausius-Clapeyron equation was applied and they used different techniques, mainly gravimetric method, to form isotherms for heat of sorption. The unit expressing the heat of sorption was kJ/mol, which is the unit for differential heat of sorption. The results were subject to the moisture content of the material. For instance, Sinija et al. (2008) found that the heat of sorption for green tea powder was 48.54-44.71 kJ/mol within moisture levels 1-9 g/g dry matter and for granules 47.96-44.10 kJ/mol when the moisture levels were 0.2-1.4 g/g dry matter.

Mulet et al. (1999) conducted an experiment with cauliflower and compared the results with the earlier results attained from potato starch. They used both

numerical and experimental method for determining the heat of sorption for cauliflower. For determining the water sorption isotherms Mulet et al. (1999) used the Novasina TH-2 (Axain Ltd. Systems for Air Treatment, Pfäffikon, Switzerland) conductivity hygrometer and calculated the isosteric heat with the Clausius-Clapeyron equation and plotted the isosteres $\ln a_w$ versus $1/T$. The heat of sorption was also determined with differential scanning calorimetry (DSC) and thermogravimetry (TG). The samples were stabilized at different moisture contents. The heat transfer was detected as the temperature changed in DSC and the weight loss due to the increase in heat was measured with TG. Together these methods were used to compute the enthalpy of vaporization of water at different moisture contents. The objective was to obtain the moisture content as a function of heat of sorption. The modelled results showed a good correlation with the experimental results.

4.3.2 Heat of Sorption in Fabrics

Fabrics are interesting materials in terms of heat of sorption. To measure how the change in moisture content affects the temperature of fabrics is relevant information in the every-day life for consumers. Gibson and Charmchi (1997) have researched the temperature transients due to water vapour sorption in fabrics and discovered that temperature changes created by heat of sorption associated with water sorption can be up to 10-20°C. They experimented with seven different materials to evaluate the transport properties. The materials consisted of natural fibres like wool, silk, cotton, and a mixture of natural and synthetic fibres wool-polyester mixture, nylon-cotton mixture, and the purely synthetic fibres nylon and polyester. The results of the experiment were compared with the results gained from numerical methods and they indicated good correlation. The results showed that wool has the highest rise in temperature (12.1°C) within the moisture load from 0 to 100% RH and polyester has the lowest, only 1.9°C. Cotton and silk had nearly the same rise, 9.8°C for cotton and 9.7°C for silk. The wool-polyester mixture had significant rise of 8.7°C and nylon and nylon-cotton mixture had a rise of 7.9°C. The results are shown in Figure 6. These results demonstrate that

natural fibres insulates better with increasing moisture content than the synthetic ones.

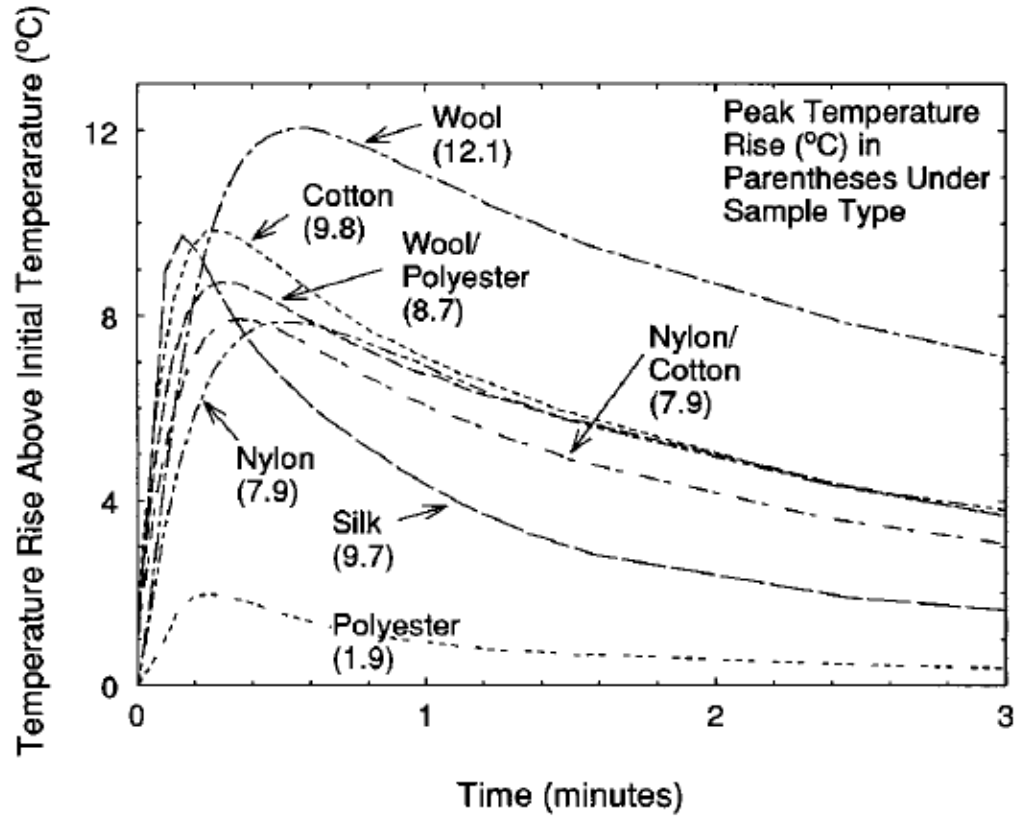


Figure 6 Temperature changes due to water vapour sorption for seven fabrics during step change in relative humidity from 0.0 to 1.0 (Gibson & Charmchi, 1997).

Crank (1975), who has researched diffusion in textiles, plotted the effect of the thickness of cotton fabric with the rise in temperature as a result of moisture sorption and Figure 7 resembles the results achieved by Gibson and Charmchi (1997).

Crank (1975) states that another problem of practical interest is to investigate the temperature change accompanied with the sorption of vapour in solid materials, where the temperature rise is due to the heat of condensation given up at the surface of the solid and the heat of mixing can be neglected. Heat of condensation denotes the heat that is released by the substance during condensation.

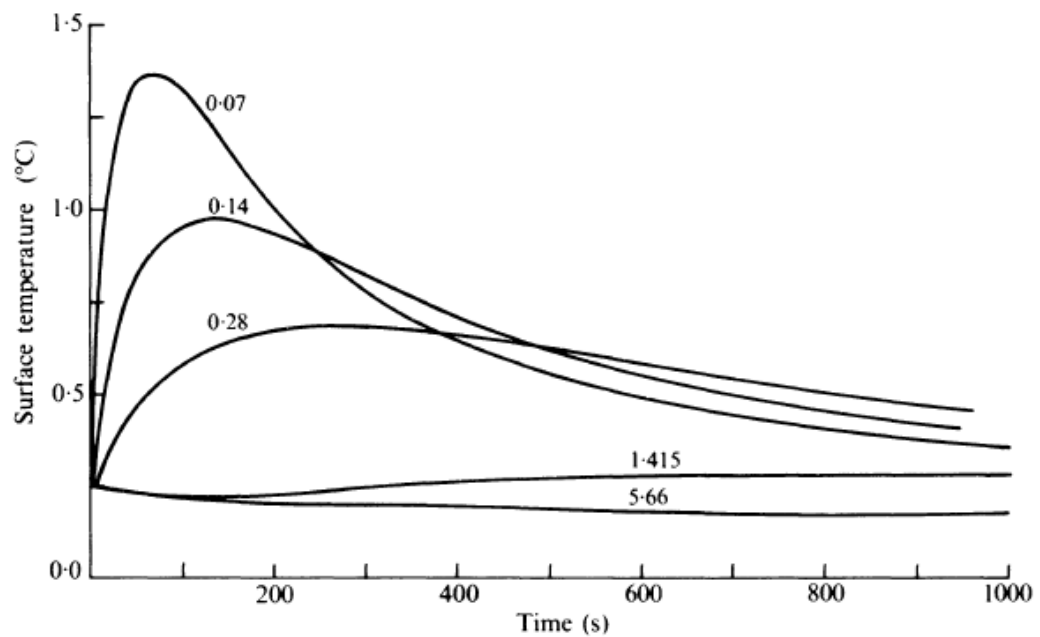


Figure 7 Variation in surface temperature with time presented as an excess over 35°C. Numbers on curves are sheet thicknesses in centimetres. (Crank, 1975)

4.3.3 Heat of Sorption in Wood

A few studies have been conducted about the heat of sorption of wood. One of them was research by Koumoutsakos et al. (1999), who experimented with five softwood species; western hemlock (*Tsuga heterophylla*), WH, Douglas fir (*Pseudotsuga menziesii*), DF, western red cedar (*Thuja plicata*), RC, Sitka spruce (*Picea sitchensis*), SS, and lodgepole pine (*Pinus contorta*), LP. They investigated the enthalpy-entropy compensation in water sorption and found that enthalpy and entropy show a strong negative relationship with the moisture content. As expected, there was no clear trend between the species. The specimens were in two different thicknesses and they used only the tangential direction. The water sorption was measured at three different temperatures 30, 45 and 60°C and the relative humidity ranged from 95% to 25% and back to 95%. The heat of sorption was calculated by using the Hailwood-Horrobin model and the isotherms were formed using non-linear regression. As a result they discovered that all enthalpy values were negative verifying the strong attractive forces between the water molecules and the cell-wall sorption sites. Also both the enthalpy and entropy values decreased as the moisture content of wood increased. This demonstrates that the attraction forces of water molecules by wood decrease along with the

increase in MC. Koumoutsakos et al. (1999) detected differences between wood species in the adsorption and desorption curves.

Researchers in Norway have simulated bathroom conditions in terms of moisture buffering, latent heat exchange and temperature changes in wood. Korsnes (2012) wrote her Master's thesis on moisture and heat transfer of indoor surfaces. She also considered the effect of ventilation. According to Korsnes (2012) a rise in temperature in bathroom conditions was 2.5°C, which was recorded to be solely due to the latent heat of wood. The floor area was 7.3 m² and wall and ceiling area was 35.4 m². Case 1 bathroom had the walls and ceiling covered with untreated wooden panels and tile flooring. Case 2 bathroom surfaces were impermeable materials. The rate of ventilation was only 0.25 1/h and the exposed wooden surfaces retained the RH below 68% during the entire moisture exposure. In the reference case, without wooden surfaces, the RH reached 100% almost immediately after the moisture load, and the RH was still 84% after 2 hours with the 0.25 1/h ventilation rate. These results are shown in Figure 8.

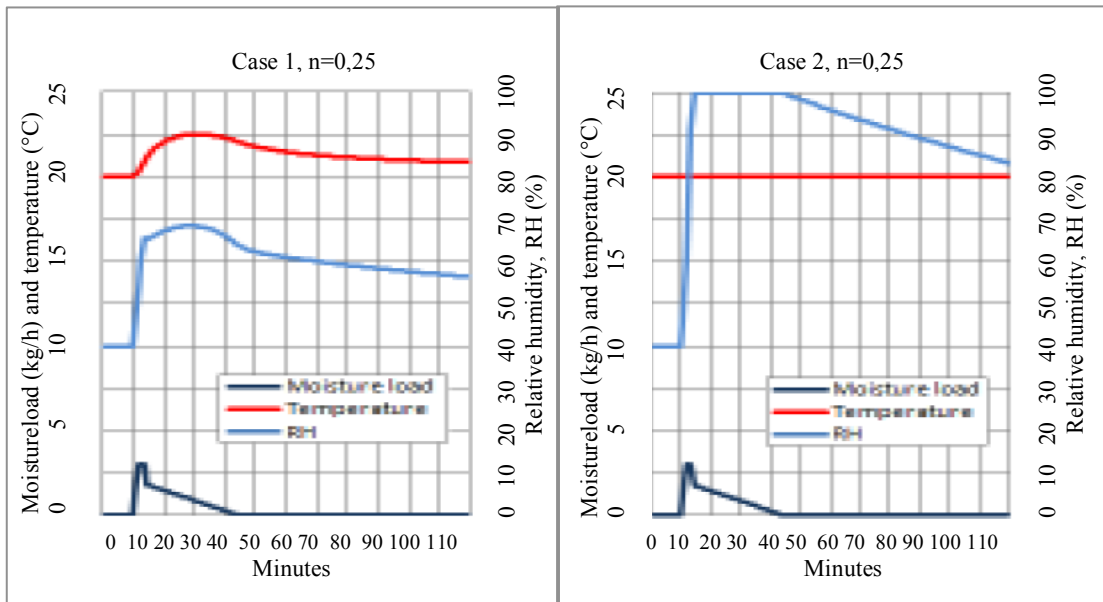


Figure 8 Values of the moisture load, indoor temperature and RH during a two hour period (displayed in minutes) in both the permeable case 1 and the impermeable case 2 with ventilation rate of 0.25 1/h (Korsnes, 2012).

The results obtained by Korsnes (2012) clearly demonstrate that hygroscopic room surfaces, such as wood panelling, may considerably reduce RH variations

due to alternating moisture loads, and that the latent heat exchange affects the room temperature. Stabilizing the RH at a desired level can enable a decrease in the indoor temperature, and in various cases the ventilation rates can be reduced without affecting the comfort or health of the residents. According to Korsnes (2012) neglecting these effects can lead to oversized ventilation, heating and air-conditioning equipment.

Brueckner et al. (2012) conducted further experiments with latent heat exchange of wood. The experiment was a part of WEEE (Wood- Energy, Emission, and Experience) project conducted by the Norwegian Institute of Wood Technology. The project investigated the suitability of wooden buildings in energy efficient constructions providing a healthy environment for the occupants. Brueckner et al. (2012) experimented with untreated spruce (*Picea abies*) and pine (*Pinus sylvestris*) heartwood panels cut tangentially. Two samples were examined simultaneously; one untreated panel and one panel covered with low density polyethylene (LDPE) film which was used as a reference material. The experiment was carried out in a controlled climate through periods of 24 hours with cyclic changes in RH. First, the RH was set to 90%, where the panels were equilibrated for 12 hours. Then the RH was decreased to 20% for a duration of 12 hours. Finally, the RH was increased rapidly back to 90% RH. This cycle was repeated three times. The surface temperatures of spruce and pine panels were measured by thermography with a FLIR E50 infrared camera and three type K (chromel – alumel) thermocouples. The moisture adsorption and desorption were detected using load cells. The results showed a 3°C rise in temperature in both spruce and pine with increasing RH. The temperature rise in the covered reference samples was $1.0 \pm 0.25^\circ\text{C}$. There were also temperature differences between the earlywood and latewood, the tangential and radial areas, and the species. The surface temperature of spruce rose by 2°C and the difference between the latewood and earlywood was 1.1°C after half an hour from the moisture load. The surface temperature of pine rose only 1.5°C, and the difference between the earlywood and latewood was 0.55°C. Also spruce seemed to retain the heat longer than pine.

4.4 Problems with Numerical Methods and Modelling

The problem of using general equations to determine the coupled diffusion of heat and vapour are the simplifying assumptions made. The one-dimensional model neglects factors such as the convective transfer of energy and mass through the porous structures in textiles and also radiative transfer. (Gibson & Charmchi, 1997) Moreover, when using the isotherms formed with Clausius-Clapeyron equation the uncertainties increase significantly at low moisture contents, since the greatest change occurs there (Chirife & Iglesias, 1992).

Hill et al. (2010) demonstrate that although the Clausius-Clapeyron is widely and almost exclusively applied to determining the heat of sorption certain caution should be acknowledged. If sorption is presumed to be irreversible according to the laws of thermodynamics the Clausius-Clapeyron equation should not be applied since the equation proves the oscillating isotherm to be reversible (Stamm & Loughborough, 1934).

Künzel and Kiessl (1996) consider modelling to be a qualified method for simulating the moisture and heat behaviour of buildings. However, they also think that even the best models cannot replace experimental results, because modelling cannot allow for unpredictable conditions, which may occur in field test. The simulated models should be always verified with experimental measurements. Experimental techniques provide a more reliable option to determine heat of sorption than the numerical techniques.

5 Experimental Techniques

Experimental methods provide more reliable data than numerical methods. Experiments, such as thermal analysis and sorption measurement, can be applied to explain the moisture and thermal behaviour of wood. After reliable experimental results have been achieved they can be used for modelling e.g. the moisture and heat transfer and energy consumption of buildings.

5.1 Moisture Sorption and Permeability Testing

This chapter presents different experimental methods for measuring the water vapour sorption and permeability. Some of these methods also include the measurement of temperature transients, but the heat of sorption is generally calculated and modelled with the Clausius-Clapeyron equation.

5.1.1 Water Vapour Permeability

Researcher Phillip Gibson developed Dynamic Moisture Permeation Cell (DMPC) test arrangement for measuring water vapour sorption in fabrics (Gibson, 1995). The DMPC can be used to obtain steady-state diffusion or diffusion/convection properties, or records of temperature transients due to the sorption for materials subjected to step changes in relative humidity. With this method it is also possible to measure the water vapour concentration change on one side as the relative humidity is changed on the other side of the sample. This gives the information about the sorption kinetics of the material. (Gibson and Charmchi, 1997)

McCullough et al. (2003) compared different methods to measure the water vapour permeability, and thermal and water vapour resistance. Water vapour transmission rate of waterproof, windproof and breathable fabrics was measured according to JIS L 1099: Method B2, Testing Methods for Water Vapor Permeability of Clothes. Another standard for measuring the water vapour transmission of materials is called ASTM E 96: Procedure B and Procedure BW,

1999, which is a Standard test method for measuring the water vapour transmission of fabrics. The difference between Procedures B and BW is in the arrangement of the instrumentation. Upright cup method is used in Procedure B, whereas Procedure BW uses the inverted cup method. (McCullough et al., 2003)

Other methods that McCullough et al. (2003) used were based on evaporative resistance: ISO 11092, Textile B Physiological Effects B Measurement of Thermal and Water Vapor Resistance under Steady State Conditions and Part B of ASTM F 1868, Standard Test Method for Thermal and Evaporative Resistance of Clothing Materials Using a Sweating Hot Plate. The test measures the amount of power required to heat the plate to the same temperature as the skin when water vapour is evaporating from the surface of the plate and diffusing through a fabric into the environment. The principle of the method is to have the sample placed on a hot plate and an airflow hood is then placed on the top of the sample.

5.1.2 Water Sorption

Falabella et al. (1989) measured the heat of sorption of maize by means of an electronic hygrometer, which was a Novasina Thermoconstanter Humidat TH2 meter (Novasina AG CH-8050 Zurich). The advantage of this equipment is that it can directly measure the isostere lines. Kitic et al. (1986) describes the operational principle.

Dynamic Vapour Sorption (DVS) analysis is one of the simplest means to study the moisture interaction of water molecules (Agrawal et al., 2004). The samples for DVS measurements are relatively small and used for testing small amounts of material. The apparatus contains two measurement containers for the sample and the reference mounted from the arms of a microbalance, which measures the change in mass as the relative humidity varies. The RH is controlled with nitrogen gas and a mixture of nitrogen gas and water vapour. The system is located in a thermostatically controlled cabinet. The principle is that the RH changes only after the moisture content of the sample is equilibrated. (Hill et al., 2010)

5.2 Thermal Analysis

Thermal properties of materials can be detected by the means of thermal analysis. The relevant methods in terms of measuring the thermal properties of wood are thermometry, calorimetry, heat flow sensors, thermogravimetry and thermal imaging. These methods are described below in more detail.

5.2.1 Temperature Measurement

The most common ways of thermometry are liquid-in-gas thermometers, resistance thermometers and thermocouples. Thermometry basically measures the temperature change in a material. The classic mercury thermometers are good for measuring the temperature from air and liquid, but not sufficient for solids. A better solution for detecting the temperature of solid materials is resistance temperature detectors (RTD), which measure the temperature by correlating the resistance of the RTD material with temperature (Wunderlich, 1990). The thermocouple is more commonly used device. It consists of two dissimilar conductors that connect at one or more spots where a temperature difference is experienced by the different conductors. The difference between the spots and the reference material produces a voltage. (Gray & Finch, 1971)

5.2.2 Heat Measurement

Differential Scanning Calorimetry (DSC) is an optional experimental method for measuring the heat of sorption instead of applying Clausius-Clapeyron equation. DSC is based on the phase changes within the material, which is detected with thermocouples. The amount of material is relatively small when using DSC. The samples also need to be oven-dry when placed into the device. Bound water is difficult to detect by DSC analysis. (Agrawal et al., 2004)

Heat Flow Sensors measures the local heat flux density in one direction. The idea is to detect the heat flow from the temperature changes of the surfaces of material as the bottom part is placed against a cold surface. The sensor method has also

the possibility to calculate heat conductivity when the heat flow and temperature change are known. (Irvine, 1993)

5.2.3 Measuring Weight Change Subjected to Heat Exchange

Thermogravimetry is a method where the weight change of a sample is detected as the thermal conditions are varied. The sample is placed on an arm of a thermobalance and this system is placed in a furnace. The temperature is measured with thermocouples. (Wunderlich, 1990)

5.3 Thermal Imaging

Thermography or infrared thermal imaging can be defined as the process of capturing and measuring variations of infrared radiations emitted by objects under inspection. The principle of operation of the camera is transforming the information into two-dimensional visible imagery in which each radiation energy level is represented by a colour gradient. In the context of buildings, thermal cameras can capture and measure variations in temperature levels on various building surfaces. (Golparvar-Fard et al., 2013; López et al., 2013) The wavelengths of different radiations are shown in Figure 9.

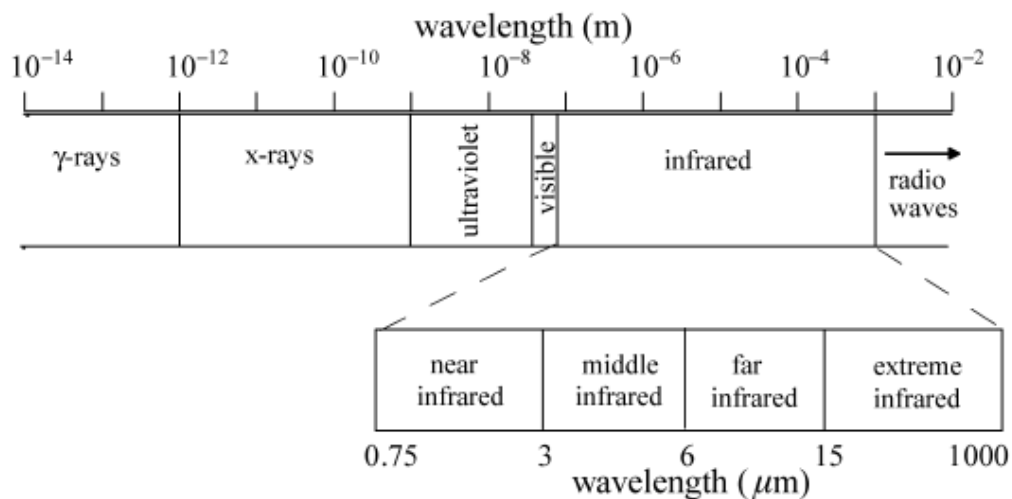


Figure 9 Schematic representation of the infrared spectrum (Meola, 2006).

The simplest way to demonstrate the temperature differences in a certain space or between materials is to use thermal camera. Today, thermography has gained wide acceptance among energy inspectors as a visual method for sensing building energy performance. Thermal camera imaging can help locate heating and cooling losses, which can be attributed to structural problems, moisture leakages and performance problems. (Golparvar-Fard et al., 2013) In addition to the energy inspection of buildings, thermal cameras are used for instance in the paper industry for quality control (Bulota, 2008).

5.3.1 Challenges in Thermal Imaging

Thermal cameras can be applied in various investigations where energy performance problems are indicated, but the method for those purposes is considered to be rather time-consuming and labour-intensive, because of the need to analyse large amounts of additional data. This is considered to be a challenge (Golparvar-Fard et al., 2013; Ham et al. 2014).

One of the most important and difficult factors in thermal imaging is the determination of emissivity (ϵ), which characterises the surface of materials and determines the ability to radiate energy. The emissivity of a substance depends on the wavelength of radiation, the viewing direction, the surface geometry, and the temperature, thus the emissivity changes as the temperature and water content change (López et al., 2013). Therefore, the determination of emissivity is quite complicated. Even though thermal imaging is a dexterous and easy method to determine thermal actions, uncertainty about the emissivity remains. Even different substances might have different emissivity values, which provide false information about the temperature. Also the angle of view can affect the emissivity even if the substance is the same. However, these challenges are recognised among the industry. López et al. (2013) has measured the emissivity values of various wood species. These values are shown in Table 1.

Table 1 Emissivity for different wood species subjected to different temperatures (López et al., 2013).

Sample test piece	-25°C _a	-10°C	5°C	40°C	60°C
<i>Pine</i>	0.966	0.965	0.930	0.855	0.835
<i>Moabi</i>	0.977	0.975	0.940	0.860	0.830
<i>Beech</i>	0.985	0.975	0.965	0.876	0.850
<i>Oak veneer</i>	1.000	0.990	0.980	0.887	0.855
<i>Cherrywood</i>	1.000	0.990	0.970	0.900	0.865
<i>Sapele</i>	1.000	0.990	0.980	0.880	0.860
<i>Oak</i>	1.000	0.990	0.990	0.910	0.880
<i>Ipe</i>	1.000	0.990	0.990	0.920	0.890

^aDue to the camera's capability it isn't possible to obtain emissivity values greater than 1.

Summary of the Literature Review

Wood is a hygroscopic material that interacts with the surrounding relative humidity by sorption. Combining this property with the heat transfer wood offers great possibilities for improving the indoor air quality and thermal comfort indoors.

The moisture and heat transfer of wood have been investigated by experimental and numerical methods. The problem with the numerical methods is that the effects of changing conditions and anisotropy of wood have not been taken into consideration. Experimental methods for determining the moisture and heat transfer of wood exists, but a method to determine the heat of sorption without numerical method is lacking.

Heat of sorption of wood can be detected as a surface temperature change, which can be observed with IR imaging during sorption. This method is used in the experiment of this thesis and is described in chapters 6 and 7.

6 Materials and Methods

6.1 Materials

The objective for the material selection was to compare hardwood and softwood species and due to availability two species were used for the experiments: birch (*Betula pendula*) and pine (*Pinus sylvestris*), of which both the sapwood and heartwood were used. Another objective was to investigate the effect of the initial MC, thus samples with MC 5% and MC 0% were compared. Also concrete was used as a reference material in one experiment. The wood samples were cut such a way that the surface grain orientation was transverse, radial or tangential. The orientations are shown in Figure 10.

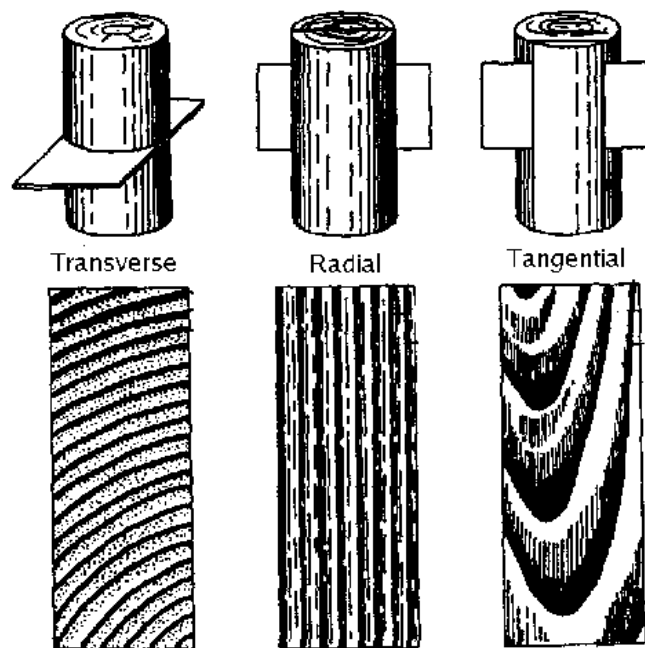


Figure 10 The surface grain orientations of wood (Wood Science, 2014).

6.1.1 Birch (*Betula pendula*)

The birch samples were cut from planks sawn from a green wood log, which was obtained from Otaniemi, Espoo. The planks were conditioned in an environment, where the RH was 50% and temperature 23°C, for two months until equilibrated to constant weight. The mass was monitored at first once a week and as the mass

approached the equilibrium the planks were weighed daily. 20 samples were cut into 20x20x20 mm sized pieces from 200x20x20 mm sticks cut along the grain. They were placed in oven with 103°C for 24 hours. Afterwards, the samples were weighed, and measured with slide calliper. The density of the oven dry birch was 640 kg/m³. After, the samples were placed in a salt chamber with RH of 32% and temperature of 23°C to condition for one week during which the samples reached MC of 4.84%.

6.1.2 Pine (*Pinus sylvestris*)

The green wood, which was obtained from Evo Natura in Southern Finland, was cut in three disks and stored in a freezer before further cutting. The thawed pieces were cut in four segments along the grain and then placed to dry in a room with temperature of 40°C and 12% RH for three days. After that the 20 sapwood and 40 heartwood samples were cut from the segments to 20x20x20 mm pieces. The cubes were cut as clear sapwood or heartwood as possible. The pieces were placed to an oven with temperature of 50°C and weighed two times a day to control when the samples had reached constant weight. After this the samples were weighed and measured. The density of the oven dry sapwood was 511 kg/m³ and the heartwood 497 kg/m³. Next the sapwood samples and 20 of the heartwood samples were placed in a salt chamber with RH of 32% and temperature of 23°C to condition. The rest of the heartwood samples were placed in a desiccator with RH of 1% and 23°C to maintain the constant weight. The sapwood samples were conditioned for 5 days and the heartwood samples for one week. The MC of pine heartwood after conditioning was 4.68% and pine sapwood 4.91%. The different conditioning times were due to the timetable of the experiment.

After conditioning all the samples were taped with aluminium tape from five surfaces so that five samples had the transverse surfaces exposed, five tangential surfaces exposed and, five radial surfaces exposed. Five reference samples were covered with LDPE based plastic kitchen film known as Elmukelmu (Eskimo). It was chosen because water will not permeate the plastic, and moisture would not

condensate on the surface of the film. The samples were weighed again after taping and conditioning.

6.1.3 Birch and concrete

Birch was also used for comparing the temperature change with concrete. Birch samples were the same that were prepared for the first experiment. Only difference was that they were conditioned for three weeks in salt chamber with 32% RH and 23°C during which the samples reached MC of 5.48%, so the difference between the shorter and longer condition periods was minor. Despite the conditioning, the sample preparation followed the same procedure as described earlier.

The concrete samples were prepared from expressed concrete manufactured by Fescon. The mass was prepared by mixing 10 ml of water to 100 g of the concrete powder. The maximum particle size of the concrete was 3 mm. The mass was compressed in an ice cube tray to achieve similar cubes to the wooden samples. The samples were left to dry in room conditions for 4 hours and then placed in the salt chamber with 32% RH and 23°C for 24 hours. The samples were also covered with aluminium tape so that only one surface was left open to achieve similar setting to the wooden samples. The density of the concrete was 1543 kg/m³ and the MC after conditioning 0.87%.

6.2 Instruments

A thermographic camera FLIR E60 (FLIR Systems, 2013) was used to depict the temperature change on the sample surfaces. Main application for this model is scanning thermal differences mostly in building materials and also as a tool for modelling. This camera features a detector consisting of an uncooled microbolometer with focal plane arrays (FPA) of 320x240 pixel resolution, and it operates in spectral range from 7.5 to 13 µm (FLIR Systems, 2013). The recorded thermograms were analysed using the FLIR Tools+ software and the data for

thermographs was exported to Excel. The properties of the camera are shown in Table 2.

Table 2 Properties of FLIR E60 thermal camera (Infradex, 2014).

Resolution	320x240
Temperature range	-20°C to 650°C
Thermal resolution, sensitivity @ 30°C	<0.050°C / 50 mK
Digital zoom	2x, 4x
Image frequency	60 Hz
Optics	25°, 15° (narrow), 45° (wide)
Accuracy	+/- 2 % or 2°C

The experiment was conducted in a RUMED Climatic Test Cabinet. The conditions during adsorption were RH 80% and 23°C, and during desorption RH 33% and 23°C. The air velocity in the climate cabinets was 0.5 m/s. The samples were conditioned in salt chambers. The conditions of the salt chamber with RH 80% were maintained with saturated solution of NaCl, and with RH 32% with saturated solution of MgCl₂.

The mass change was monitored for every one minute during the adsorption with Precisa 205 A SCS scale with accuracy of 0.0001 g. Scale that was used for weighing before sorption was Precisa XT 920M with accuracy of 0.001 g and after sorption it was Mettler AT400 with accuracy of 0.0001 g.

6.3 Determining the Emissivity and Transmission

Thermography is based on capturing and measuring infrared radiation emitted by objects, thus emissivity is a crucial factor while determining the temperatures of the inspected material. Therefore, the emissivity values were determined for each species, grain orientation, references and concrete. The method was to use a reference emitter at the same temperature as the material under investigation.

The sample under investigation was covered with black electric tape, which has emissivity value of 0.95 at 48.8°C (López et al., 2013). The sample was placed on

a hot plate that was heated to 50°C, and it was held on the hot plate for 2 minutes. After the surface had heated, a thermogram was taken. The parameters of the camera were set according to surrounding conditions (RH 30%, temperature 23°C, distance 0.5 m) and the emissivity of the black tape (0.95). The surface temperature of the black tape and the sample were captured, and the emissivity value was adjusted so that the temperature of the sample corresponded that of the black tape. The emissivity value of the sample was achieved as a result.

Shiny surfaces reflect some of the emissivity of the environment, and thus the transmission of the plastic had to be determined. The test involved aluminium foil, a cupboard cup filled with hot water, black electric tape, and the plastic foil used for the samples (Figure 11). The emissivity value of the camera was set to 1.00. First, the reflective temperature was determined with capturing a thermogram of the aluminium foil placed on a hard surface. The temperature detected from the image gives the reflective temperature and must be entered to the camera's settings menu (Figure 11, point 1). Next, the black tape was placed on the surface of the cup and it was filled with boiling hot water (Figure 11, point 2). It was allowed to sit for one minute to stabilise in temperature. Then the thermogram was captured and the temperature of the black tape was recorded (Figure 11, point 3). Then the cup with the tape was covered with the plastic foil and again a thermogram was captured. An external lens is used in the figure (point 4), but in this case the lens was replaced with the plastic foil. The temperature of the black tape showed a lower temperature through the plastic foil due to transmission loss. Like in the emissivity test, again the emissivity of the picture with plastic foil was adjusted to meet the temperature of the plain tape (Figure 11, point 5). This emissivity value represents the transmission value, and it needs to be multiplied with the emissivity value of the target that is measured, e. g. if the emissivity of an object is 0.8 and it is covered with plastic with transmission value of 0.9, the actual emissivity would be 0.72. Also, the camera has an "external optics" correction feature where the transmission value can be entered and the camera fixes the emissivity automatically.

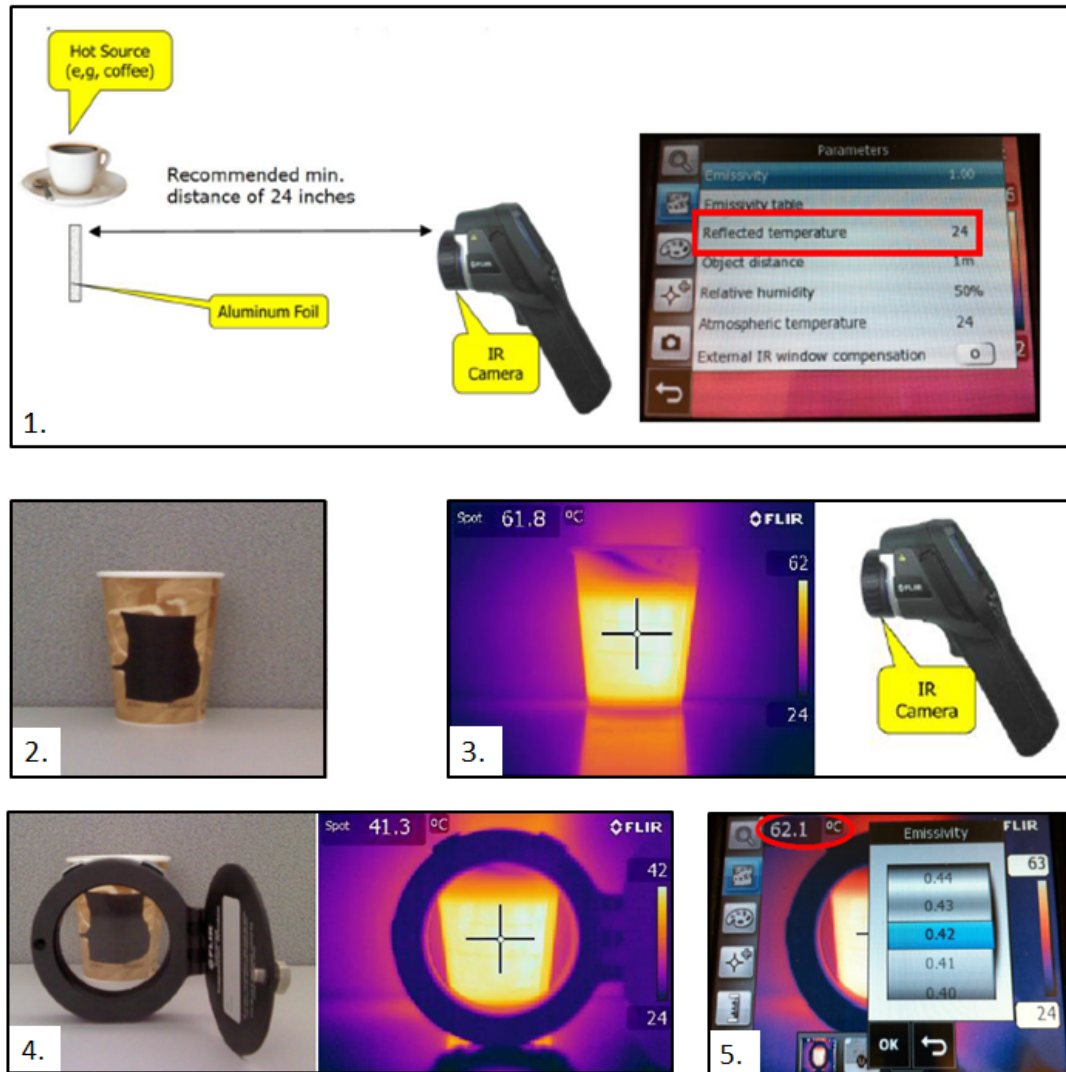


Figure 11 The description of the transmission measurement (Orlove, 2014).

6.4 The Experimental Method

The objective of this experiment was to discover the temperature change on the surface of solid wood subjected to relative humidity variations. Also the differences between birch and concrete were compared.

The procedure was conducted by observing the surface temperature change with FLIR E60 thermal camera on the surface of the samples during adsorption and desorption. The conditions in the adsorption cabinet were 80.5% RH and 23.4°C, and in the desorption cabinet 33.5% RH and 23°C. The conditions were chosen according to the living space where similar humidity fluctuations could be

observed, e.g. bedroom or kitchen. The camera was standing on a tripod facing down and placed inside of the cabinet (Figure 12). It was connected to the computer that streamed the video as sequence files to FLIR Tools + software. The samples were placed on a plastic plate next to the tripod, and a logger, which recorded the RH and temperature every one minute, was placed next to the samples. During the adsorption the plastic plate was lying on a scale. The setting is shown in Figure 12 and the thermogram of the sample setting in Figure 13.

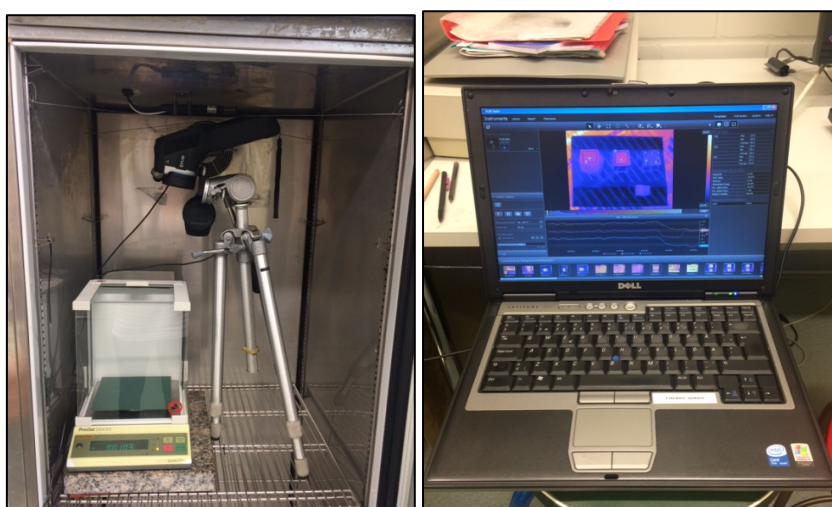


Figure 12 The experimental setting and the computer with FLIR Tools + program.

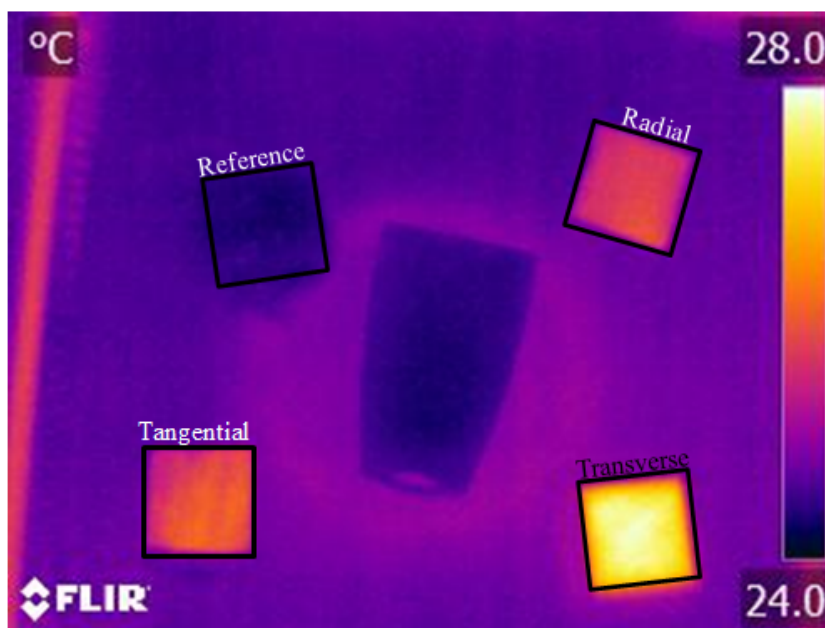


Figure 13 Thermogram of the samples during the adsorption.

Five sample categories were investigated: birch, pine sapwood, pine heartwood, dry pine heartwood and one where birch was compared with concrete. The categories were divided in five groups of four samples. One group consisted of four samples: one transverse, one tangential and one radial surface, and one reference sample, except for the last group the reference was concrete (Figure 14). The oven dry densities and moisture contents before adsorption and desorption are shown in Table 5 under Chapter 7. Five parallel recordings were performed to acknowledge the variations between the samples, which describe the reliability of the results.

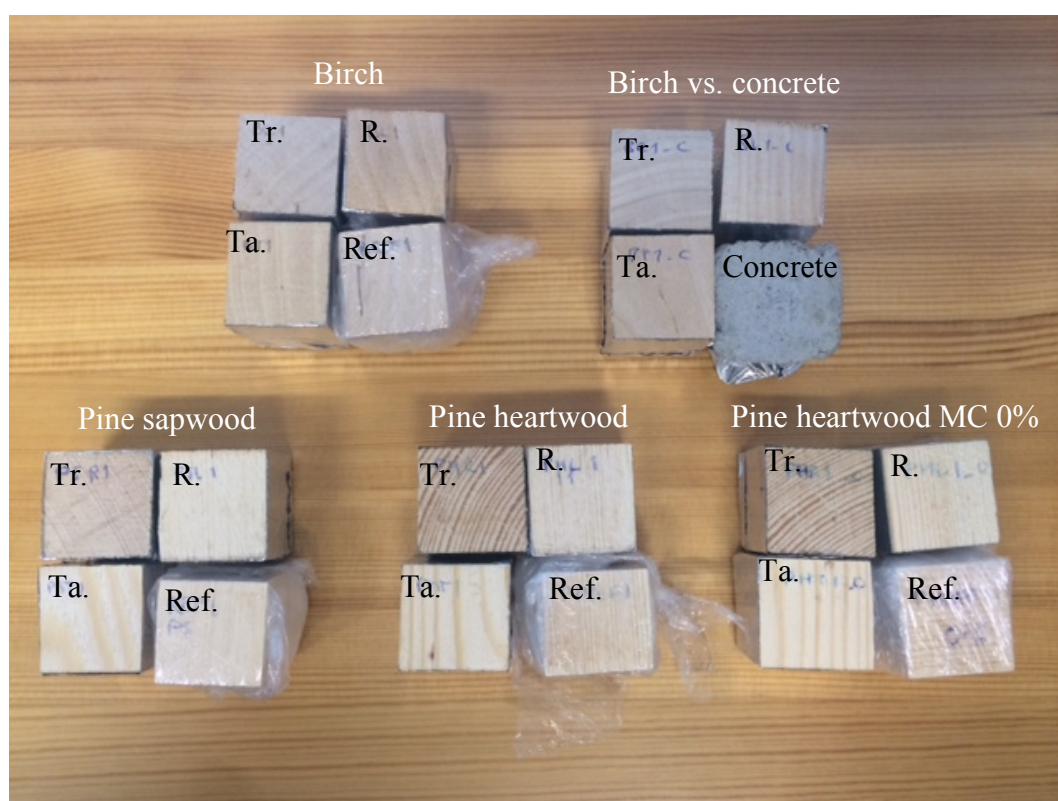


Figure 14 Categories: birch, pine sapwood, pine heartwood, pine heartwood MC 0% and birch vs. concrete. Group (grain orientations): transverse (Tr.), radial (R.), tangential (Ta.) and reference (Ref.)/concrete.

The department of Forest Products Technology is located in two buildings. The samples were conditioned in the salt chamber in building two and the experiment was carried out in building one. Before transporting the samples to the other building they were weighed. The samples were carried in a cool box made of Styrofoam that had been inside of the salt chamber with the samples to attain the

same conditions as the samples. Then the samples were carried in the box to building one to the climate cabinet. Simple flow diagram of the procedure is shown in Figure 15.

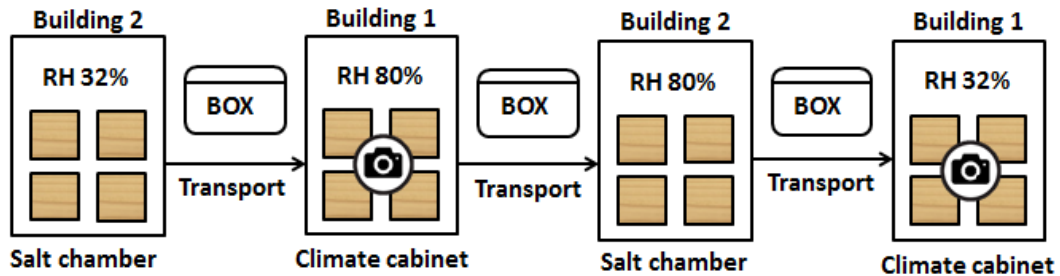


Figure 15 Flow diagram of the process progression. The samples were conditioned in a salt chamber and the temperature changes were recorded in climate cabinets as the moisture conditions changed.

Once in the room with the climate cabinets, the samples were placed on a scale inside the adsorption climate cabinet. All the four samples were on a same scale. The recording was initiated immediately after the samples were set and the cabinet door closed. The duration of the recording was one hour and the frame rate was one frame for every five seconds. The duration was determined by preliminary tests. After the recording the samples were weighed and carried back to the building with salt chambers and placed in a salt chamber where the RH was 80% and temperature 24°C. The samples were left to condition for one week to wait for desorption phase.

Desorption part was conducted similarly as the adsorption part except the samples were placed now inside of the desorption cabinet and they were not on a scale. This procedure was repeated for all the groups according to the schedule in Table 3.

Table 3 *The schedule of the experiment.*

Day 1	<i>Adsorption</i>	Birch (5 repetitions)
Day 2	<i>Adsorption</i>	Pine heartwood MC 0% (5 repetitions)
Day3	<i>Adsorption</i>	Pine sapwood (5 repetitions)
Day 4	<i>Adsorption</i>	Pine heartwood (5 repetitions)
Day 5	<i>Desorption</i>	Birch (5 repetitions)
Day 6	<i>Desorption</i>	Pine heartwood MC 0% (5 repetitions)
Day 7	<i>Desorption</i>	Pine sapwood (5 repetitions)
Day 8	<i>Desorption</i>	Pine heartwood (5 repetitions)
Day 9	<i>Adsorption</i>	Birch & concrete (5 repetitions)
Day 10	<i>Desorption</i>	Birch & concrete (5 repetitions)

7 Results and Discussion

The results of the experimental part are presented in this chapter. First, the initial values for the samples and conditions are shown. Second, the methodology and the sample properties are discussed, next the results are presented by species and discussed, and finally the results are also presented and discussed by anatomical orientation.

The tables present the initial conditions of the samples and the environment where the samples were stored. The initial conditions of the storage environment are shown in Table 4.

Table 4 Initial conditions where the samples were stored before and after the tests.

	RH (%)	T (°C)
<i>Salt chamber RH 32 %</i>	32	23
<i>Salt chamber RH 80 %</i>	80	24
<i>Desiccator</i>	1	23

Table 5 shows the average oven dry densities and initial moisture contents of the samples before adsorption and desorption tests. The moisture contents of the samples before the adsorption do not vary between the directions and reference since they were conditioned uncovered. However, before desorption the samples were already taped and only one surface was open, which led to a difference in MC.

Table 5 Average oven dry densities, and moisture contents before adsorption and desorption of the samples.

	ρ (kg/m ³)	MC _{adsorption} (%)	MC _{desorption} (%)
Birch			
<i>Transverse</i>	620	4.82	13.87
<i>Radial</i>	672	4.97	7.53
<i>Tangential</i>	627	4.81	7.61
<i>Reference</i>	644	4.74	5.99
Concrete	1543	0.87	1.07
Birch (concrete)			
<i>Transverse</i>	643	5.34	8.81
<i>Radial</i>	643	5.48	6.21
<i>Tangential</i>	626	5.62	6.44
Pine sapwood			
<i>Transverse</i>	520	4.89	12.67
<i>Radial</i>	511	5.00	9.33
<i>Tangential</i>	512	5.03	8.93
<i>Reference</i>	502	4.74	5.91
Pine heartwood			
<i>Transverse</i>	525	4.64	11.72
<i>Radial</i>	488	4.76	7.78
<i>Tangential</i>	486	4.77	8.18
<i>Reference</i>	488	4.69	5.81
Pine heartwood, dry			
<i>Transverse</i>	538	0 [*]	11.83
<i>Radial</i>	539	0 [*]	6.15
<i>Tangential</i>	510	0 [*]	6.43
<i>Reference</i>	514	0 [*]	4.01

(*The initial MC is considered to be near to zero.

Tables 6, 7 and 8 include the measured emissivity values for the grain orientations of birch, pine sapwood and heartwood, as well as for references and concrete. The tables show also the temperature at which the values were determined. The transmission of the plastic film was also determined as described in Section 6.3 and the value was found to be 0.9.

Table 6 Emissivity values of birch in three grain orientations, reference and concrete.

Birch	T (°C)	□
<i>Transverse</i>	41.6	0.80
<i>Radial</i>	44.9	0.80
<i>Tangential</i>	38.3	0.815
Reference	44.4	0.865
Concrete	42.5	0.71

Table 7 Emissivity values of pine sapwood in three grain orientations and reference.

Pine sapwood	T (°C)	□
<i>Transverse</i>	44.7	0.85
<i>Radial</i>	39.8	0.83
<i>Tangential</i>	40	0.81
Reference	39.9	0.84

Table 8 Emissivity values of pine heartwood in three grain orientations and reference.

Pine heartwood	T (°C)	□
<i>Transverse</i>	40	0.85
<i>Radial</i>	45.5	0.84
<i>Tangential</i>	43.8	0.815
Reference	39.8	0.83

7.1 Analysing the Methodology

The development of the methodology was one objective of the thesis and the experimental method was used for the first time as it was in our department. The experimental method had unexpected effects on the results and they are discussed in this chapter.

The emissivity was determined with a hot plate and the problem was the low heat conductivity and thermal diffusivity of wood (Kärkkäinen, 2007). The surface of the sample was in contact with the hot plate but depending whether the grain orientation was transverse or radial the heating time varied. Even though the surface was heated, the heat did not transfer throughout the sample. The less the heat was penetrated the faster the surface was cooling due to the heat convection caused by airflow. Also the cooling rate was different for the exposed wooden surface and the part covered with the electric tape. Thus, by the time the thermograph was taken the actual surface temperature appeared uneven between the wood and the tape and affected the determination of emissivity. The difference in cooling of the surfaces might have resulted in inaccurate emissivity values, which can cause erroneous thermographs. However, the temperature difference between the sample and the tape was confirmed with thermowire, and there was no difference. The emissivity values were obtained at approximately 40°C and the determined values were 0.8-0.85, which corresponds with the results obtained by López et al. (2013). Nevertheless, when the emissivity values were determined at lower temperatures, approximately 30°C, the values were around 0.7. According to López et al. (2013) the emissivity should increase as the temperature decreases, thus the results obtained in 30°C appears different. Nevertheless, when defining the emissivity the temperature between the material in question and the environment should be significant, e.g. if the emissivity is measured at room temperature, the material should be heated to 40°C (Infradex, 2014). Thus the temperature change is noticeable and the emissivity value is more reliable.

The samples were transported in a cool box between the building with salt chamber and climate cabinet. Even though the conditions were similar between

the salt chambers and climate cabinets, and the box was stored in the salt chamber, the transportation might have affected the temperature of the samples. During colder days it was clear that the initial surface temperature of the samples was lower than desired. This was discovered in the thermographs of pine heartwood during adsorption as well as pine sapwood and dry heartwood during desorption. Also the conditions in the room with the climate cabinets varied during some days. The default setting in the room was RH 50% and temperatures of 23°C, but on some days the RH dropped near to 30%.

The conditions in the salt chambers, climate cabinets, and desiccator were monitored. Always when the door of the salt chamber was opened, the RH and temperature decreased or increased according to the surrounding room conditions. The RH could vary from 75 to 80% in the chamber with 80% RH and in the other the RH could vary from 28 to 34%. The temperature could have varied between 22.5 and 24°C.

The conditions to which the climate chamber was set varied a bit from the actual conditions. The RH was set to 75%, but the recorded RH was 80%. The temperature was stable most of the time, but moving of the samples caused fluctuation in the RH. As the door of the climate cabinet was opened the RH varied, but the temperature remained steady. However, the possible error caused by the RH change due to opening the door was investigated. The door opening did not appear to have an effect on the desorption thermographs.

Also the dry pine heartwood samples were stored in a desiccator with RH of 1% and it was kept in a room with the climate chambers. The conditions of the room were approximately RH 50% and 23°C, thus always when the lid of the desiccator was opened to take the samples out some amount of moisture might have entered. This has possibly led to an increase of the surface temperatures of the dry pine heartwood samples before recording began, which can be observed as a higher initial temperature of the samples (Figure 39). The ideal situation would have been that the samples had been conditioned in the climate cabinets where the

experiment was conducted. This would eliminate the error that was caused by transporting the samples between the two buildings.

Two scales were used in the experiment: one in the building with the salt chambers and one with the climate cabinets. The samples were weighed with Precisa XT 920M scale after drying in oven and before the sorption experiments, and the scale used for weighing after sorption was Mettler AT400. The samples weighed with Precisa scale weighed 0.002 g more than with the Mettler scale. This difference is included in the results, thus there should not be error in the MC results. However, the results would be more reliable and comparable if only one scale was used or the scales would be calibrated. Even better, if the mass change could be monitored simultaneously during adsorption and desorption.

7.2 Analysing the samples

A simple explanation for the variation between the MC and temperature results of individual samples is difficult to define, since the factors affecting them are many. Surface roughness, density, initial moisture content and the amount of earlywood and latewood are all properties of the samples that had an effect on the results. The explanation for the variety of MC values as well as temperature is more of a combination of multiple properties.

The properties had an impact on the sorption, which again affected the temperature changes. The rougher surface of the sample results in greater surface area, thus increasing the moisture sorption. Also the variation of the densities of the samples led to differences between the moisture distributions. Denser samples had lower moisture sorption than the more porous samples, since the denser samples contain less air, which increases the thermal conductivity. The initial moisture content seemed to have greater impact in desorption. The closer the initial moisture contents between the samples were the closer the produced thermographs were. The magnitude of the effect was greater for the transverse grain orientation. The ratio of earlywood and latewood results in a variety of moisture contents. In softwood the earlywood is more porous than latewood, thus

the samples containing more earlywood have greater moisture sorption. In hardwoods the earlywood and latewood are more homogenous and thus more difficult to distinguish (Kärkkäinen, 2007; Sjöström, 1993). The greater impact on moisture transfer in birch samples could be the amount of pith rays.

One factor affecting the difference between the adsorption and desorption thermographs could be the conditioning of the samples. They were conditioned before the adsorption un-taped, thus all the surfaces were open and the samples were able to reach approximately the same MC. After the adsorption the samples were conditioned taped, with only one surface open, at RH 80% for one week. This led to differentiation of the moisture contents between the surface grain orientations (Table 5) and very likely have had an effect on the difference of adsorption and desorption thermographs.

The pine samples were all dried in oven at 50°C, and even though they were dried for several days, some moisture might have remained. Also the densities of pine heartwood and sapwood appear to be the other way around (Table 5). Usually the heartwood is considered to be denser than sapwood (Kärkkäinen, 2007). The difference in density between heartwood and sapwood is 15 kg/m³, which is considered to be rather low. However, the accumulation of extractives might affect the increasing density of heartwood, thus if the wood is very young or old, or cut from the top, the amount of extractives might be very low and result in lower density. Also, as the samples were cut from pine where the difference of sapwood and heartwood was not clear the certainty of having samples containing only sapwood or heartwood is unclear.

The thermograph figures represent the average results of the thermal imaging experiment. Some of the recordings were erroneous due to distraction in filming process, belated initiation of the recording, and movement of the samples resulting in inconsistent data. The average figures exclude these erroneous results. All the results are presented in the Appendices.

7.3 Birch

Figure 16 shows the average values of the change in moisture content and the error bar describes the minimum and maximum values of the samples. The transverse grain orientation of the birch had the greatest change in moisture content during adsorption and desorption. The radial and tangential grain orientations behaved quite similarly and the reference did not gain nor lose moisture during sorption as expected.

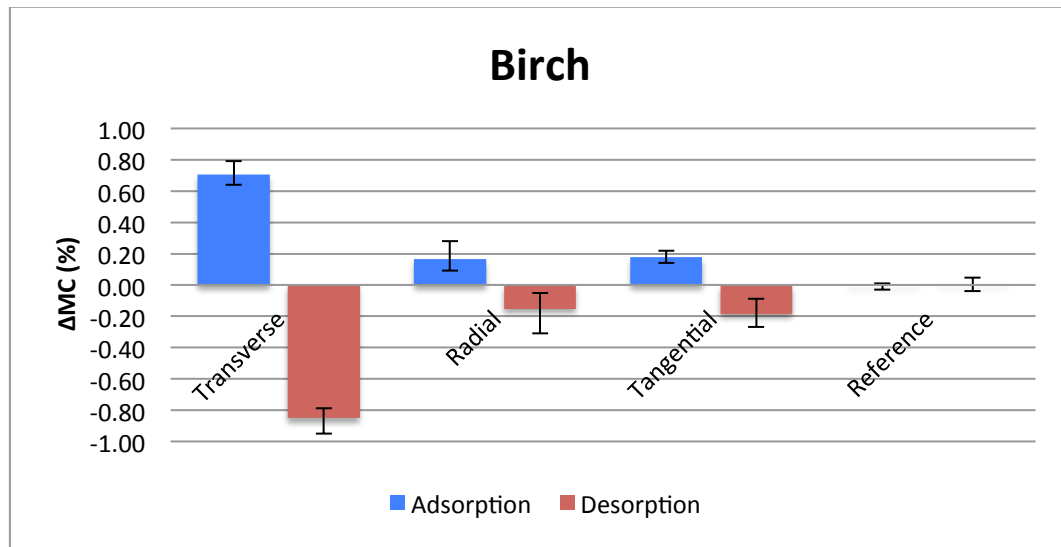


Figure 16 Changes of moisture content during adsorption and desorption in birch in three grain orientations and in reference during 1 hour.

The transverse surface clearly adsorbs and desorbs more moisture than the tangential and radial surfaces. Roughly speaking, the fibre cells can be pictured as a capillary (Al Hodali, 1997). The moisture is transported along the capillary deeper inside of the wood, but on tangential or radial surface, the capillary is though cut in half, thus the moisture cannot penetrate that deeply. The moisture transfer is naturally more complicated than that, since the moisture movement appears also between the fibres along the pith rays and pores in the cell wall and by diffusion, although slowly (Kärkkäinen, 2007).

The amount of desorbed moisture was a bit greater than the adsorbed moisture. This might be due to the sorption kinetics, and here it seems that the rate of

desorption is more rapid than that of adsorption. Generally the adsorption occurs faster than desorption, but desorption reaches the maximum MC faster than adsorption (Hill, 2010). The faster rate of desorption than adsorption can be applied in liquid water sorption, but in terms of water vapour the situation is more complicated. In this case it could be due to the greater amount of energy required for creating the hydrogen bonds during adsorption than breaking the bonds during desorption (Wood Handbook, 2000). Also the starting MC was higher in the desorption cycle than the end of the adsorption cycle.

The temperature changes correlate with the moisture content changes to some extent as it can be observed from Figure 17. The temperature is expected to rise on the surface during adsorption due to positive sorption enthalpy (Engelund et al., 2013) and the heat of sorption. The transverse surface had the greatest increase in temperature during adsorption. Since it adsorbed more moisture it also released the more heat. The surface temperature of the reference sample also rose, which was unexpected. This occurred also in the subsequent experiments. This could be accounted for the condensed moisture on the surface of plastic. The sample was wrapped with the plastic foil in multiple layers and moisture could have accumulated in the gaps between the layers, which appeared as an increase in temperature. The change in temperature might be also due the heat radiation of the plastic. Until further notice the cause for the temperature change remains uncertain.

The temperature change during desorption was significantly smaller than that of adsorption, which does not correlate with the change in moisture content. However, this could be expected since the samples had not most likely reached EMC and rather than desorbing from that moisture content, the MC was increased to a higher level and desorption begun from there. The same result can be observed in the following results. Still the transverse grain orientation showed the greatest reaction.

The effect of desorption on the decrease in temperature is more complicated and could be accounted for the sorption kinetics, and the internal heat and moisture transfer in wood. As explained earlier, the samples probably have not reached EMC during the conditioning before desorption. Thus as the surface dries first as a result of low RH the moisture begins to be released from within the sample. Consequently, adsorption and desorption occurs simultaneously within the sample, which could lead to simultaneous heat adsorption and desorption.

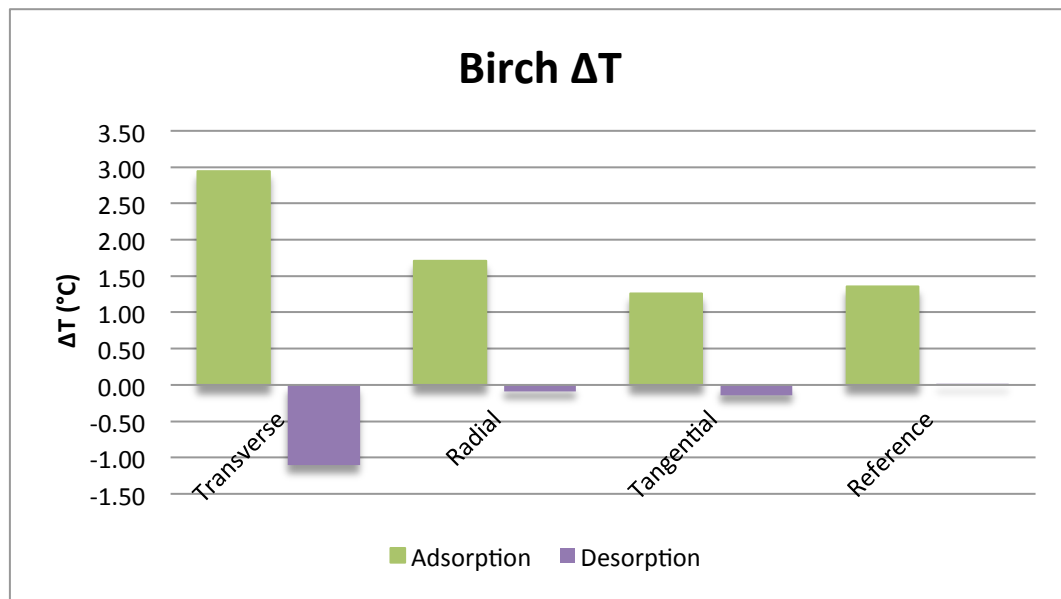


Figure 17 Differences between the initial and maximum temperature changes of grain orientations of birch and reference during adsorption and desorption during 1 hour.

Figure 18 shows the thermographs of the birch samples during adsorption from RH 32% to RH 80% at 23°C. The rate of the temperature rise is very rapid and linear in the beginning, and it occurs in few minutes from the beginning of the adsorption and then it begins to stabilise to the surrounding temperature. The linear rise in the beginning could be due to the occupation of the sorption sites on the surface (Hill, 2010). First, the free hydroxyl groups in the fibre cell walls are occupied and the bonding releases heat, thus increasing the temperature rapidly. After the sorption sites on the surface are occupied the water molecules bond with the hydroxyl groups of the deeper layers. The temperature rise of the transverse surface is significantly greater than that of radial and tangential surface. The radial

and tangential surfaces behave almost identically due to the homogenous structure of birch (Kärkkäinen, 2007).

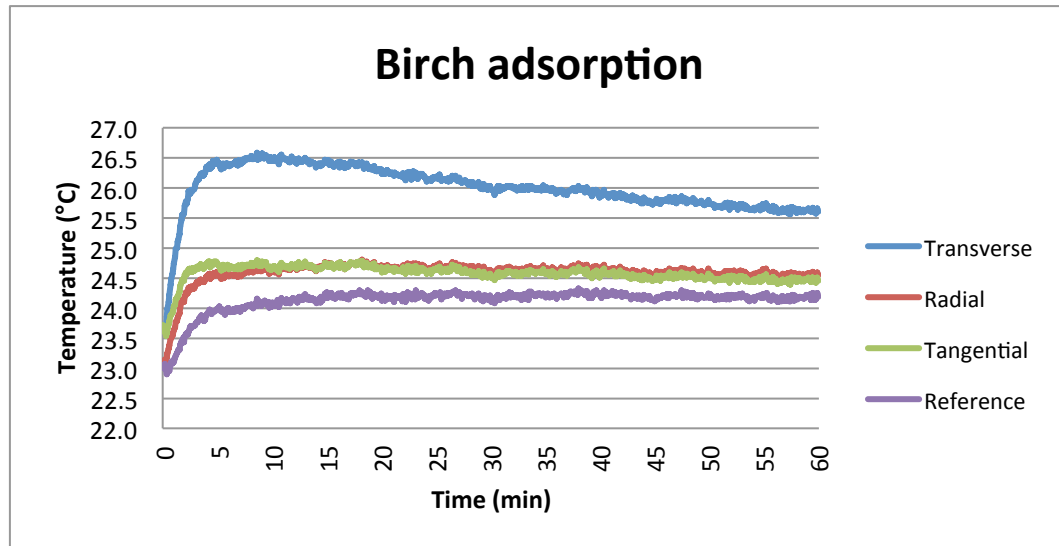


Figure 18 Temperature changes of birch samples and reference when the samples are placed in climate cabinet with RH 80%.

Figure 19 shows the MC change of all the samples combined irrespective of the orientation during the adsorption. All the four samples (transverse, radial, tangential, reference) were on the same scale, since it would have been impossible to have individual scales for the samples and fit them into climate cabinet and record the thermographs. It seems that the MC increases quite linearly compared to the thermograph. However, the thermal camera captures only the surface reaction and the water molecules are attached first on the surface, thus resulting in rapid rise in surface temperature, even though the increase in moisture content continues. Also, the MC change appears linear, although adsorption is an exponential process. However, the time to achieve EMC takes longer than one hour, thus the MC change might appear on the linear part of the curve (Hill, 2010).

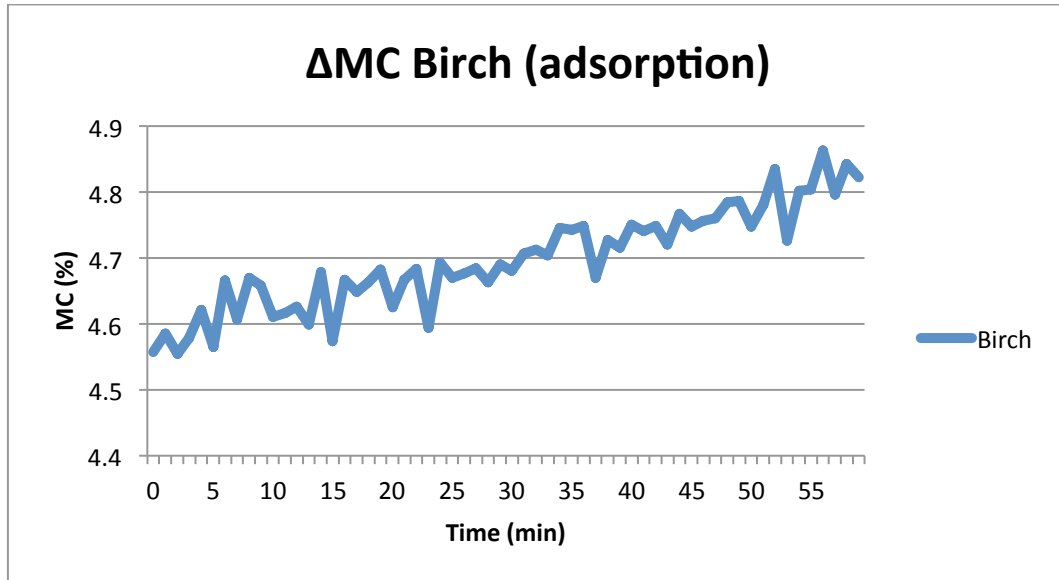


Figure 19 The average change in MC of all the birch samples (transverse, radial, tangential and reference) summed during adsorption.

The conditions during adsorption remained steady (Figure 20). The problem with this experiment was that the RH and temperature were logged only every half hour, thus the information is incomplete.

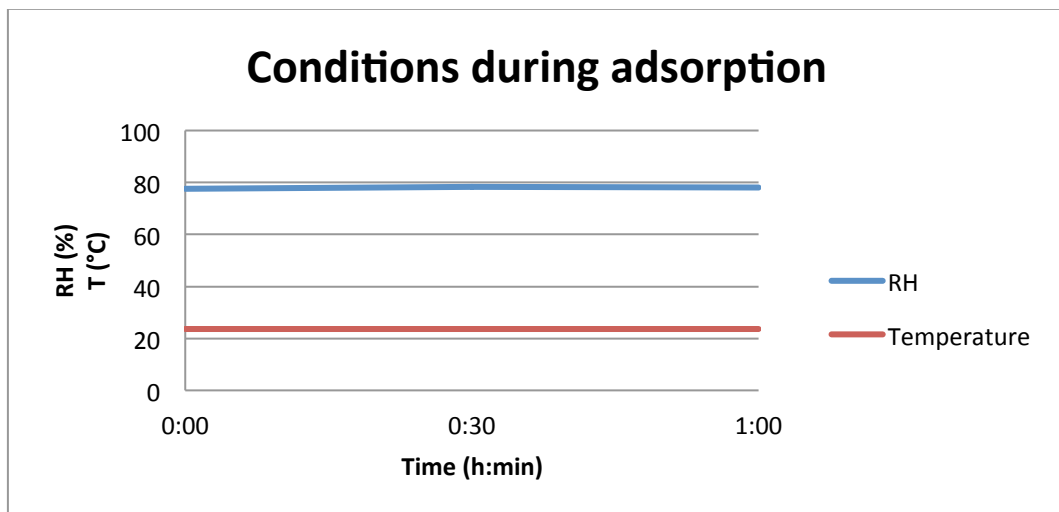


Figure 20 Conditions in climate cabinet during adsorption of the birch samples.

Desorption of birch samples (Figure 21) differed from the other desorption experiments. The conditions during desorption are shown in Figure 22. The difference between the experiment with birch samples and the other experiments was that the birch samples were not moved between the two buildings, but within the same room. Thus, here is no clear drop and then rise in temperatures as the

other graphs have. However, in the fifth parallel test the thermograph was similar to the subsequent desorption thermographs (Appendix 7, Figures 19 and 20). First, it appeared as the transporting between the two buildings would have caused the drop in temperature, but since one of the experiments with birch samples had also the same behaviour, it is unlikely to be the reason. However, this could have been one day when the conditions in the room with the climate cabinets differed from the default conditions. The RH could have been lower than usual, around 30% instead of 50%, which would have not caused a rise in RH in the cabinet as the door was opened as during the other recordings. But as the last parallel test was recorded the RH could have risen back to 50%, thus causing the usual rise in RH within the cabinet while opening the door. This might have affected the desorption results of the last parallel desorption experiment as well as the subsequent desorption experiments.

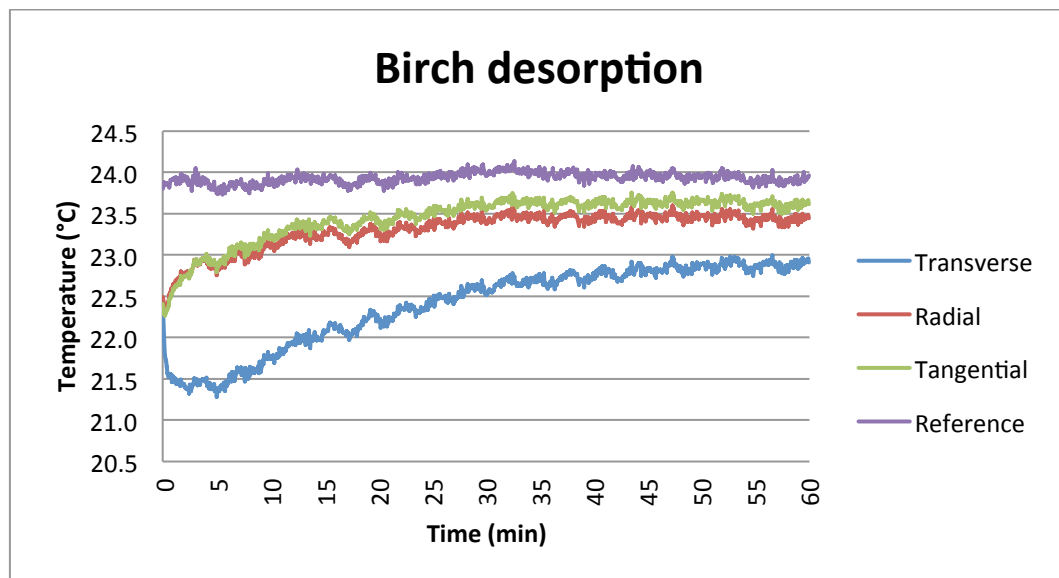


Figure 21 Temperature changes of birch samples and reference when the samples are placed in climate cabinet with RH 33%.

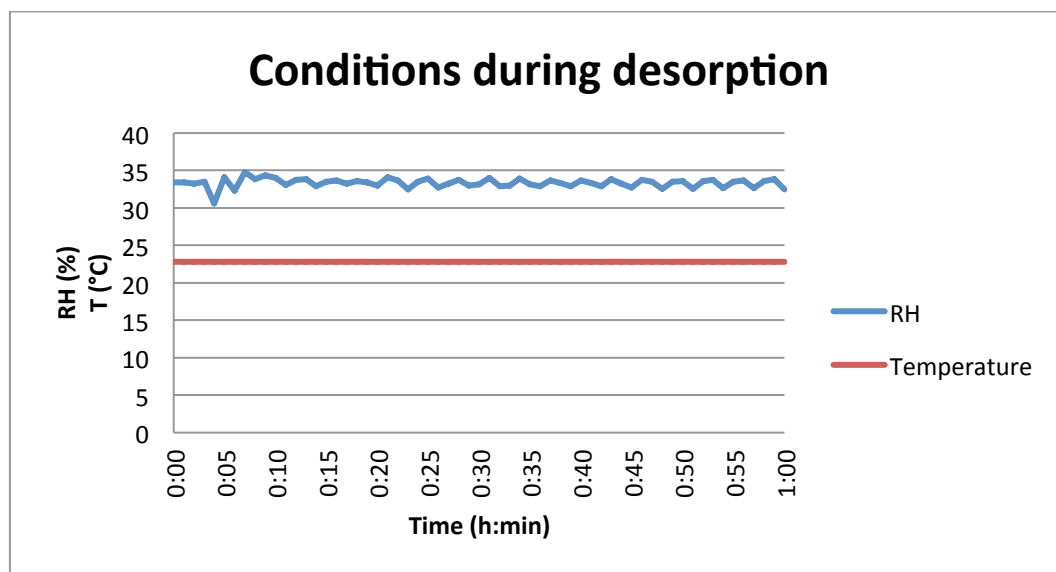


Figure 22 Conditions in climate cabinet during desorption of the birch samples.

7.4 Pine Sapwood

The changes in moisture content (Figure 23) were quite similar to the birch samples. The moisture gain with the transverse surface was quite the same, and greater with radial and tangential grain orientations. Desorption of pine sapwood was greater in all grain orientations than for birch samples. This indicates that pine sapwood is more active with moisture than birch, which is denser than pine sapwood (Table 5). Also, the structure of pine sapwood is more porous at the microscopic scale than birch (Kärkkäinen, 2007), which would confirm the greater MC variation. However, birch contains 32.4% hemicelluloses and pine only 28.5% (Sjöström, 1993) denoting that it would attract more moisture than pine, since hemicelluloses are mostly responsible for forming the hydrogen bonds. On the other hand, the question is not only about the amount of hemicelluloses, but the accessibility.

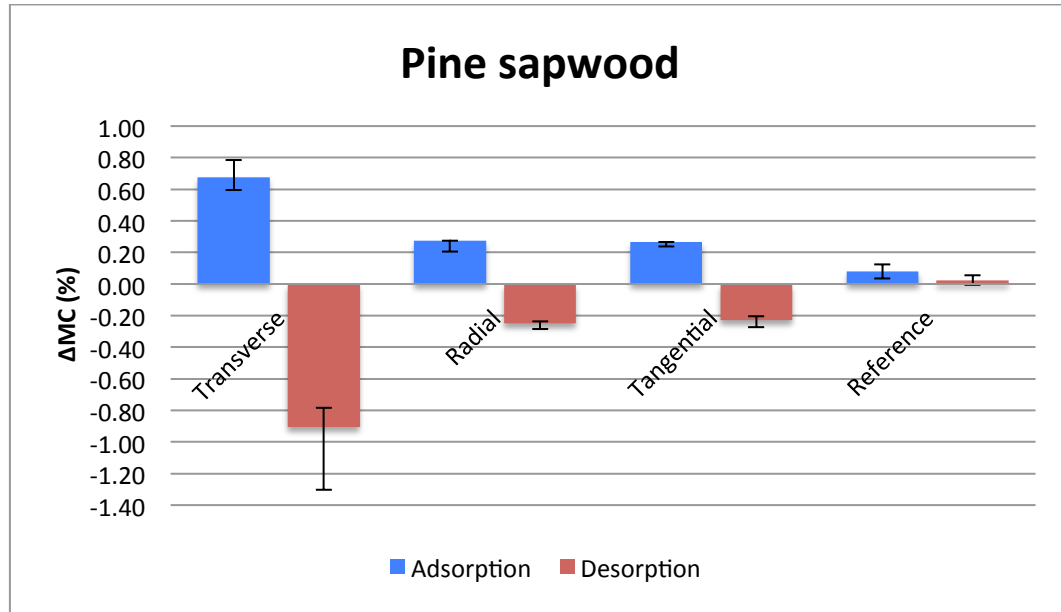


Figure 23 Changes of moisture content during adsorption and desorption in pine sapwood in three grain orientations and reference during 1 hour.

The transverse surface of pine sapwood samples had the greatest increase in temperature during adsorption and decrease during desorption compared to the radial and tangential surfaces (Figure 24). Again the surface temperature of the reference rose as well for the same reasons as the reference in birch samples. The difference between the temperature of tangential and transverse surfaces was quite low (Figure 25) perhaps because the tangential surface had greater amount of earlywood than latewood compared to radial surface. The recording of the thermal camera indicated that the parts with earlywood were warmer than the parts with latewood. Same as for MC, this could be due to greater porosity of earlywood (Sjöström, 1993). Also, the tangential and radial surfaces behave similarly in the beginning when the rise was linear and then the temperature of the radial surface cooled faster than the tangential.

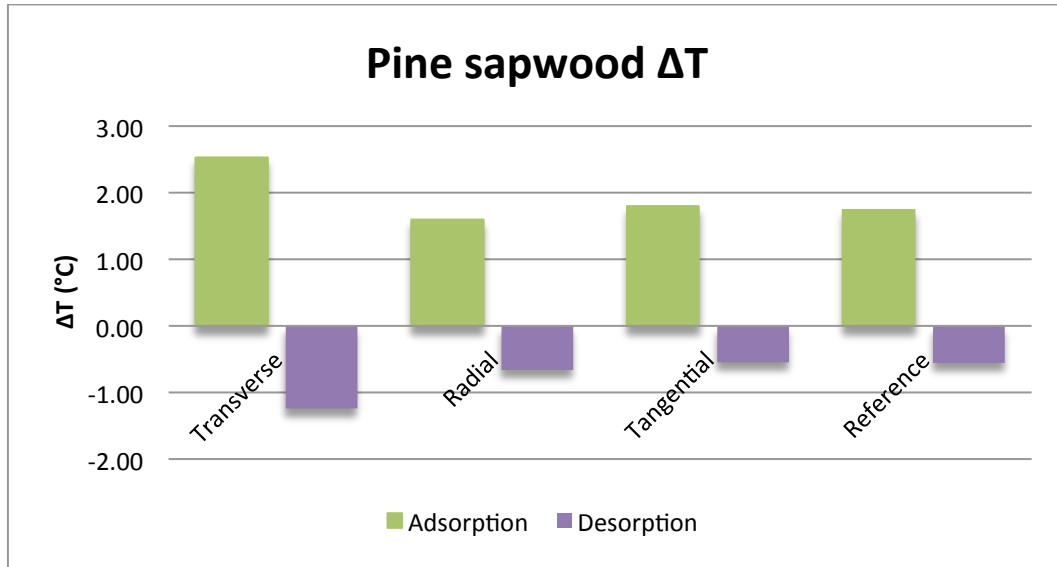


Figure 24 Differences between the initial and maximum temperature changes of grain orientations of pine sapwood and reference during adsorption and desorption during 1 hour.

Even though the temperature increase of the radial and tangential surfaces was almost the same, the radial surface cooled faster than the tangential (Figure 25). The conditions during adsorption are shown in figure 27. The radial and tangential surfaces of the birch samples behaved more similarly, but pine is more heterogeneous (Kärkkäinen, 2007) thus the behaviour of the radial and tangential surfaces diverges.

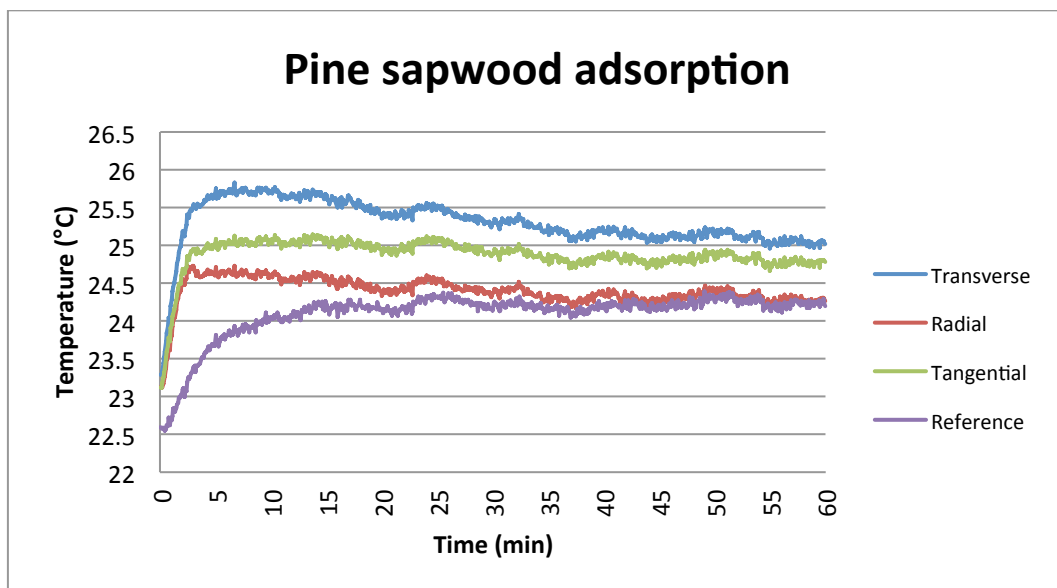


Figure 25 Temperature changes of pine sapwood samples and reference when the samples are placed in climate cabinet with RH 80%.

The MC increase is linear (Figure 26), and the overall change appears to be similar with the MC change of birch. Thus, if the sorption was comparable between birch and pine sapwood, the reasons for the difference in temperature variations are something else, such as the factors listed in Section 7.2.

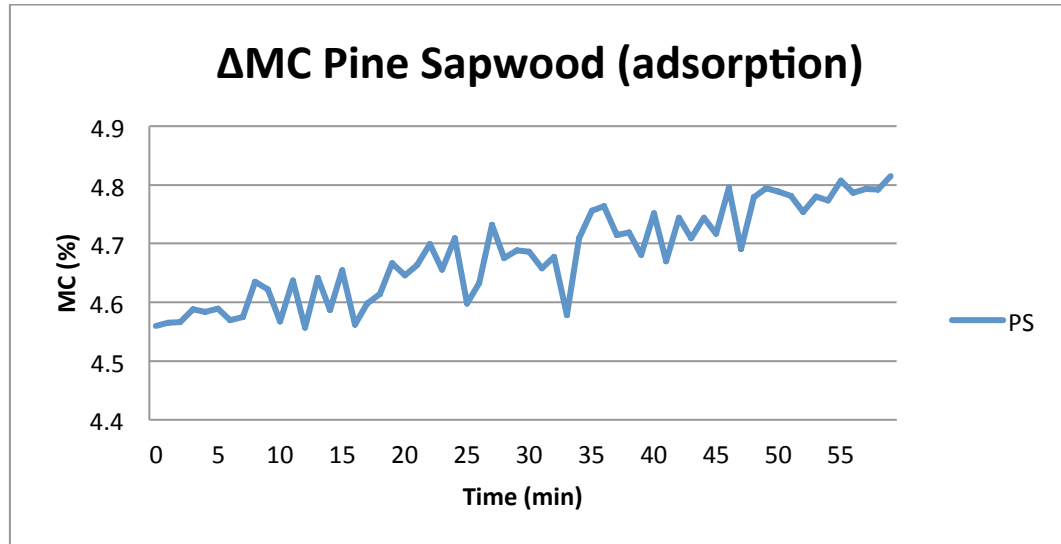


Figure 26 The average change in MC of all the pine sapwood samples (transverse, radial, tangential and reference) summed during adsorption.

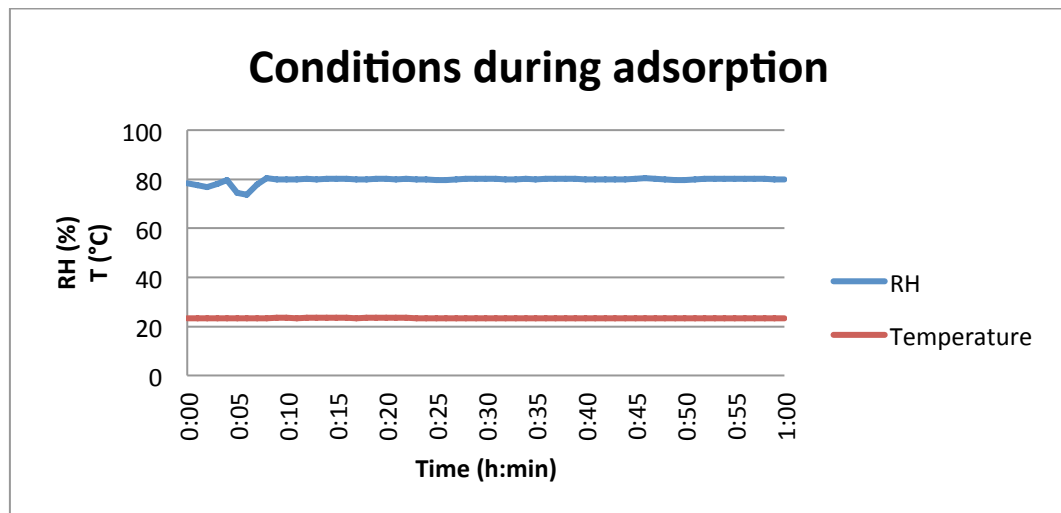


Figure 27 Conditions in climate cabinet during adsorption of the pine sapwood samples.

The temperature change during desorption behaved rather differently from the adsorption (Figure 28). First, the temperature of all the samples decreased rapidly and increased almost as fast as it had decreased. The decrease occurred faster than the increase in adsorption. The duration of the temperature decrease and the return

to initial temperature are presented in Appendix 14, Table 1. First, it seems that the temperature decreases subjected to desorption, but then it starts to increase almost as rapidly as it first decreased, and this might be due to the internal moisture, which is transferred to the surface after the surface has dried. Also, as mentioned in the Section 7.2, the heat of sorption increases with decreasing moisture content, which leads to heat release from inside the sample, and to surface temperature increase. In contrast to birch, instead of having a simultaneous decrease and increase temperature, the decrease occurs first and then the increase. This same behaviour occurs with pine heartwood (Figure 35), dry pine heartwood (Figure 42) and the experiment comparing birch and concrete (Figure 48).

Also, the conditions in Figure 29 show that the RH in the cabin rose in the beginning, most likely due to the opening of the door. It appears from the graphs that the temperature of the samples begins to increase as the RH of the cabinet rises, which might interfere with desorption. However, as mentioned above, the effect of opening the doors on the heat of desorption was proven not to have a clear impact.

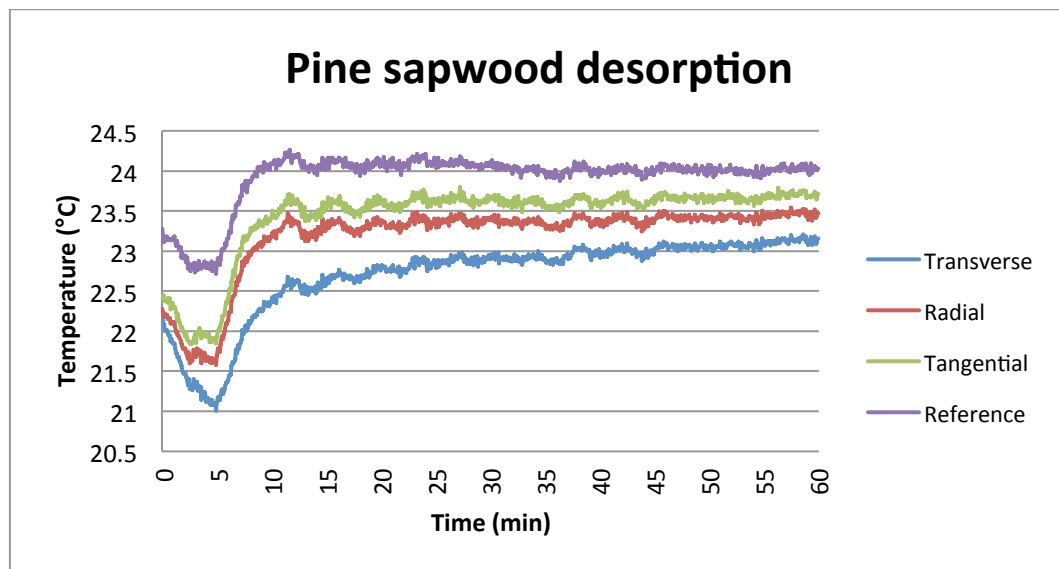


Figure 28 Temperature changes of pine sapwood samples and reference when the samples are placed in climate cabinet with RH 33%.

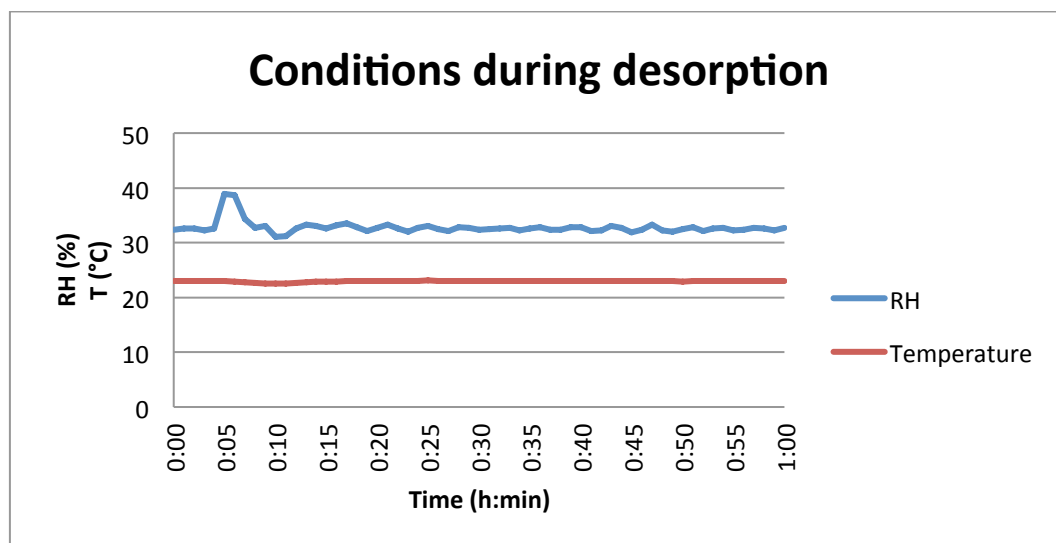


Figure 29 Conditions in climate cabinet during desorption of the pine sapwood samples.

7.5 Pine Heartwood

According to Kärkkäinen (2007) pine heartwood and sapwood are clearly distinguishable. The sapwood is visibly darker in colour, which is caused mostly by extractives. Also, there is a clear difference between the moisture content of pine sapwood and heartwood in the green state: sapwood contains more moisture than heartwood. All the cells that transport moisture are in the sapwood, and the heartwood consists of dead cells that store the nutrients. Sapwood is divided in two parts according to its physiological functions: the outer layer with transportcell zone and the inner layer as a storagecell zone. (Kärkkäinen, 2007)

The moisture contents of the pine sapwood and heartwood behave accordingly (Figure 30). The adsorption is lower with pine heartwood than with pine sapwood, although the difference is barely noticeable with the radial and tangential surfaces. This could be attributed to the function of sapwood and heartwood cells. The task of sapwood cells is to transport moisture and thus the sorption was greater than with heartwood. The cells of heartwood are intended for storage. (Kärkkäinen, 2007) Also the chemical composition, as the amount of hydrophobic compounds, of pine softwood and heartwood affects the sorption. The initial MC of pine sapwood samples was also a bit higher than of pine heartwood samples.

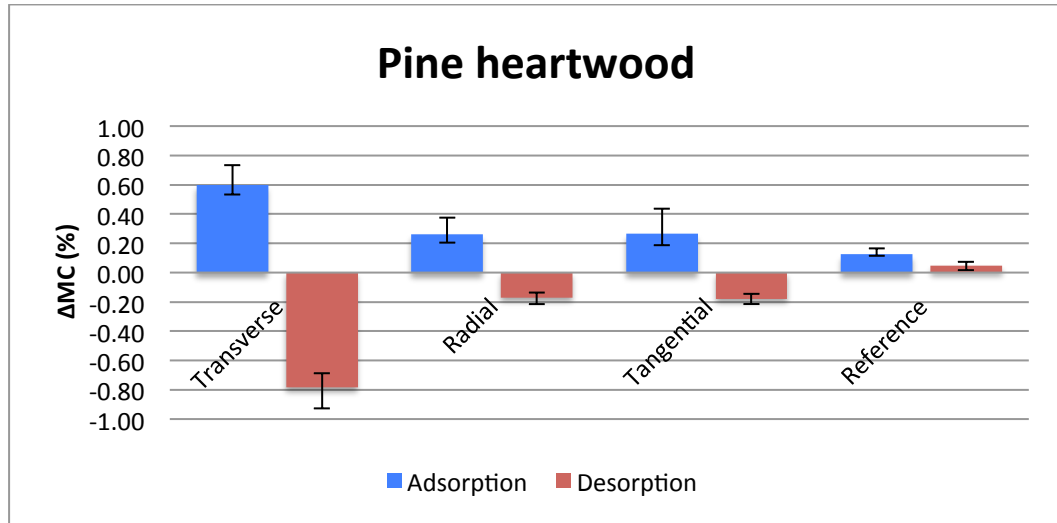


Figure 30 Changes of moisture content during adsorption and desorption in pine heartwood in three grain orientations and reference during 1 hour.

The temperature increase of the samples was the highest with the pine heartwood compared to the other categories (Figure 31). However, the initial temperature of the samples was approximately 1°C lower than with the previous samples, which is possibly due to the transportation between the buildings. This would affect the temperature increase, thus the increase could be assumed to be 1°C less. That day was colder than the other days and this could have affected the temperature inside of the box and therefore the samples. The temperature decrease during desorption was on a smaller scale than the rise in temperature, as in the previous results.

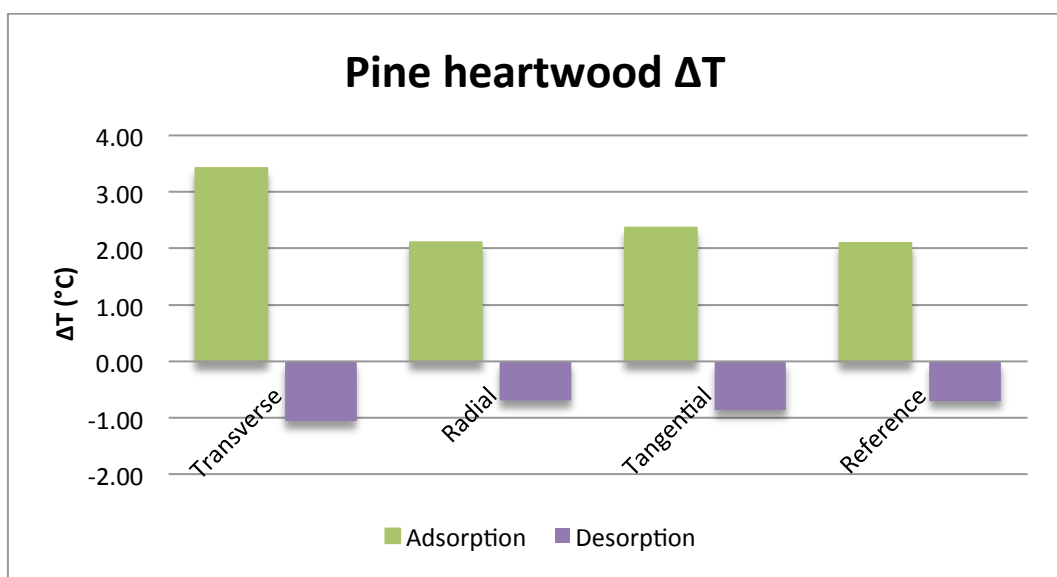


Figure 31 Differences between the initial and maximum temperature changes of grain orientations of pine heartwood and reference during adsorption and desorption during 1 hour.

The thermographs are comparable with the previous results and the samples reach the same temperature as the pine sapwood samples (Figure 32). It appears that the difference between these two is negligible. However, it would have been expected that the sapwood and heartwood would show some difference. The similarity could be attributed to the cutting of the samples. Even though the samples were cut as clear heartwood and sapwood as possible, the sapwood samples may have contained some heartwood and vice versa. Also, according to Kärkkäinen (2007) the sapwood is divided in two sections, the outer layer and the inner layer next to the heartwood. This inner layer is more like a mixture of heartwood and sapwood, and most of the samples were cut right from near to the heartwood.

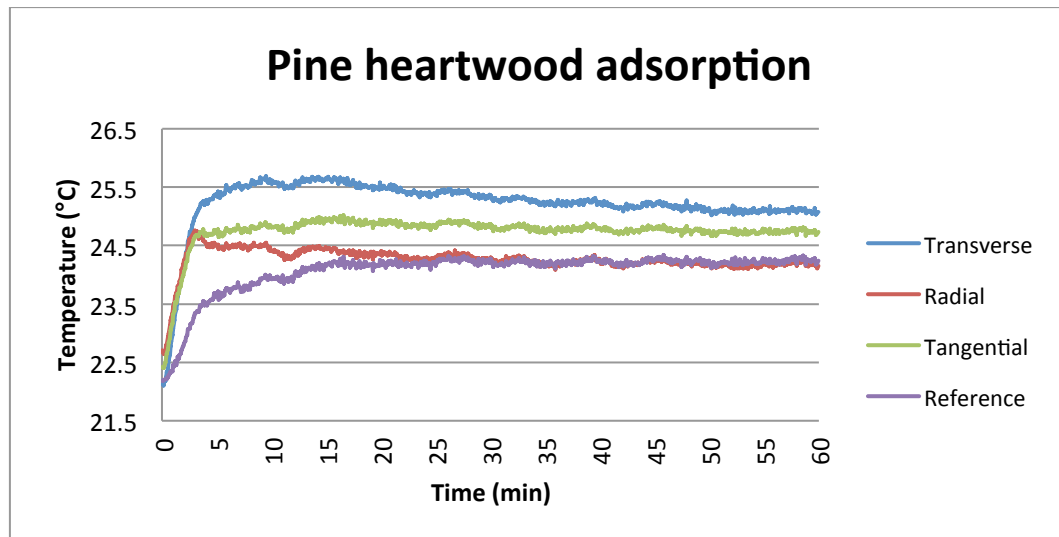


Figure 32 Temperature changes of pine heartwood samples and reference when the samples are placed in climate cabinet with RH 80%.

The MC change is once again linear (Figure 33), but the values are lower than those of birch or pine sapwood. Pine heartwood contains more hydrophobic compounds, such as extractives and lignin (Sjöström, 1993), which could result in lower sorption than birch or pine sapwood. The pine sapwood samples were denser than the heartwood samples, which affected the lower temperatures of the heartwood.

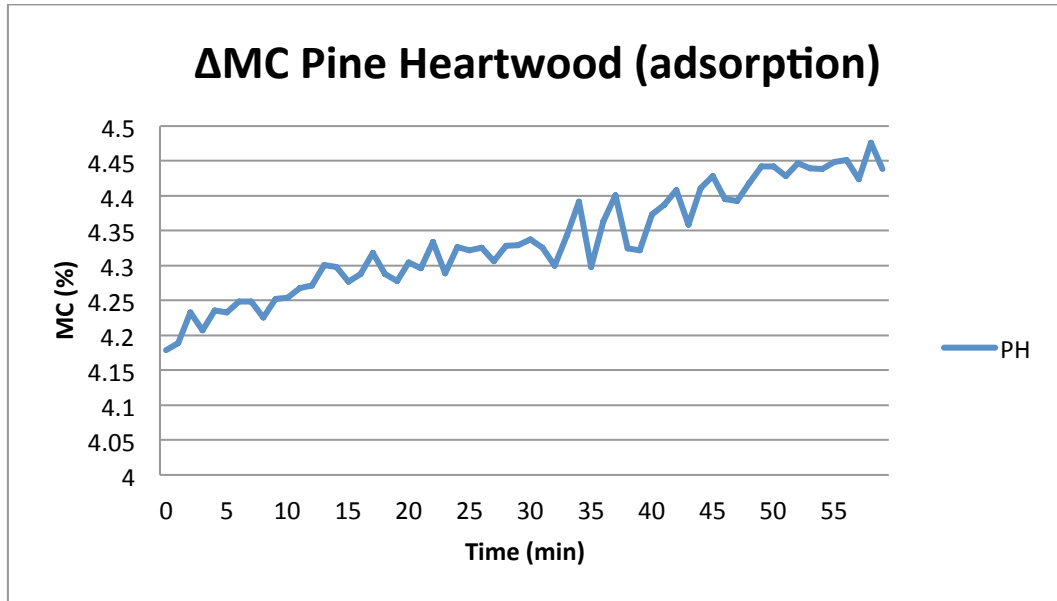


Figure 33 The average change in MC of all the pine heartwood samples (transverse, radial, tangential and reference) summed during adsorption.

The conditions remained stable during the recording (Figure 34) except for a small drop at 5 minutes. This could be an error due to a calculating the average values of the conditions or caused by a system error.

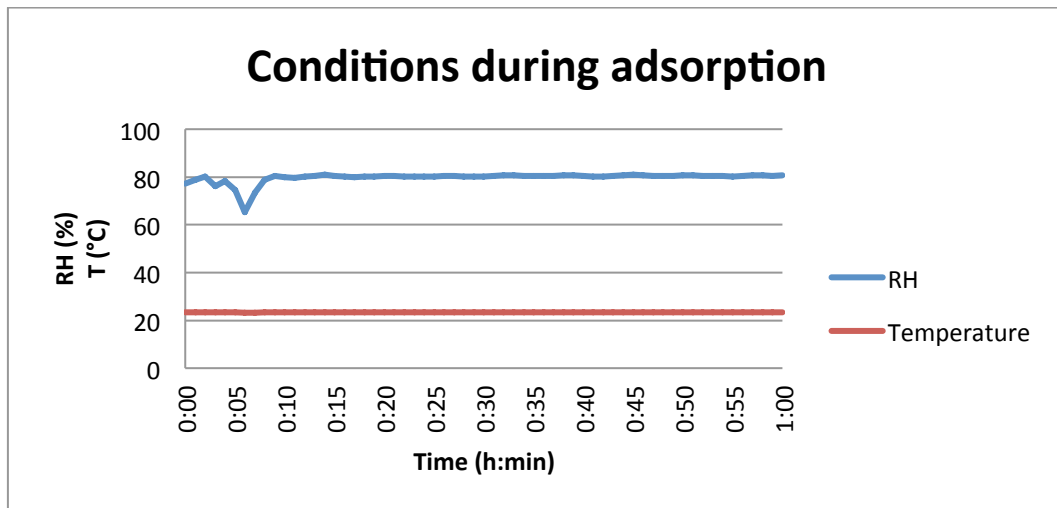


Figure 34 Conditions in climate cabinet during adsorption of the pine heartwood samples.

The temperature curves during desorption have first a decrease in temperature and nearly immediately a rise to the surrounding temperature, as pine sapwood had (Figure 35). The only difference is that the transverse surface temperature was closer to the radial surface temperature than with the pine sapwood due to the

smaller difference in initial moisture contents between the transverse and radial surfaces. The conditions (Figure 26) peaked again a while after initiating the test.

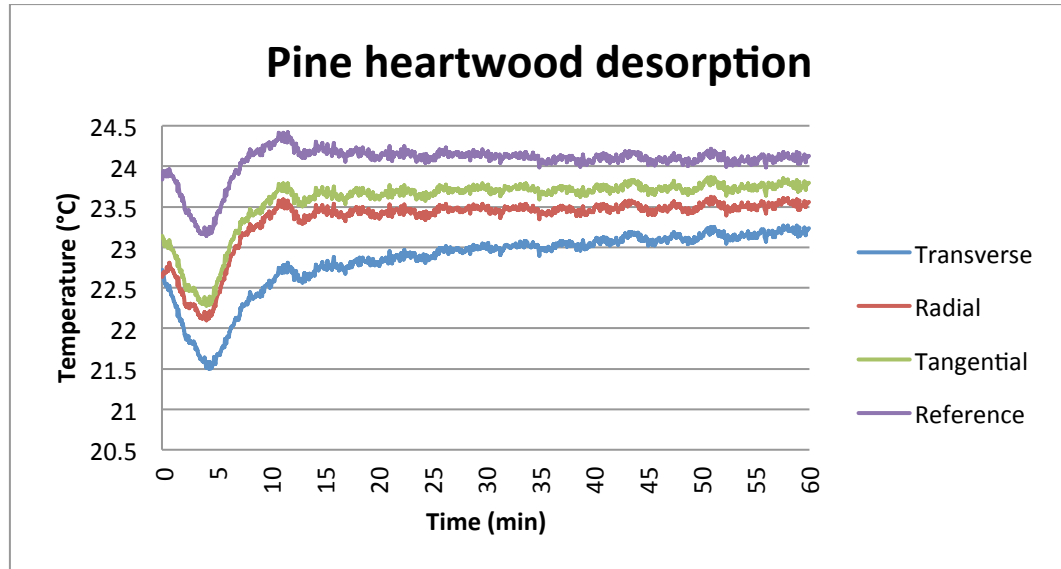


Figure 35 Temperature changes of pine heartwood samples and reference when the samples are placed in climate cabinet with RH 33%.

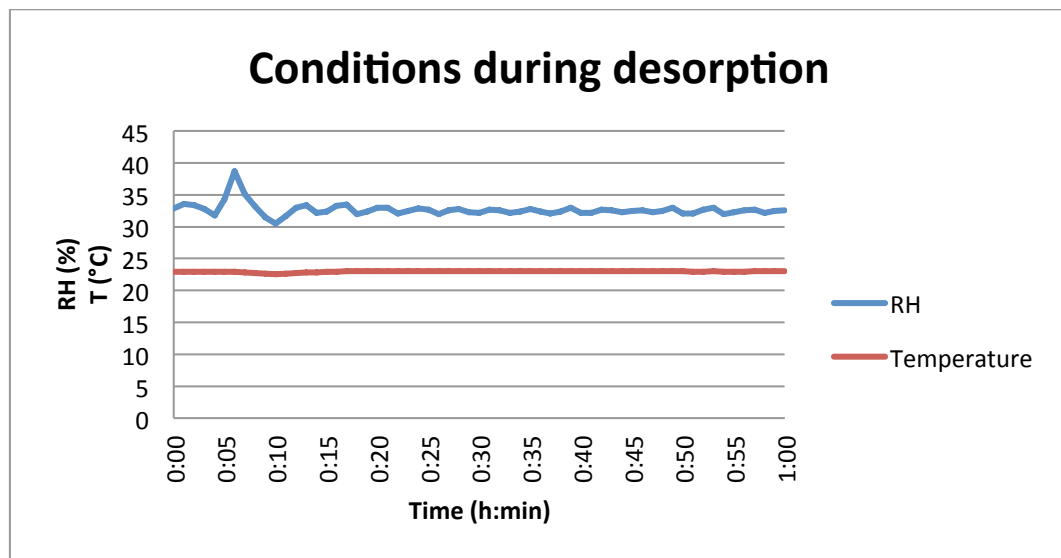


Figure 36 Conditions in climate cabinet during desorption of the pine heartwood samples.

7.6 Dry Pine Heartwood

The dry pine sapwood samples had the highest adsorption and reached the highest temperatures. The adsorption was nearly double the values of conditioned pine heartwood (Figure 36). The sorption is faster with lower moisture contents (Yazdani et al. 2006), which caused the greater adsorption.

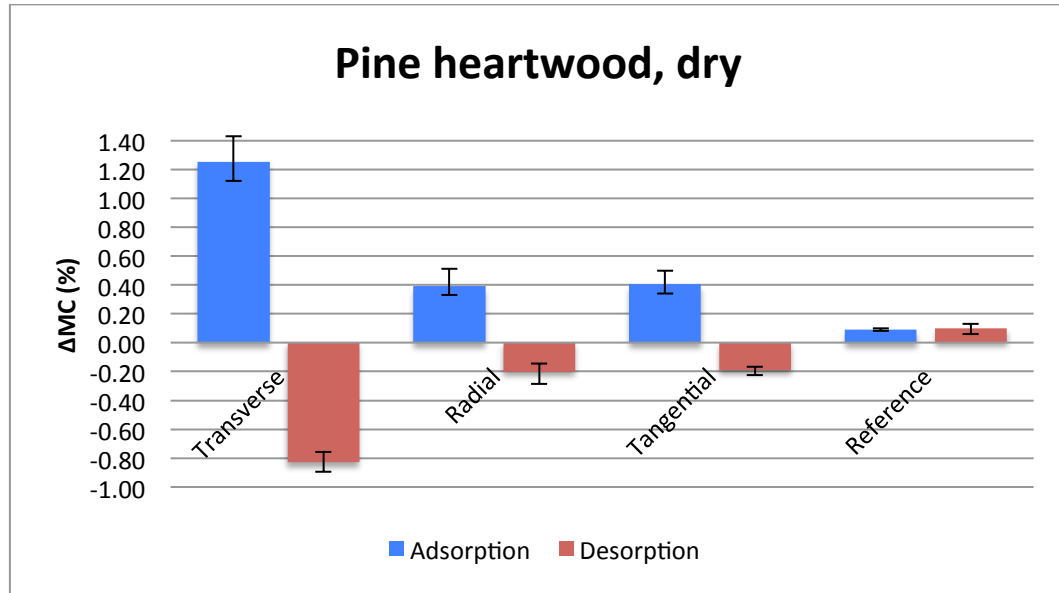


Figure 37 Changes of moisture content during adsorption and desorption in dry pine heartwood in three grain orientations and reference during 1 hour.

The changes between the initial and the highest temperature during adsorption are the lowest for dry pine heartwood (Figure 38), but yet the temperature values are the highest (Figure 39). The initial temperatures of the dry pine heartwood samples are nearly 2°C higher compared to birch (Figure 18) and pine sapwood (Figure 25) thermographs. This could be due to the fact mentioned in the analysis of the methodology that moisture might have entered the desiccator where the samples were stored. Furthermore, the samples could have adsorbed moisture during moving the samples from the desiccator to the climate cabin. Thus, the adsorption might have already initiated before the recording begun and led to an increase on the surface temperature. And since the samples were approximately oven dry the adsorption would be very aggressive in the beginning (Engelund, 2013).

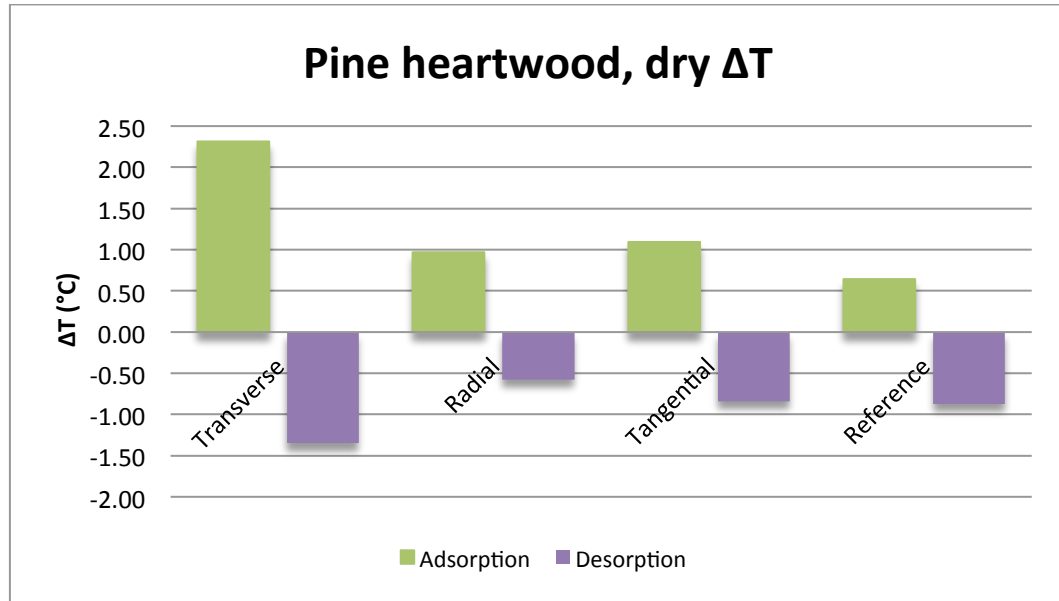


Figure 38 Differences between the initial and maximum temperature changes of grain orientations of dry pine heartwood and reference during adsorption and desorption during 1 hour.

Engelund et al. (2013) illustrated that the larger the initial moisture contents the lower the temperature rise during adsorption. Also, the lower the MC the less heat required to increase the temperature (Siikanen, 2008). The case can also be observed in figure 39, where the transverse surface temperature increases to 27.5°C and the tangential and radial to approximately 26°C. Compared to the conditioned pine heartwood the difference is 2°C for the transverse surface and 1.3°C for the radial and tangential surfaces. The behaviour of the reference sample differs from the other adsorption thermographs. This could be due to the fact that these samples were stored in the desiccator in the same room with the climate cabinet. Thus, the surface temperature of the reference sample is more stable. The drop in the beginning might be caused by the temperature difference between the sample and the climate cabinet.

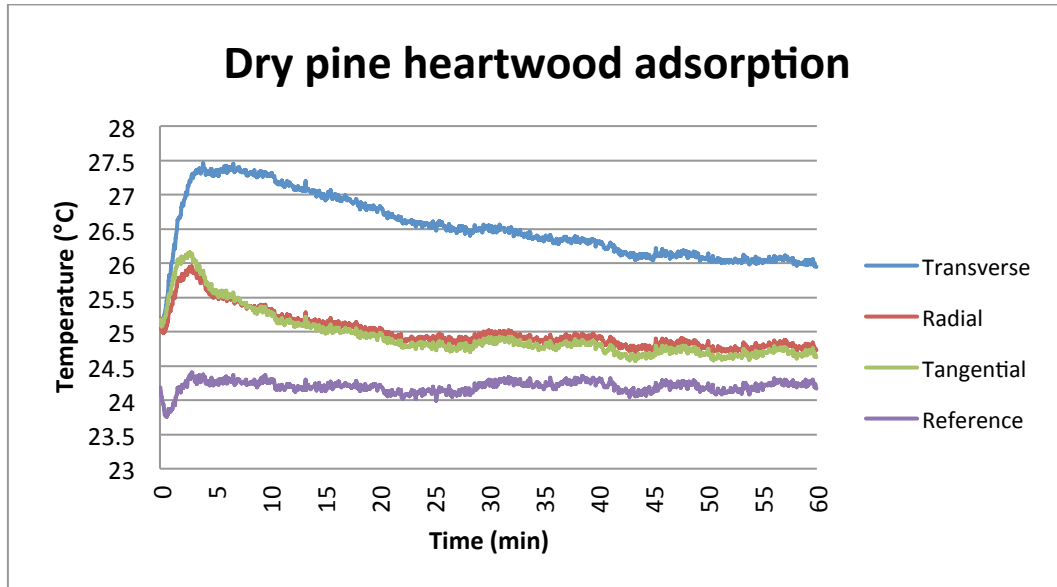


Figure 39 Temperature changes of dry pine heartwood samples and reference when the samples are placed in climate cabinet with RH 80%.

The overall MC increase of the dry pine sapwood samples appears linear (Figure 40), but it could be interpreted that the diagram curves slightly at the end. Perhaps the MC begins to approach the equilibrium according to the exponential form, which is usually the form of the adsorption curve.

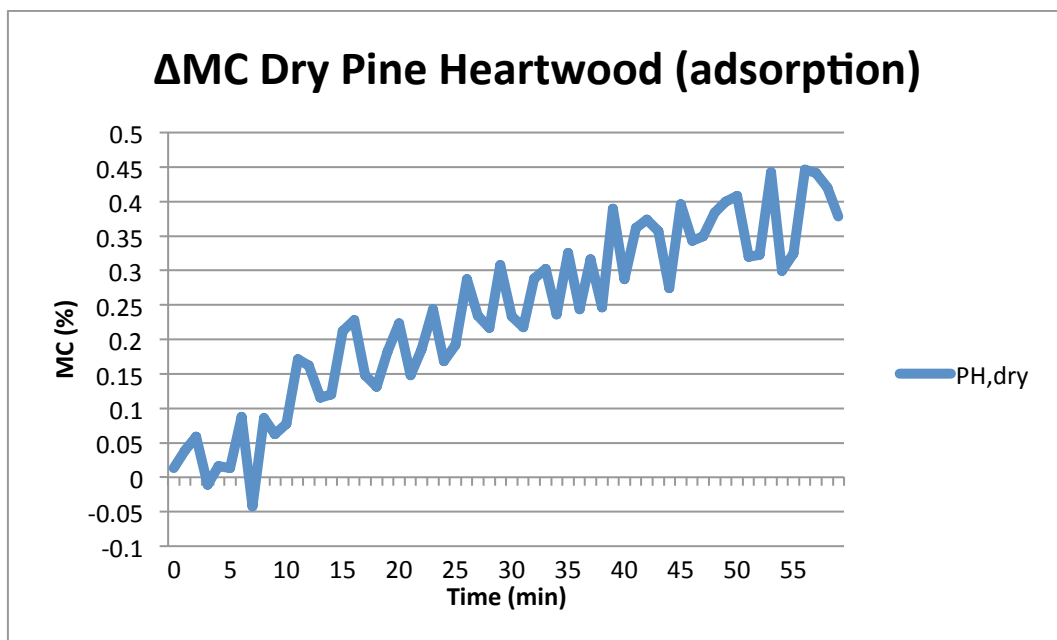


Figure 40 The average change in MC of all the dry pine heartwood samples (transverse, radial, tangential and reference) summed during adsorption.

As the adsorption of the birch samples, the logger did record the conditions only once in half an hour, thus the results do not give a realistic picture of the conditions (Figure 41).

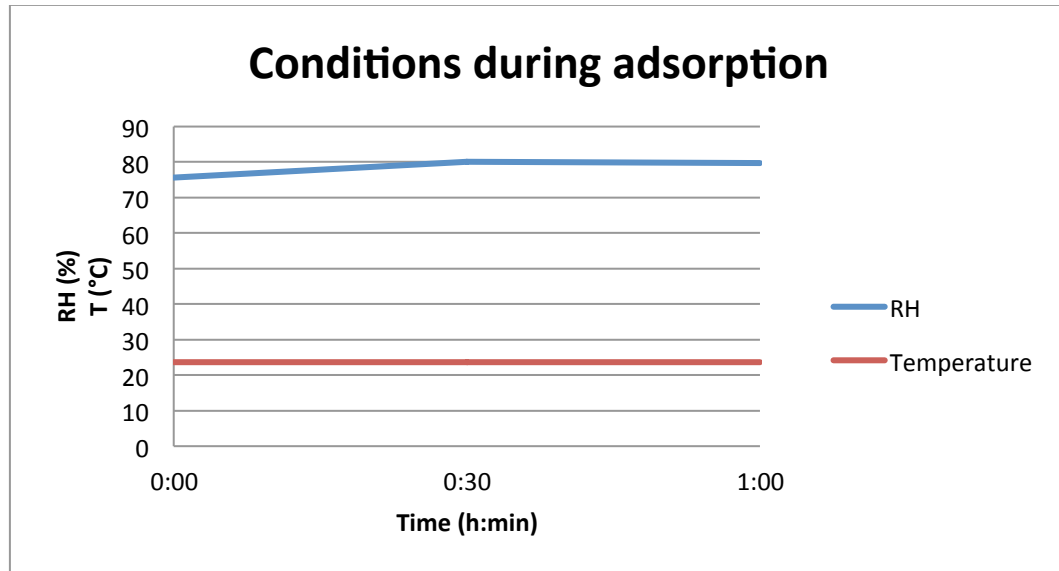


Figure 41 Conditions in climate cabinet during adsorption of the dry pine heartwood samples.

The thermographs during desorption are similar with the previous results (Figure 42) and also the conditions have the similar rise in RH as the previous diagrams (Figure 43). The tangential and radial surfaces show almost indistinguishable differences, but the temperature of transverse surface decrease almost double compared to the radial and tangential surface temperatures. The steep decrease in the beginning could be due to the more hydrophobic structure of pine heartwood.

Compared to the conditioned pine heartwood the initial moisture contents before desorption varied between the grain orientations (Table 5). The difference of the initial MC between the transverse (11.83%) and the radial (6.15%) surface is greater with dry heartwood samples than the conditioned pine heartwood (transverse 11.72% MC and radial 7.78% MC), which can be observed as greater difference in thermographs. Also, the radial (MC 6.15%) and tangential (MC 6.43%) surfaces have approximately the same MC with dry heartwood samples, whereas the difference is greater with the other heartwood samples (radial MC 7.78% and tangential MC 8.18%). This results in smaller difference between radial and tangential thermographs for dry pine heartwood samples.

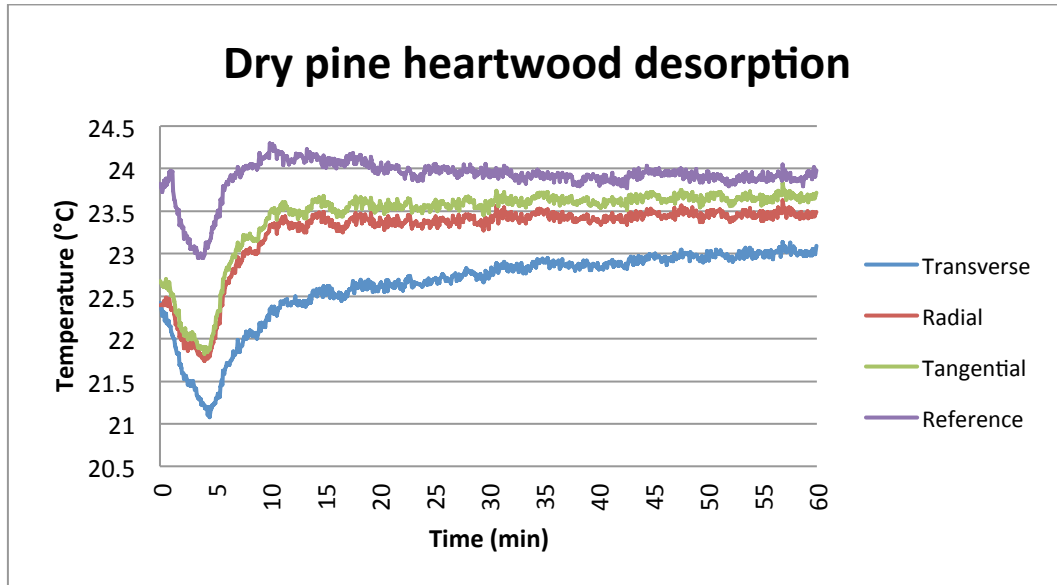


Figure 42 Temperature changes of dry pine heartwood samples and reference when the samples are placed in climate cabinet with RH 33%.

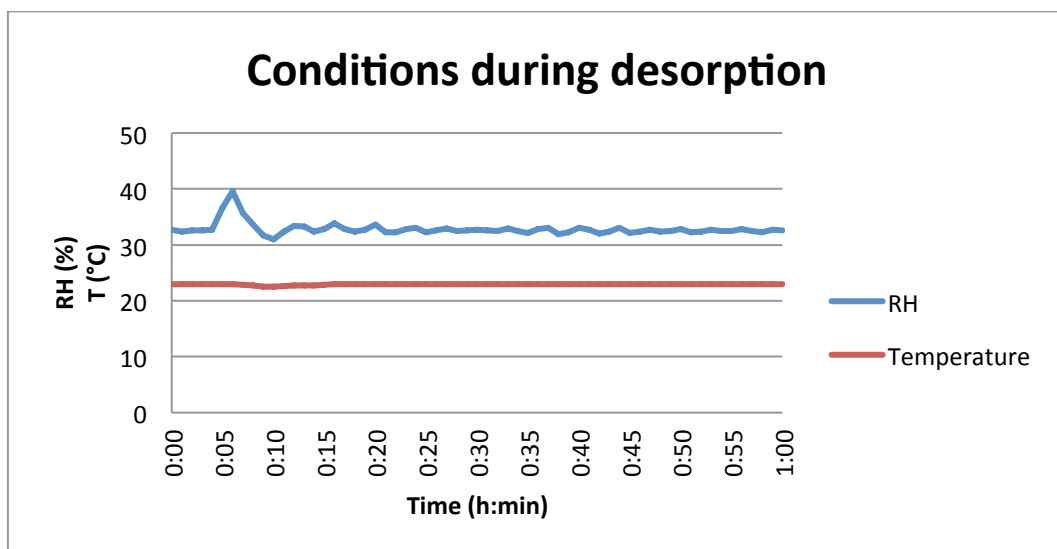


Figure 43 Conditions in climate cabinet during desorption of the dry pine heartwood samples.

7.7 Birch and Concrete

One objective of the experiment was to compare the heat of sorption of wood and concrete. Concrete is the most common building material, which is why it was chosen. It has also porous structure and it adsorbs moisture. (Khan, 2002) According to figure 3 the sorption of concrete is far lower than the sorption of wood. The results behave accordingly (Figure 44). The adsorption of concrete is the lowest compared to birch samples. And during desorption instead of decreasing the MC actually increases. This might be due the short conditioning

time. The concrete samples were conditioned only one day before adsorption and desorption, thus the MC of the samples was rather uneven between and within the samples.

The sorption of the birch samples is far lower than the sorption of the previous samples. This is due to the different conditions in the climate chamber. The same RH and temperature values as before were entered to the program of the cabinet, but the actual RH was not equivalent with the program. The temperature remained stable. Thus, the actual RH during the adsorption was 70% (Figure 47) and during desorption it was around 34% (Figure 49). This affected the adsorption of the samples.

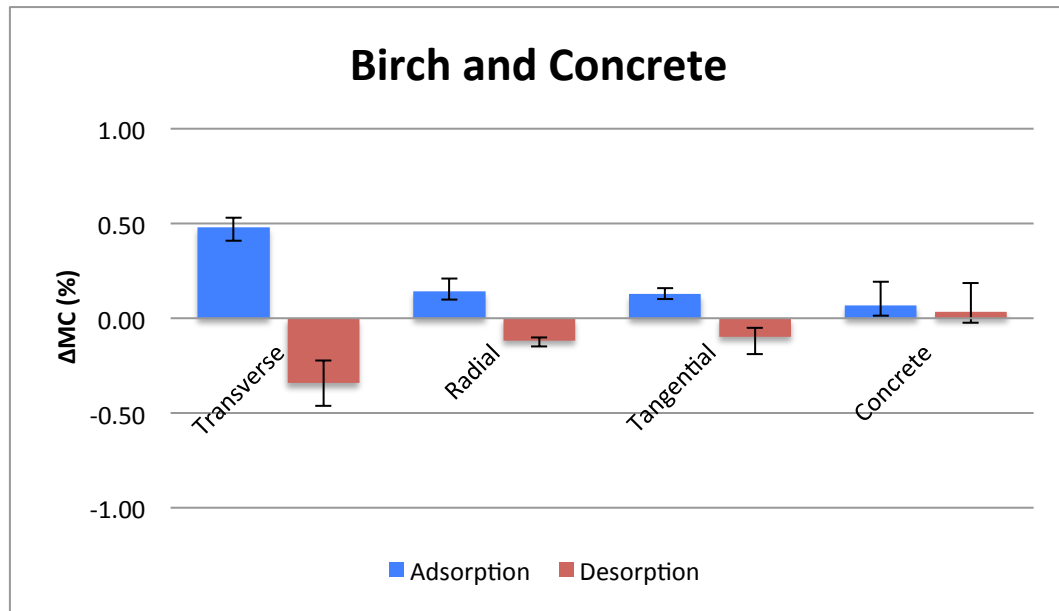


Figure 44 Changes of moisture content during adsorption and desorption in birch in three grain orientations and concrete during 1 hour.

The results for temperature change during adsorption and desorption are shown in figure 45. Concrete has a similar temperature changes as the wooden samples even though it had a minor change in MC. Also, the concrete thermograph reaches the same temperature as the radial and tangential surfaces (Figure 46). The high temperature might be due to the emissivity value of concrete, which was only 0.71 compared to that of birch samples' 0.8. The lower the emissivity value the higher the temperature (López et al., 2013). Also, the tabular values for concrete vary

from 0.63 to 0.92 depending on the roughness of the surface (Engineering Toolbox, 2015; Infrared Thermography, 2015). However, the emissivity does not affect the magnitude of temperature change.

The temperature changes in concrete are not due to the moisture sorption, thus it may be attributed to the structure and thermal properties of concrete. The heat transfer in concrete is subjected to the constituents of concrete and the proportions, e.g. thermal conductivity of the rocks used as aggregates vary from 1.163 and 8.6 W/mK (Khan, 2002) and depending on the MC and porosity the values will vary. The thermal conductivity of the concrete used in the experiment is unknown, thus the assessment of the thermal properties is challenging. Also, the age, the casting and composition of concrete have major effect on its properties, thus the results could be very different with more mature concrete. Generally concrete conducts heat more effectively than wood, which might affect the surface temperature change.

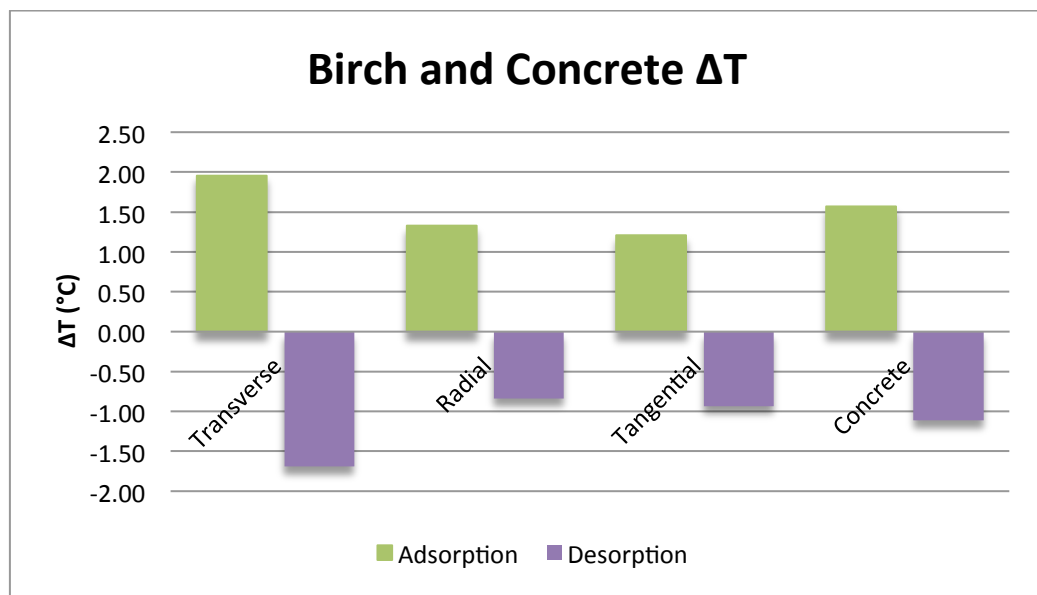


Figure 45 Differences between the initial and maximum temperature changes of grain orientations of birch and concrete during adsorption and desorption during 1 hour.

The thermograph resembles the thermograph of the birch samples above (Figure 46). The radial and tangential surfaces have similar temperature increase and the thermograph of transverse surface lies above them. The interesting part here is the

concrete thermograph, which reaches the maximum temperature after the wood samples. It does not have that peak in the beginning, thus the concrete surface heats up bit slower than wood. The conditions have an unusual drop at 5 minutes as previous results have (Figure 47).

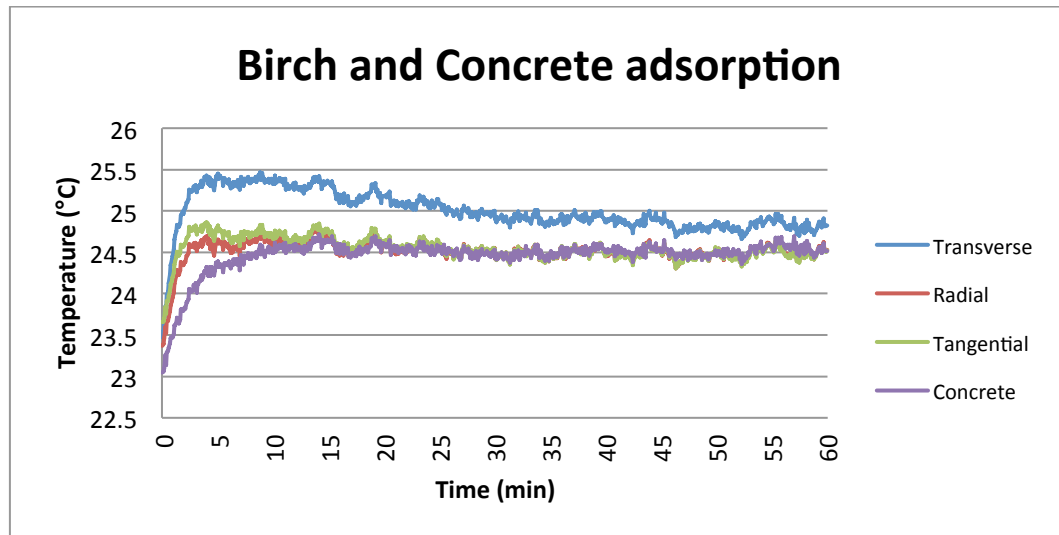


Figure 46 Temperature changes of birch and concrete samples when the samples are placed in a climate cabinet with RH 70%.

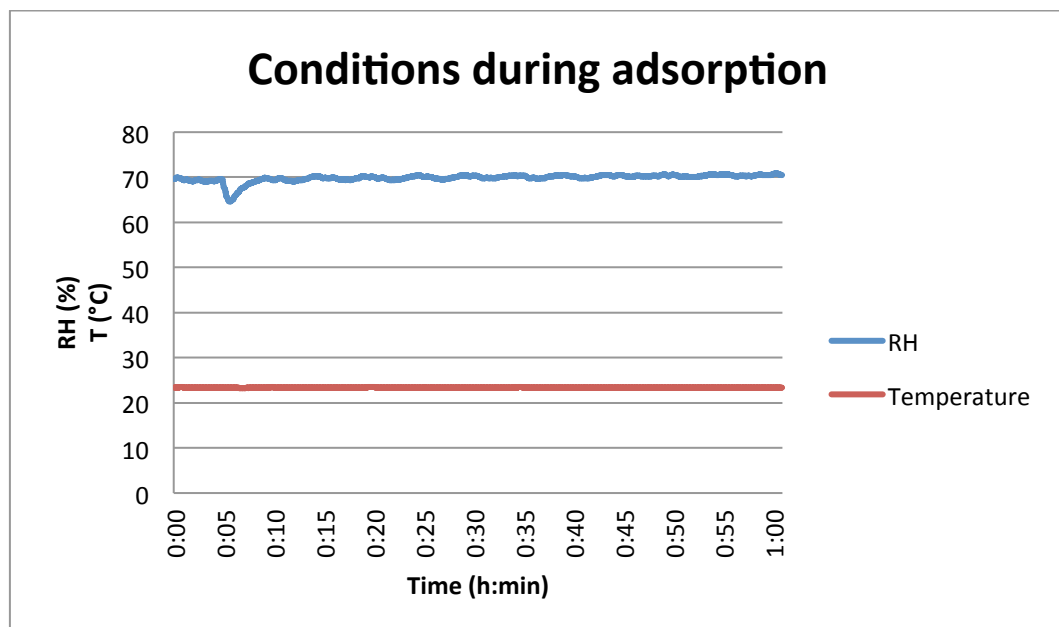


Figure 47 Conditions in climate cabinet during adsorption of the birch samples and concrete.

The thermographs during desorption have a steep drop and then rise in temperature (Figure 48). The steep drop might be due to the slightly lower temperature in the climate cabinet (22.7°C) compared to the previous results (23°C). The thermographs of the radial and tangential surfaces are almost the same, and this appears to correlate with the initial moisture contents (Table 5). The difference between the moisture contents of these and the transverse sample is noticeable and the similar effect can be observed from the thermographs. Concrete has almost similar curve, but the initial surface temperature is higher than the wooden samples. This might be again due to the emissivity value. Also the thermograph of concrete appears to be a bit more stable than the wood samples.

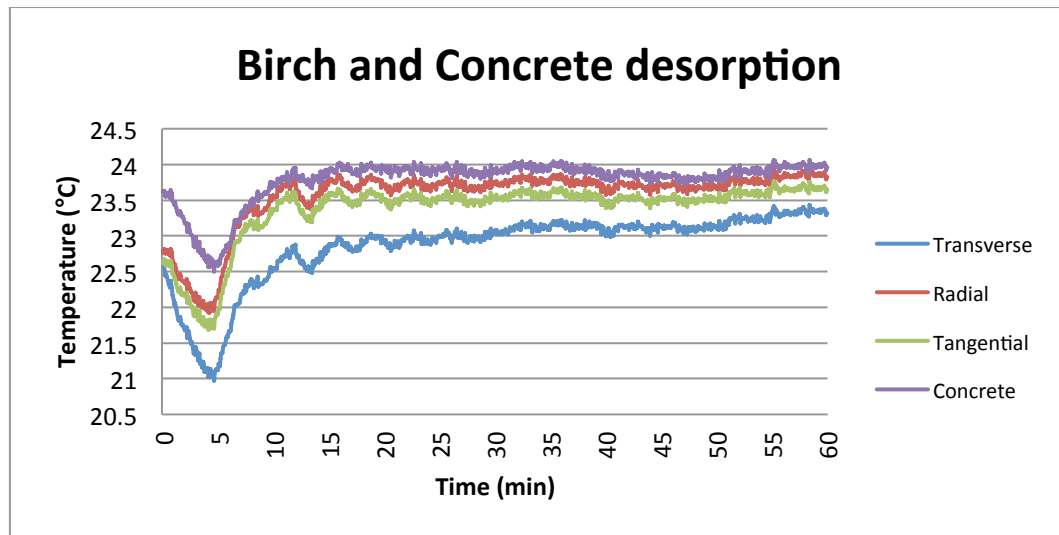


Figure 48 Temperature changes of birch and concrete samples when the samples are placed in a climate cabinet with RH 34%.

The change in the conditions was observed now at the same rate as the recording so the logging interval was once in every five seconds (Figure 49). The recording begins after the samples are placed in the climate cabinet and the door is closed, thus the RH has risen as the door was opened, but it is not observed in the diagram. Also, the RH increases at the end, but this can be due to the opening the door at the end.

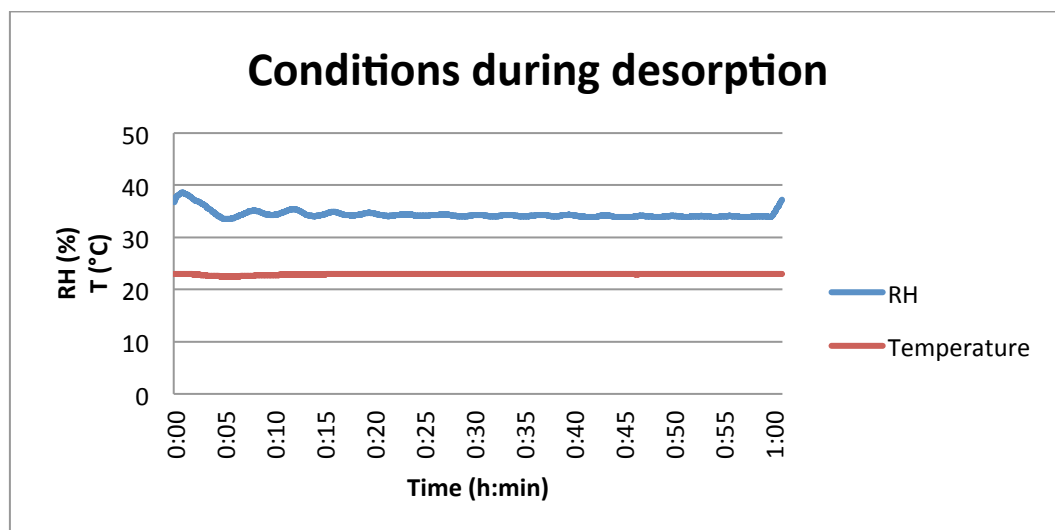


Figure 49 Conditions in climate cabinet during desorption of the birch samples and concrete.

7.8 Transverse Grain Orientation

Transverse direction (Figure 50) had the greatest variation between the species. Other directions seemed to behave quite similarly. Transverse surface is the most adsorbing surface compared to tangential and radial surfaces. Thus the adsorption and the resulting temperature rise could have occurred even before the test had begun which could have resulted in the variation between the initial temperatures.

Dry pine heartwood reached the highest temperature, as expected. It had the greatest moisture uptake, thus leading to the highest temperature during adsorption. Also birch seemed to have greater rise than pine (sapwood and heartwood). Pine sapwood and heartwood had the smallest rise in temperature of the wood samples, and the difference was small between them. As mentioned before, pine is more porous than birch (Kärkkäinen, 2007), which could indicate that the heat diffusion is faster from the surface to inner parts of the sample resulting in smaller temperature rise on the surface. Denser species also conduct heat better, thus the heat could be transported from inside the sample more effectively thus increasing the temperature (Siikanen, 2008). Also, the initial moisture content has an effect on the temperature differences between the dry and conditioned pine heartwood. Compared to the transverse direction concrete has the lowest rise in temperature. Concrete does not have a similar capacity to adsorb

moisture as wood has on the transverse surface, thus the increase in temperature is low compared to wooden samples.

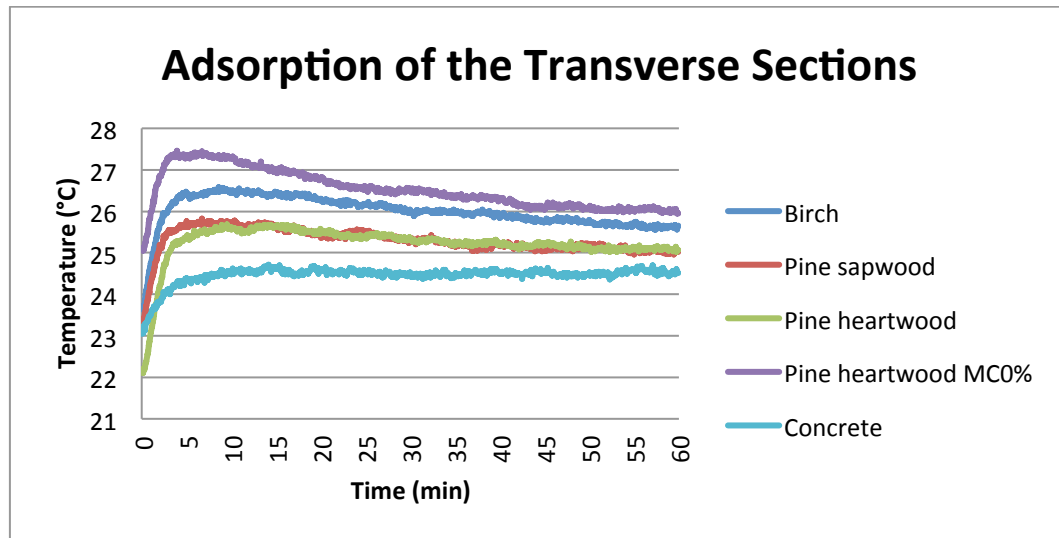


Figure 50 Comparison between temperature changes of different species in transverse direction and concrete during adsorption.

The difference between the thermographs of the wood samples during desorption are minor compared to the adsorption thermographs (Figure 51). The thermograph of birch is incomparable with other thermographs due to the difference in methodology compared to the other samples. Dry pine heartwood and pine sapwood have almost identical thermographs and conditioned pine heartwood is situated a bit higher. The form of the curves still very similar and also the magnitude of the temperature decrease is approximately the same for all the samples.

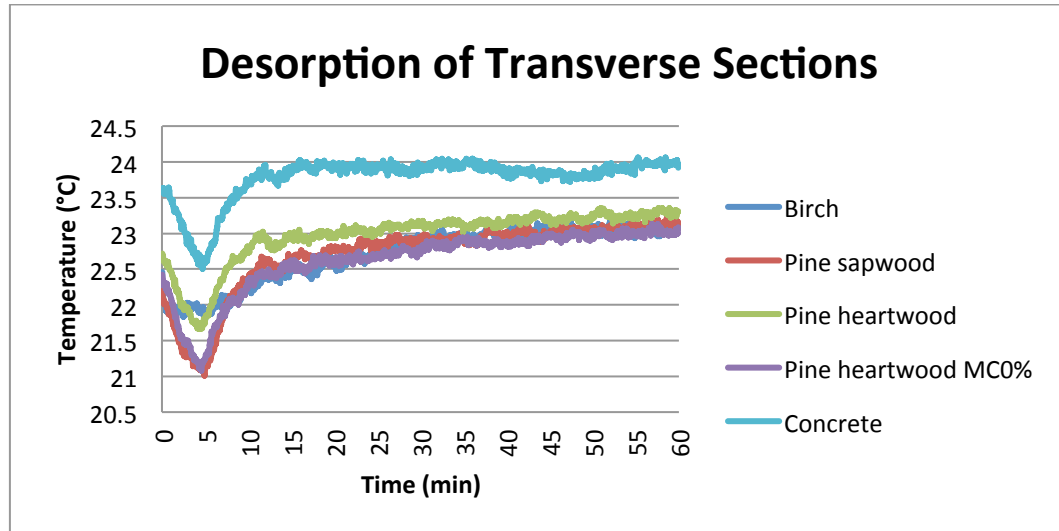


Figure 51 Comparison between temperature changes of different species in transverse direction and concrete during desorption.

7.9 Radial Grain Orientation

The differences between the radial thermographs are very minor, except for dry pine heartwood (Figure 52). The situation with dry pine heartwood is the same as with the transverse section: the temperature has risen already before the recording. Even though the differences are minor it is possible to distinguish that conditioned pine heartwood and sapwood have steeper angle after reaching the maximum temperature, whereas the thermograph of birch is smoother. This might be due to the composition of the structure, as the structure of birch is more homogenous (Kärkkäinen, 2007) the angle is more gradual. The amount of earlywood and latewood in the pine could cause the sharper angle, since temperature of the latewood could decrease more rapidly and affect the total temperature of the surface. Concrete has similar thermograph as birch, thus they may have more similar structure than with heterogeneous pine.

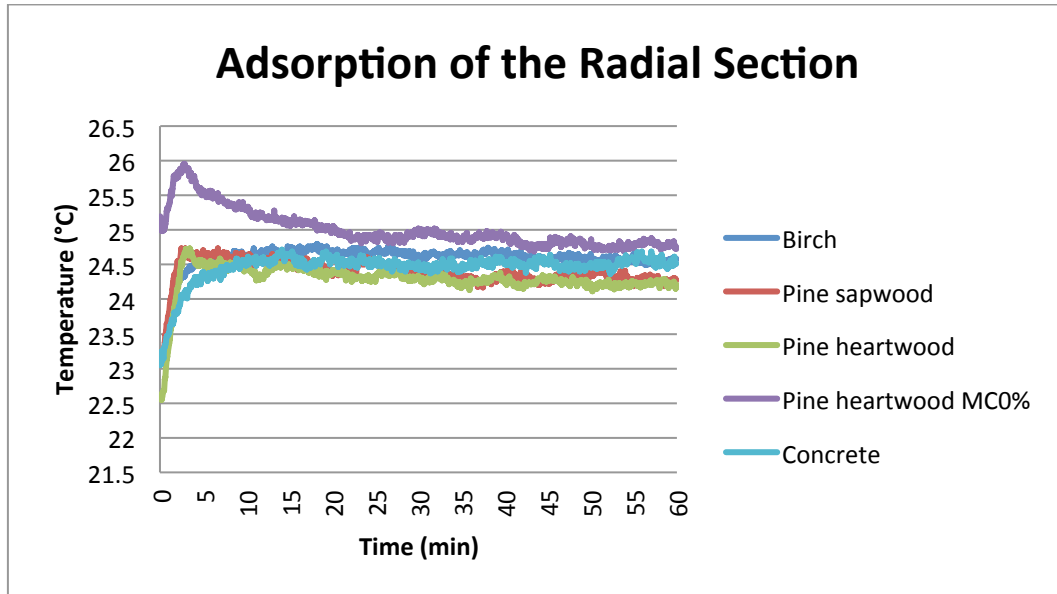


Figure 52 Comparison between temperature changes of different species in radial direction and concrete during adsorption.

As for adsorption thermographs the desorption thermographs are also hardly distinguishable (Figure 53) and even less distinguishable than with the transverse surfaces. Here the difference between concrete and wooden samples is smaller than with the transverse surface, because radial surface desorbed less moisture than the transverse direction.

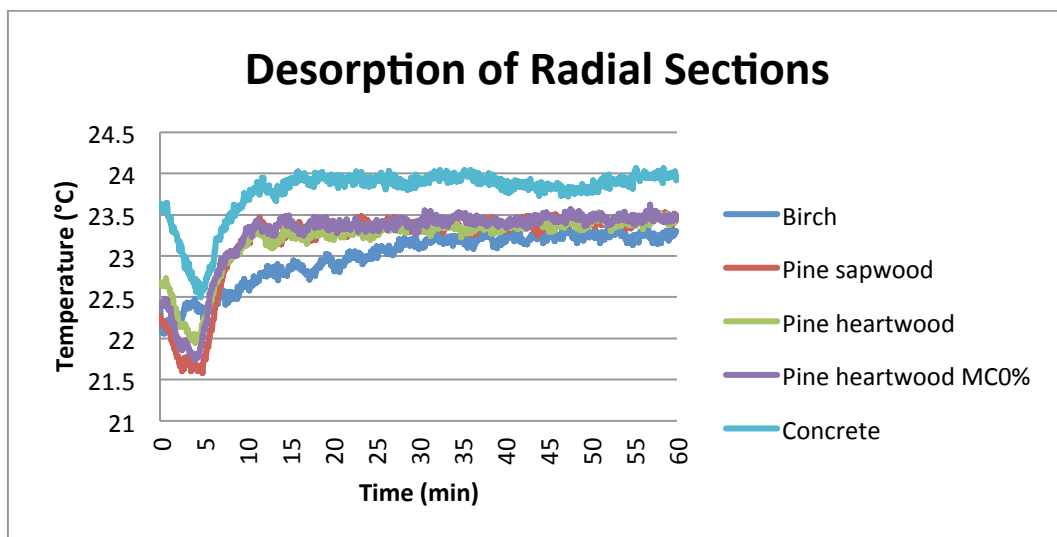


Figure 53 Comparison between temperature changes of different species in radial direction and concrete during desorption.

7.10 Tangential Grain Orientation

The thermographs follow the radial thermographs (Figure 54). Only difference is that the thermographs combine nearly to one temperature after 20 minutes. Also the angles of the conditioned pine heartwood and sapwood are not as steep as with radial thermographs. It appears that the tangential surfaces the earlywood area was dominant, which would affect the smoother curve.

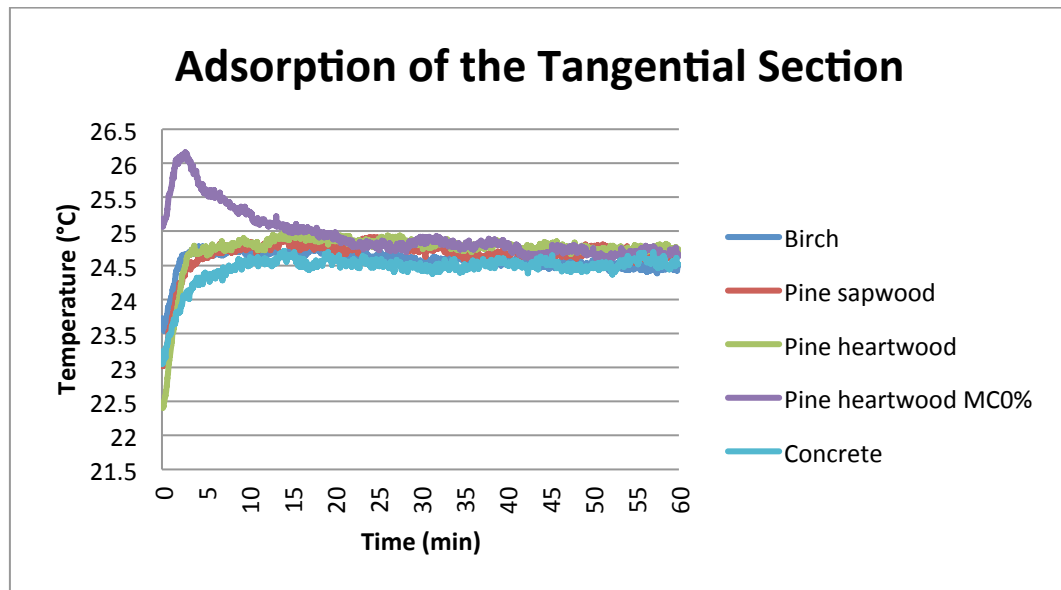


Figure 54 Comparison between temperature changes of different species and concrete in tangential direction during adsorption.

As the adsorption thermographs also the desorption thermographs are even closer together compared to transverse and radial surfaces (Figure 55). Only the initial temperatures vary.

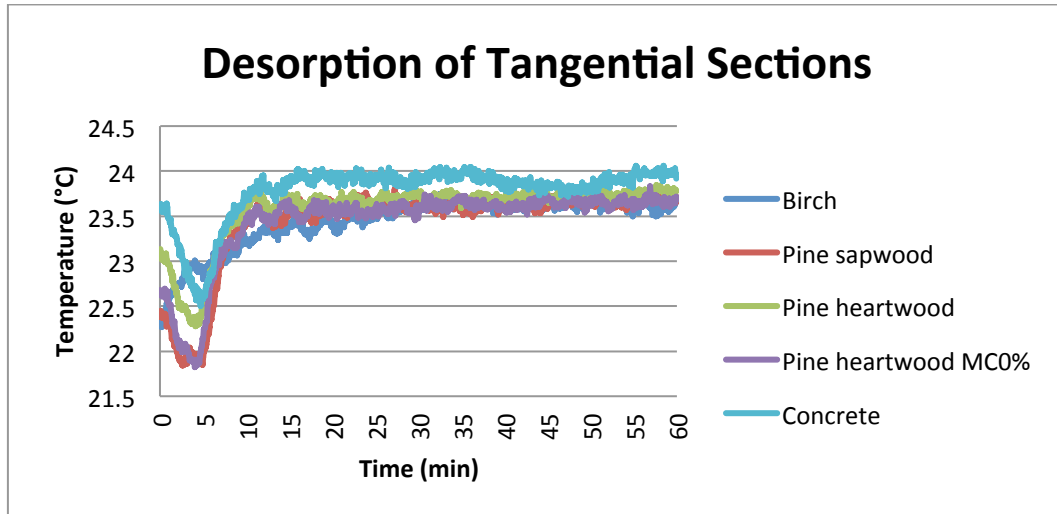


Figure 55 Comparison between temperature changes of different species in tangential direction and concrete during desorption.

7.11 Reference and Concrete

A wooden sample covered with plastic film was chosen as a reference material and concrete was also one reference material, because they have very different material properties the wood (Yang et al., 2012). Plastic film was impermeable and concrete has been a research topic in building material investigation together with wood (Padfield, 1998).

However, the resulted thermographs were quite unexpected. It was assumed that the surface temperature of the plastic or the concrete samples would not increase (Figure 56) nor decrease (Figure 57) as the surface temperatures of the wooden samples.

The reference samples of birch, pine sapwood and heartwood produced similar thermographs (Figure 56). Only the reference of dry pine heartwood and reference had different behaviour. The dry pine heartwood samples were stored in desiccator in the same room with the climate cabinet, whereas the others were in salt chambers in the other building. Also, the temperature in the desiccator might have been higher than in the salt chamber, thus showing first a decrease in the surface temperature and then an increase.

Concrete is more porous (Khan, 2002) and reacts to humidity changes, thus showing a greater increase in temperature than the references covered with plastic film.

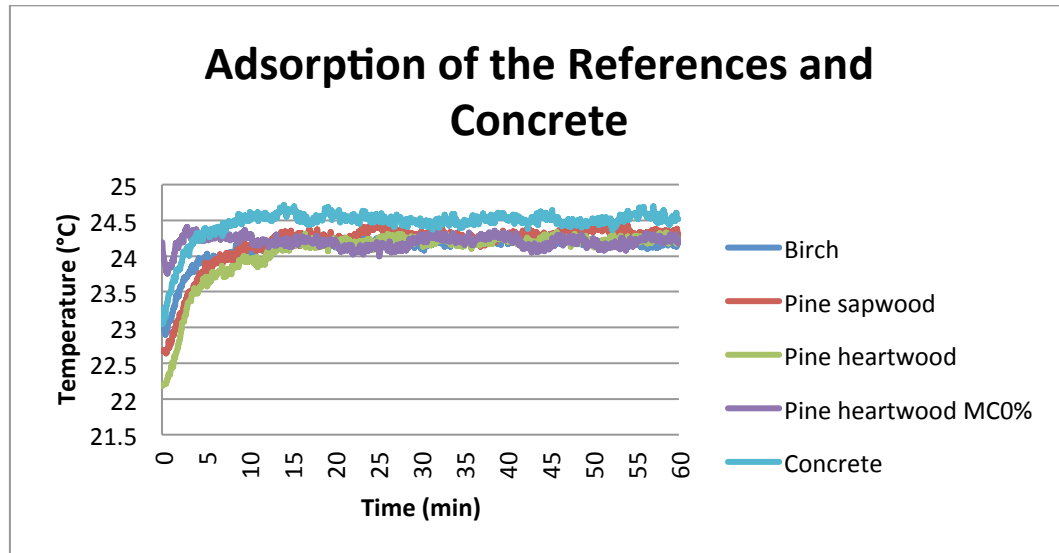


Figure 56 Comparison between temperature changes of the reference samples of birch, pine sapwood and heartwood, dry pine heartwood, and concrete during adsorption.

The references had similar temperature changes during desorption except for birch reference (Figure 57). Birch had the only reference that remained steady during desorption, which would be expected, since the plastic should be impermeable. However, the temperature changes are not caused by the sorption in case of the reference or concrete, but something else.

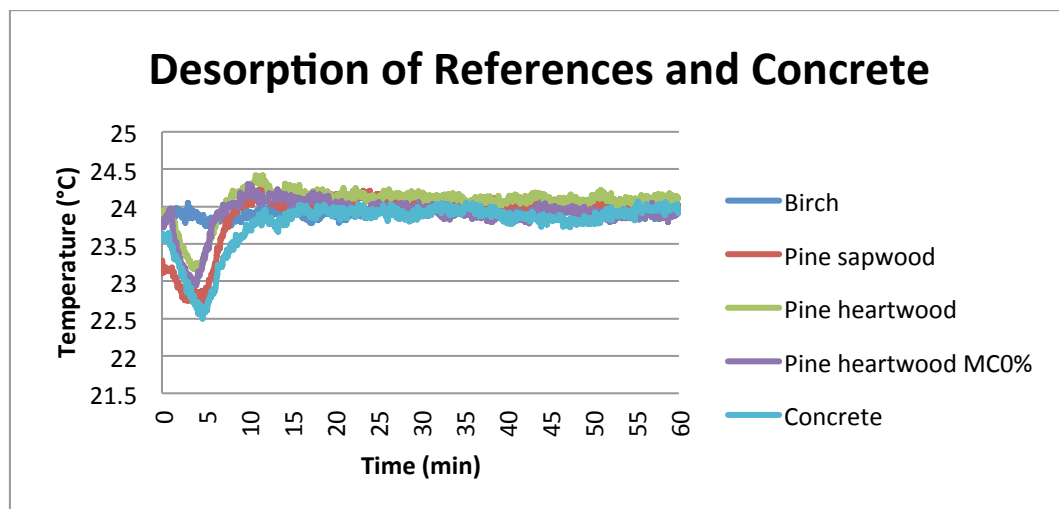


Figure 57 Comparison between temperature changes of the reference samples of birch, pine sapwood and heartwood, dry pine heartwood, and concrete during desorption.

8 Conclusions

The experiment was conducted in different building than the samples were stored and conditioned. The ideal situation would have been that the samples were the same temperature as the climate cabinet where the experiment was run. Still it can be seen in the results that during the colder days the initial temperature of the samples was a bit lower than during the warmer days. Also, the conditions during the transportation of the samples between the buildings were not recorded, thus the effect of the transportation on the temperature change is not certain.

The salt chambers used for the experiment were not the best possible equipment for conditioning the samples, since the RH and temperature in the surrounding environment were unstable. For the future research the experiment should be conducted only in one space and the samples should be conditioned at the same place as the experiment is conducted. Also, the conditions during the experiment should be observed at all times and at same rate as the recording.

The duration of the experiment should be extended so that the samples would reach EMC before initiating desorption. This might produce more comparable results between adsorption and desorption. Also the order between the adsorption and desorption could be the other way around and the experiment could consist of multiple continuous cycles instead of only one where the adsorption and desorption are recorded separately.

One major subject of speculation was the emissivity of the samples. The emissivity of wood varies somewhat between the species, individual trees and also the grain orientations. Further research should be conducted on emissivity values of different wood species, grain orientations and modified wood surfaces.

The samples should be conditioned in the same state before adsorption and desorption. Either all should be open from each surface or one surface open. Also

all the samples should have the same initial MC, and the effect of volume and thickness of the samples should be investigated.

The anisotropic structure of wood causes internal variation and there is also variation between trees, thus the amount of parallel samples should be far greater and the samples should be from different logs.

Transverse surface had clearly the greatest temperature changes at least during adsorption. The temperature rise on the transverse surface of dry pine heartwood was 3.8°C, of birch 2.9°C, and of pine heartwood and sapwood 2.2°C. The decrease in temperature during desorption was 1.35°C for dry pine heartwood 1.24°C for pine sapwood, 1.1°C for birch and 1.05°C for pine heartwood. The transverse surface should be utilised for instance in wall panels or ceilings.

The radial surface had also change in temperature subjected to sorption, but the changes were not as significant as on transverse surface. The temperature rise on the radial of pine heartwood surface was 1.6°C, of birch and pine sapwood 1.7°C, and of dry pine heartwood 2.5°C. The decrease in temperature during desorption of radial pine heartwood surface was 0.7°C, of pine sapwood 0.66°C, of dry pine heartwood 0.58°C, and of birch 0.1°C.

The tangential surface had bit greater temperature changes than the radial surface. The temperature rise of the tangential surface of dry pine heartwood was 2.6°C, pine sapwood 1.8°C, birch 1.26°C and pine heartwood 1.2°C. The temperature of pine heartwood surface decreased during desorption 0.86°C, of dry pine heartwood 0.84°C, of pine sapwood 0.55°C, and of birch 0.14°C. The mixture of tangential and radial wood is commonly used in interior panels and construction materials. The benefits due to thermal comfort are not the greatest, but still it has an impact on the perceived thermal comfort.

Pine sapwood and heartwood had similar temperature changes. Yet the uncertainty whether the samples were clearly heartwood and sapwood remains.

The clarity of the heartwood and sapwood samples can be confirmed by cutting the sapwood near to the bark and heartwood near to the core, and the samples should be small enough to accomplish this.

The initial moisture content had a visible effect on the temperature changes. At least if the surface is completely dry the rise in temperature will be significant.

Concrete is more comparable with the radial and tangential surfaces of wood. The greatest difference or advantage compared to concrete could be achieved with transverse surfaces. The reason for the temperature changes of reference and concrete are unresolved for the time being and this should be investigated in the future. The age, manufacturing method and history of concrete affects the properties of concrete, thus the cause for the temperature change cannot be verified.

The effect of sorption kinetics on heat of sorption should be investigated. The difference of rate of adsorption and desorption during heat of sorption could be valuable information while analysing the phenomenon, and also for the practical applications.

Next it would be interesting to compare the effect of different permeable and impermeable surface treatments and modifications on heat of sorption. Even though the plastic film was impermeable the temperature changes were comparable with the wooden samples, which would indicate that impermeable treatment would not prevent the heat of sorption. Further research should be conducted with the transverse surface and also with rotary peeled wood.

The effect of the temperature change subjected to moisture sorption could be worthwhile in environments with significant humidity variations during the day, for instance the kitchen, bedroom or dressing room.

References

Absetz, I. 1999. Moisture transport and sorption in wood and plywood: theoretical and experimental analysis originating from wood cellular structure. Doctoral Thesis. Helsinki University of Technology Laboratory of Structural Engineering and Building Physics. Espoo, Finland. 190 p. ISBN: 951-22-4642-2.

Agrawal, A. M., Manek, R. V., Kolling, W. M. & Neau, S. H. 2004. Water distribution studies within microcrystalline cellulose and chitosan using differential scanning calorimetry and dynamic vapor sorption analysis. *Journal of pharmaceutical sciences*. Vol. 93:7. pp. 1766–1779.

Akanbi, C. T., Adeyemi, R. S. & Ojo A. 2006. Drying characteristics and sorption isotherm of tomato slices. *Journal of Food Engineering*. Vol. 73:2. pp. 157–163.

Al Hodali, R. 1997. Numerical Simulation of an Agricultural Foodstuffs Drying Unit Using Solar Energy and Adsorption Process. Doctoral Thesis. Université Libre de Bruxells, Belgium. 309 p.

Avramidis, S., & Siau, J. F. 1987. Experiments in nonisothermal diffusion of moisture in wood. *Wood Science and Technology*. Vol. 21:4. pp. 329–334.

Brunauer, S., Emmett, P. H. & Teller, E. 1938. Adsorption of gases in multimolecular layers. *American Chemical Society Journal*. Vol. 60. pp. 309–319.

Brueckner, C., Nore, K. & Nyrud, A. Q. 2012. Investigating latent heat exchange of untreated wood panels. In: 8th meeting of the Northern European Network for Wood Science and Engineering (WSE). Kaunas, Lithuania. September 13th-14th. pp. 70–78.

Bulota, M. 2008. Study on the assessment of moisture content in birch veneer. Master's Thesis. Helsinki University of Technology, Espoo, Finland. 70 +12 p.

Chen, C. 2006. Obtaining the isosteric sorption heat directly by sorption isotherm equations. *Journal of Food Engineering*. Vol. 74:2. pp. 178–185.

Chirife, J. & Iglesias, A. 1992. Estimation of the Precision of Isosteric Heats of Sorption Determined from the Temperature Dependence of Food Isotherms. *Lebensmittel - Wissenschaft + Technologie*. Vol. 25:1. pp. 83–84.

Crank, J. 1975. *The Mathematics of Diffusion*. 2nd edition. Oxford: Clarendon Press. Brunel University Uxbridge. 414 p. ISBN 0-19-853344-6.

Dinwoodie, J.M. 2000. *Timber, it's nature and behaviour*. 2nd edition. New York, USA: London: E & FN Spon with the support of the Centre for Timber Technology and Construction at BRE. 257 p. ISBN 0-419-25550-8.

Engelund, E. T., Thygesen, L. G, Svensson, S. & Hill, C. A. S. 2013. A critical discussion of the physics of wood–water interactions. *Wood Science Technology*. Vol. 47:1. pp. 141–161.

Engineering Toolbox, 2015. Emissivity coefficients of some common materials. [online]. http://www.engineeringtoolbox.com/emissivity-coefficients-d_447.html.

Fagerholm, N-E. 1986. *Termodynamiikka* 479. Tekijä ja Otakustantamo. Gummerus Oy, Jyväskylä. 382 p. ISBN 951-671-327-0.

Falabella, M. C., Aguerre, R. J. & Suárez, C. 1989. Determination of the Heat of Water Vapor Sorption by Means of Electronic Hygrometers. *Lebensmittel - Wissenschaft + Technologie*. Vol. 22. pp. 11–14.

Frandsen, H. L., Svensson, S. & Damkilde, L. 2007. A hysteresis model suitable for numerical simulation of moisture content in wood. *Holzforschung*. Vol. 61. pp. 175–181.

García-Pérez, J. V., Cárcel, J. A., Clemente, G. & Mulet, A. 2008. Water sorption isotherms for lemon peel at different temperatures and isosteric heats. *LWT - Food Science and Technology*. Vol. 41:1. pp. 18–25.

Ghodake, H. M., Goswami, T. K. & Chakraverty, A. 2007. Moisture sorption isotherms, heat of sorption and vaporization of withered leaves, black and green tea. *Journal of Food Engineering*. Vol. 78:3. pp. 827–835.

Gibson, P., Kendrick, C., Rivin, D., Charmchi, M. & Sicuranza, L. 1995. An Automated Dynamic Water Vapor Permeation Test Method. *Journal of Industrial Textiles*. Vol. 24:4. pp. 322–345.

Gibson, P. & Charmchi, M. 1997. The Use of Volume-Averaging Techniques to Predict Temperature Transients Due to Water Vapor Sorption in Hygroscopic Porous Polymer Materials. *Journal of Applied Polymer Science*. Vol. 64:3. pp. 493–505.

Golparvar-Fard, M. & Ham, Y. 2013. Automated Diagnostics and Visualization of Potential Energy Performance Problems in Existing Buildings Using Energy Performance Augmented Reality Models. *Journal of Computing in Civil Engineering*. Vol. 28:1. pp. 17–29.

Gray, W. T. & Finch, F. I. 1971. How accurately can temperature be measured? *Physics Today*. Vol. 24:9. pp. 32–40.

Ham, Y. & Golparvar-Fard, M. 2014. Three-Dimensional Thermography-Based Method for Cost-Benefit Analysis of Energy Efficiency Building Envelope Retrofits. *Journal of Computing in Civil Engineering*.

Hameury, S. 2005. Moisture buffering capacity of heavy timber structures directly exposed to an indoor climate: A numerical study. *Building and Environment*. Vol. 40:10. pp. 1400–1412.

Hellier, C. 2001. Handbook of nondestructive evaluation. McGraw-Hill
U.S. 594 p.

Hill, C. A. S., Forster, S. C., Farahani, M. R. M., Hale, M. D. C., Ormondroyd, G. A. & Williams, G. R. 2005. An investigation of the cell wall micropore blocking as a possible mechanism for the decay resistance of anhydride modified wood. *International Biodeterioration & Biodegradation*. Vol. 55:1. pp. 69–76.

Hill, C. A. S., Norton, A. J. & Newman, G. 2010. The water vapour sorption properties of Sitka spruce determined using a dynamic vapour sorption apparatus. *Wood Science and Technology*. Vol. 44:3. pp. 497–514.

Infradex Oy. 2014. FLIR Exx –series. Infradex Oy. Web. 27. February. 2015. [online]. <http://www.infradex.com/exx.html>

Infrared Thermography. 2015. Emissivity Values for Common Materials. [online]. <http://www.infrared-thermography.com/material-1.htm>

Irvine, T. F. 1993. Advances in heat transfer. London: United Kingdom. Vol. 23. Academic Press. ISBN 0-12-020023-6

Kalamees, T., Korpi, M., Vinha, J. & Kurnitski, J. 2009. The effects of ventilation systems and building fabric on the stability of indoor temperature and humidity in Finnish detached houses. *Building. Environment*. Vol. 44:8. pp. 1643–1650.

Kanda, M., Kawai, T., Kanega, M., Moriwaki, R., Narita, K. & Hagishima, A. 2005. A simple energy balance model for regular building arrays. *Boundary-Layer Meteorology*. Vol. 116:3. pp. 423–443.

Karlsson, M. 2000. Papermaking Part 2, Drying. Jyväskylä, Finland: Gummerus Oy. Fapet Oy. 496 p. Papermaking Science and Technology 9. ISBN 952-5216-09-8.

Khan, M. I. 2002. Factors affecting the thermal properties of concrete and applicability of its prediction models. Building and Environment. Vol 37:6. pp. 607–614.

Kitic, D., Favetto, G. J., Chirife, J. & Resnik, S. L. 1986. Measurements of water activity in the intermediate moisture range with the Novasina Thermoconstanter humidity meter. Lebensmittel- Wissenschaft und – Technologie. Vol. 19. pp. 297–301.

Korsnes, S. K. 2012. Moisture and heat transfer of indoor surfaces. Master's Thesis. Norwegian University of Science and Technology. Trondheim, Norway.

Koumoutsakos, A. & Avramidis, S. 1999. Enthalpy-entropy compensation in water sorption by various wood species. Holz als Roh- und Werkstoff. Vol. 57:5. pp. 379–382.

Künzel, H. M., Kiessl, K. 1996. Calculation of heat and moisture transfer in exposed building components. International Journal of Heat and Mass Transfer. Vol. 40:1. pp. 159–167.

Kwiatkowski, J., Woloszyn, M. & Roux, J-J. 2009. Modelling of hysteresis influence on mass transfer in buildings materials. Building and Environment. Vol. 44:3. pp. 633–642.

Kärkkäinen, M. 2007. Puun rakenne ja ominaisuudet. Hämeenlinna, Suomi: Tekijä ja Metsäkustannus. 468 p. ISBN 978-952-5694-10-9.

López, G., Basterra, L. A., Acuña, L. & Casado M. 2013. Determination of the Emissivity of Wood for Inspection by Infrared Thermography. *Journal of Nondestructive Evaluation*. Vol. 32:2. pp. 172–176.

McCullough, E. A., Kwon, M. & Shim, H. 2003. A comparison of standard methods for measuring water vapour permeability of fabrics. *Measurement Science and Technology*. Vol. 14:8. pp. 1402–1408.

Meola C., G. M. Carlomagno. 2006. Application of infrared thermography to adhesion science. *Journal of Adhesion Science Technology*. Vol 20:7. pp. 589–632.

Mohamed, L., Kouhila, M., Jamali, A., Lahsasni, S. & Mahrouz, M. 2005. Moisture sorption isotherms and heat sorption of bitter orange leaves (*Citrus aurantium*). *Journal of Food Engineering*. Vol. 67:4. pp. 491–498.

Mulet, A., Garcia-Reverter, J., Sanjuan, N. & Bon, J. 1999. Sorption isosteric heat determination by thermal analysis and sorption isotherms. *Journal of Food Science*. Vol. 64. pp. 64–68.

Ojanen, T. & Salonvaara, M. 2004. Comparison of measured and simulated moisture buffering results. In: Paper to IEA ECBCS Annex 41, Working meeting. Glasgow, Scotland. 27th-29th of October 2004. 12 p.

Olek, W., Weres, J., & Guzenda, R. 2003. Effects of thermal conductivity data on accuracy of modelling heat transfer in wood. *Holzforschung*. Vol. 57:3. pp. 317–325.

Orlove, G. 2014. Easy IR Window Transmission Measurement. Infrared Training Center, FLIR Systems. Technincal Publication. 4 p.

Padfield, T. 1998. The role of absorbent building materials in moderating changes of relative humidity. Ph.D. Thesis. Department of Structural Engineering and Materials. Lyngby, Technical University of Denmark. 150 p.

Rode, C. & Grau, K. 2008. Moisture buffering and its consequence in whole building hygrothermal modeling. *Journal of Building physics*. Vol. 31:4. pp. 333–360.

Roth, K., Westphalen, D., Feng, M., Llana, P. & Quartararo, L. 2005. The energy impact of commercial building controls and performance diagnostics: Market characterization, energy impact of building faults and energy savings potential. TIAX LCC Technical Rep., TIAX LCC, Lexington, MA. US Department of Energy. 412 p.

Siau, J. F. 1984. Transport processes in wood. *Transport processes in wood*. 245 p.

Siikanen, U. 2008. Puurakentaminen. 6th edition. Tampere, Finland: Rakennustieto Oy. 332 p. ISBN 978-951-682-862-9.

Simonson, C.J. & Salonvaara, M. & Ojanen, T. 2001. Improving indoor climate and comfort with wooden structures. Espoo: VTT Publications 431. 298 p. ISBN 951-38-5846-4.

Simonson, C. J. & Salonvaara, M. & Ojanen, T. 2002. The effect of structures on indoor humidity – possibility to improve comfort and perceived air quality. *Indoor Air*. Vol. 12:4. pp. 243–251.

Sinija, V. R. & Mishra H. N. 2008. Moisture sorption isotherms and heat sorption of instant (soluble) green tea powder and green tea granules. *Journal of Food Engineering*. Vol. 86:4. pp. 494–500.

Sjöström, E. 1993. Wood Chemistry: Fundamentals and Applications. 2nd ed. San Diego: Academic Press. 292 p. ISBN-10: 0-12-647481-8.

Skaar, C. 1988. Wood-water relations: Moisture Sorption Thermodynamics. pp. 53–72. Berlin: Springer. 283 p. ISBN 3-540-19258-1 710.

Stamm, A. J. & Loughborough, W. K. 1934. Thermodynamics of the Swelling of Wood. J. Phys. Chem. Vol. 39:1. pp. 121–132.

Swedish Energy Agency. 2010. Energy in Sweden facts and figures 2010. Report ET2010:46. Stockholm, Sweden.

Tilastokeskus. 2015. Asumisen energiankulutus. ISSN=2323-3273. Tilastokeskus, Helsinki. [online]. <http://www.stat.fi/til/asen/index.html>

Water Activity. 2013. Theory: Water activity. [online]. <http://www.wateractivity.org/>.

Wood Handbook. 2000. Wood Handbook – Wood as an engineering material. University Press of the Pacific, Honolulu, Hawaii. Forest Products Laboratory, Forest Service, U.S. Department of Agriculture. ISBN 0-89875-082-2.

Wood Science. 2014. Wood Science: Structure of wood: Basic knowledge: Macroscopic structure of wood. [online]. <https://is.mendelu.cz/eknihovna/opory/index.pl?cast=19203>.

Wunderlich, B. 1990. Thermal Analysis. The University of Tennessee at Knoxville, Knoxville, Tennessee and Oak Ridge National Laboratory, Oak Ridge, Tennessee. Academic Press, Inc. Harcourt Brace Janovich, Publishers. 450 p. ISBN 0-12-765605-7.

Yang, X. & Fazio, P. & Ge, H. & Rao, J. 2012. Evaluation of moisture buffering capacity of interior surface materials and furniture in a full-scale experimental investigation. *Building and Environment*. Vol. 47. pp. 188–196.

Yazdani, M., Sazandehchi, P., Azizi, M. & Ghobadi, P. 2006. Moisture sorption isotherms and isosteric heat for pistachio. *European Food Research and Technology*. Vol. 223:5. pp. 577–584.

List of Appendices

Appendix 1 Equations and abbreviations for the Appendices 2-11

Appendix 2 Masses, volumes, densities and moisture contents of birch samples

Appendix 3 Masses, volumes, densities and moisture contents of pine sapwood samples

Appendix 4 Masses, volumes, densities and moisture contents of pine heartwood samples

Appendix 5 Masses, volumes, densities and moisture contents of dry pine heartwood samples

Appendix 6 Masses, volumes, densities and moisture contents of birch and concrete samples

Appendix 7 Thermographs, condition graphs and temperature changes of birch samples

Appendix 8 Thermographs, condition graphs and temperature changes of pine sapwood samples

Appendix 9 Thermographs, condition graphs and temperature changes of pine heartwood samples

Appendix 10 Thermographs, condition graphs and temperature changes of dry pine heartwood samples

Appendix 11 Thermographs, condition graphs and temperature changes of birch and concrete samples

Appendix 1 (1/3)

Equations and abbreviations for the Appendices 2-11

V_{od}	oven dry volume of the sample in cubic centimetres
ρ_{od}	oven dry density of the sample in kilograms per cubic metre
$m_{bt,RH32\%}$	mass of the sample before adsorption test in RH 32% with aluminium tape, or plastic foil in case of reference, in grams

$$MC_{bt,RH32\%} \% = \frac{m_{RH32\%} - m_{od}}{m_{od}} \times 100\%$$

$MC_{bt,RH32\%}$	moisture content of the sample after one week conditioning before the adsorption test in RH 32% as percentage
$m_{RH32\%}$	mass of the sample after conditioning in RH 32% for one week in grams
m_{od}	oven dry mass of the sample in grams

$$MC_{at,RH80\%} \% = \frac{m_{at,RH80\%} - m_{od} - m_{tape}}{m_{od}} \times 100\%$$

$MC_{at,RH80\%}$	moisture content of the sample after the adsorption test in RH 80% as percentage
$m_{at,RH80\%}$	mass of the sample after adsorption test in RH 80% with aluminium tape, or plastic foil in case of reference, in grams
m_{tape}	mass of the tape in the sample in grams

Appendix 1 (2/3)

Equations and abbreviations for the Appendices 2-6

$$MC_{bt,RH80\%} \% = \frac{m_{bt,RH80\%} - m_{od} - m_{tape}}{m_{od}} \times 100\%$$

$MC_{bt,RH80\%}$ moisture content of the sample after conditioning for one week and before the desorption test in RH 80% as percentage

$m_{bt,RH80\%}$ mass of the sample after one week conditioning and before desorption test in RH 80% with aluminium tape, or plastic foil in case of reference, in grams

$$MC_{at,RH32\%} \% = \frac{m_{at,RH32\%} - m_{od} - m_{tape}}{m_{od}} \times 100\%$$

$MC_{at,RH32\%}$ moisture content of the sample after desorption test in RH 32% as percentage

$m_{at,RH32\%}$ mass of the sample after desorption test in RH 80% with aluminium tape, or plastic foil in case of reference, in grams

$$MC_{ads} \% = MC_{at,RH80\%} - MC_{bt,RH32\%}$$

MC_{ads} change in moisture content during the adsorption from RH 32% to RH 80%

Appendix 1 (3/3)

Equations and abbreviations for the Appendices 2-6

$$MC_{des} \% = MC_{at,RH32\%} - MC_{bt,RH80\%}$$

MC_{des} change in moisture content during the desorption from
RH 80% to RH 32%

Appendix 2 (1/3)

Masses, volumes, densities and moisture contents of birch samples

Table 1 Oven dry masses, volumes and densities of birch samples of groups 1-5 and the average values.

	m_{od} (g)	V_{od} (cm ³)	ρ_{od} (kg/m ³)
Group 1			
<i>B, transverse</i>	7.333	11.34	646.8
<i>B, radial</i>	7.391	11.29	654.8
<i>B, tangential</i>	7.153	11.44	625.5
<i>B, reference</i>	7.223	11.44	631.6
Group 2			
<i>B, transverse</i>	6.316	11.74	537.9
<i>B, radial</i>	7.809	11.39	685.8
<i>B, tangential</i>	6.916	11.34	609.9
<i>B, reference</i>	7.239	11.64	622.0
Group 3			
<i>B, transverse</i>	6.580	11.69	562.8
<i>B, radial</i>	7.685	11.48	669.4
<i>B, tangential</i>	7.019	11.34	619.1
<i>B, reference</i>	7.784	11.43	680.9
Group 4			
<i>B, transverse</i>	6.538	11.69	559.2
<i>B, radial</i>	7.667	11.53	664.8
<i>B, tangential</i>	7.123	11.44	622.7
<i>B, reference</i>	7.672	11.39	673.5
Group 5			
<i>B, transverse</i>	6.328	11.74	539.0
<i>B, radial</i>	7.856	11.48	684.1
<i>B, tangential</i>	7.372	11.24	656.0
<i>B, reference</i>	6.937	11.29	614.6
Average			
<i>B, transverse</i>	6.619	11.64	568.64
<i>B, radial</i>	7.682	11.43	671.81
<i>B, tangential</i>	7.117	11.36	626.57
<i>B, reference</i>	7.371	11.44	644.46

Appendix 2 (2/3)

Masses, volumes, densities and moisture contents of birch samples

Table 2 Masses of birch samples in groups 1-5 and the average values after conditioning in RH 32% without aluminum tape or plastic foil, before the adsorption test, after adsorption test, before desorption test, after desorption test and the mass of the aluminum tape or, in case of reference, plastic foil.

	$m_{RH32\%}$ (g)	$m_{bt,RH32\%}$ (g)	$m_{at,RH80\%}$ (g)	$m_{bt,RH80\%}$ (g)	$m_{at,RH32\%}$ (g)	m_{tape} (g)
Group 1						
<i>B, transverse</i>	7.678	8.286	8.336	8.935	8.873	0.608
<i>B, radial</i>	7.753	8.288	8.309	8.564	8.541	0.535
<i>B, tangential</i>	7.489	8.315	8.331	8.510	8.491	0.826
<i>B, reference</i>	7.568	7.938	7.939	8.058	8.056	0.370
Group 2						
<i>B, transverse</i>	6.624	7.251	7.301	7.841	7.781	0.627
<i>B, radial</i>	8.186	8.894	8.905	9.073	9.059	0.708
<i>B, tangential</i>	7.25	7.855	7.868	8.090	8.074	0.605
<i>B, reference</i>	7.587	7.972	7.972	8.073	8.070	0.385
Group 3						
<i>B, transverse</i>	6.905	7.518	7.561	8.109	8.057	0.613
<i>B, radial</i>	8.059	8.652	8.669	8.850	8.841	0.593
<i>B, tangential</i>	7.363	7.946	7.956	8.140	8.128	0.583
<i>B, reference</i>	8.157	8.499	8.501	8.621	8.624	0.342
Group 4						
<i>B, transverse</i>	6.850	7.488	7.530	8.071	8.017	0.638
<i>B, radial</i>	8.093	8.545	8.553	8.721	8.712	0.452
<i>B, tangential</i>	7.471	8.009	8.023	8.203	8.191	0.538
<i>B, reference</i>	8.029	8.415	8.413	8.472	8.474	0.386
Group 5						
<i>B, transverse</i>	6.634	7.282	7.330	7.862	7.809	0.648
<i>B, radial</i>	8.227	8.953	8.960	9.105	9.101	0.726
<i>B, tangential</i>	7.722	8.420	8.430	8.597	8.590	0.698
<i>B, reference</i>	7.262	7.795	7.796	7.855	7.856	0.533
Average						
<i>B, transverse</i>	6.938	7.565	7.612	8.164	8.107	0.627
<i>B, radial</i>	8.064	8.666	8.679	8.863	8.851	0.603
<i>B, tangential</i>	7.459	8.109	8.122	8.308	8.295	0.650
<i>B, reference</i>	7.721	8.124	8.124	8.216	8.216	0.403

Appendix 2 (3/3)

Masses, volumes, densities and moisture contents of birch samples

Table 3 Moisture contents of the birch samples groups1-5 and average values before the adsorption test, after the adsorption test, the change in MC during the adsorption, MC before the desorption test, after the desorption test and the change in MC during the desorption. The equations for the moisture contents are presented in Appendix 1.

	MC _{bt,RH32%} (%)	MC _{at,RH80%} (%)	MC _{ads} (%)	MC _{bt,RH80%} (%)	MC _{at,RH32%} (%)	MC _{des} (%)
Group 1						
<i>B, transverse</i>	4.70	5.39	0.68	13.555	12.710	-0.85
<i>B, radial</i>	4.90	5.18	0.28	8.632	8.321	-0.31
<i>B, tangential</i>	4.70	4.92	0.22	7.423	7.158	-0.27
<i>B, reference</i>	4.78	4.79	0.01	6.438	6.410	-0.03
Group 2						
<i>B, transverse</i>	4.88	5.67	0.79	14.218	13.268	-0.95
<i>B, radial</i>	4.83	4.97	0.14	7.120	6.941	-0.18
<i>B, tangential</i>	4.83	5.02	0.19	8.227	7.996	-0.23
<i>B, reference</i>	4.81	4.81	0.00	6.203	6.161	-0.04
Group 3						
<i>B, transverse</i>	4.94	5.59	0.65	13.921	13.131	-0.79
<i>B, radial</i>	4.87	5.09	0.22	7.443	7.326	-0.12
<i>B, tangential</i>	4.90	5.04	0.14	7.665	7.494	-0.17
<i>B, reference</i>	4.79	4.82	0.03	6.359	6.398	0.04
Group 4						
<i>B, transverse</i>	4.77	5.41	0.64	13.689	12.863	-0.83
<i>B, radial</i>	5.56	5.66	0.10	7.852	7.734	-0.12
<i>B, tangential</i>	4.89	5.08	0.20	7.609	7.441	-0.17
<i>B, reference</i>	4.65	4.63	-0.03	5.396	5.422	0.03
Group 5						
<i>B, transverse</i>	4.84	5.59	0.76	14.001	13.164	-0.84
<i>B, radial</i>	4.72	4.81	0.09	6.657	6.606	-0.05
<i>B, tangential</i>	4.75	4.88	0.14	7.149	7.054	-0.09
<i>B, reference</i>	4.69	4.70	0.01	5.550	5.564	0.01
Average						
<i>B, transverse</i>	4.82	5.53	0.70	13.87	13.02	-0.85
<i>B, radial</i>	4.97	5.14	0.17	7.53	7.37	-0.15
<i>B, tangential</i>	4.81	4.99	0.18	7.61	7.42	-0.19
<i>B, reference</i>	4.74	4.75	0.01	5.99	5.99	0.00

Appendix 3 (1/3)

Masses, volumes, densities and moisture contents of pine sapwood samples

Table 1 Oven dry masses, volumes and densities of pine sapwood samples of groups 1-5 and the average values.

	m_{od} (g)	V_{od} (cm ³)	ρ_{od} (kg/m ³)
Group 1			
<i>PS, transverse</i>	5.482	10.89	503.4
<i>PS, radial</i>	5.944	11.18	531.6
<i>PS, tangential</i>	5.549	10.64	521.4
<i>PS, reference</i>	5.446	10.45	521.0
Group 2			
<i>PS, transverse</i>	5.636	10.08	559.3
<i>PS, radial</i>	5.275	10.17	518.7
<i>PS, tangential</i>	5.878	10.45	562.5
<i>PS, reference</i>	5.565	10.79	515.8
Group 3			
<i>PS, transverse</i>	5.819	11.24	517.7
<i>PS, radial</i>	5.318	10.60	501.8
<i>PS, tangential</i>	5.556	10.89	510.3
<i>PS, reference</i>	5.640	11.03	511.1
Group 4			
<i>PS, transverse</i>	5.716	10.17	562.0
<i>PS, radial</i>	5.921	10.45	566.6
<i>PS, tangential</i>	5.308	10.26	517.2
<i>PS, reference</i>	5.961	11.19	532.8
Group 5			
<i>PS, transverse</i>	5.745	570.1	0.565
<i>PS, radial</i>	5.910	535.7	0.476
<i>PS, tangential</i>	5.528	519.4	0.488
<i>PS, reference</i>	5.848	513.4	0.436
Average			
<i>PS, transverse</i>	5.680	10.48	541.73
<i>PS, radial</i>	5.674	10.68	531.04
<i>PS, tangential</i>	5.564	10.58	526.00
<i>PS, reference</i>	5.692	10.97	518.91

Appendix 3 (2/3)

Masses, volumes, densities and moisture contents of pine sapwood samples

Table 2 Masses of pine sapwood samples in groups 1-5 and the average values after conditioning in RH 32% without aluminum tape or plastic foil, before the adsorption test, after adsorption test, before desorption test, after desorption test and the mass of the aluminum tape or, in case of reference, plastic foil.

	$m_{RH32\%}$ (g)	$m_{bt,RH32\%}$ (g)	$m_{at,RH80\%}$ (g)	$m_{bt,RH80\%}$ (g)	$m_{at,RH32\%}$ (g)	m_{tape} (g)
Group 1						
<i>PS, transverse</i>	5.757	6.425	6.466	6.850	6.805	0.668
<i>PS, radial</i>	6.238	6.765	6.779	7.009	6.993	0.527
<i>PS, tangential</i>	5.832	6.382	6.396	6.609	6.594	0.550
<i>PS, reference</i>	5.718	6.276	6.281	6.331	6.329	0.558
Group 2						
<i>PS, transverse</i>	5.908	6.385	6.424	6.812	6.762	0.477
<i>PS, radial</i>	5.543	6.003	6.019	6.234	6.217	0.460
<i>PS, tangential</i>	6.170	6.745	6.759	6.963	6.945	0.575
<i>PS, reference</i>	5.825	6.149	6.152	6.214	6.214	0.324
Group 3						
<i>PS, transverse</i>	6.102	6.607	6.643	7.095	7.017	0.505
<i>PS, radial</i>	5.589	6.033	6.047	6.272	6.256	0.444
<i>PS, tangential</i>	5.836	6.378	6.389	6.584	6.570	0.542
<i>PS, reference</i>	5.920	6.187	6.190	6.255	6.254	0.267
Group 4						
<i>PS, transverse</i>	5.990	6.496	6.530	6.930	6.883	0.506
<i>PS, radial</i>	6.212	6.674	6.688	6.929	6.913	0.462
<i>PS, tangential</i>	5.577	6.008	6.021	6.232	6.218	0.431
<i>PS, reference</i>	6.251	6.571	6.571	6.643	6.644	0.320
Group 5						
<i>PS, transverse</i>	6.029	6.594	6.626	7.029	6.982	0.565
<i>PS, radial</i>	6.204	6.680	6.690	6.940	6.924	0.476
<i>PS, tangential</i>	5.803	6.291	6.303	6.500	6.487	0.488
<i>PS, reference</i>	6.096	6.532	6.534	6.604	6.603	0.436
Average						
<i>PS, transverse</i>	5.957	6.501	6.538	6.943	6.890	0.544
<i>PS, radial</i>	5.957	6.431	6.445	6.677	6.661	0.474
<i>PS, tangential</i>	5.844	6.361	6.374	6.578	6.563	0.517
<i>PS, reference</i>	5.962	6.343	6.346	6.409	6.409	0.381

Appendix 3 (3/3)

Masses, volumes, densities and moisture contents of pine sapwood samples

Table 3 Moisture contents of the pine sapwood samples groups1-5 and average values before the adsorption test, after the adsorption test, the change in MC during the adsorption, MC before the desorption test, after the desorption test and the change in MC during the desorption. The equations for the moisture contents are presented in Appendix 1.

	MC _{bt,RH32%} (%)	MC _{at,RH80%} (%)	MC _{ads} (%)	MC _{bt,RH80%} (%)	MC _{at,RH32%} (%)	MC _{des} (%)
Group 1						
<i>PS, transverse</i>	5.02	5.76	0.75	12.77	11.95	-0.82
<i>PS, radial</i>	4.95	5.18	0.24	9.05	8.78	-0.27
<i>PS, tangential</i>	5.10	5.35	0.25	9.19	8.92	-0.27
<i>PS, reference</i>	4.99	5.09	0.09	6.00	5.97	-0.04
Group 2						
<i>PS, transverse</i>	4.83	5.52	0.69	12.40	11.52	-0.89
<i>PS, radial</i>	5.08	5.38	0.30	9.46	9.14	-0.32
<i>PS, tangential</i>	4.97	5.21	0.24	8.68	8.37	-0.31
<i>PS, reference</i>	4.67	4.73	0.05	5.84	5.84	0.00
Group 3						
<i>PS, transverse</i>	4.86	5.48	0.62	13.25	11.91	-1.34
<i>PS, radial</i>	5.10	5.36	0.26	9.59	9.29	-0.30
<i>PS, tangential</i>	5.04	5.24	0.20	8.75	8.50	-0.25
<i>PS, reference</i>	4.96	5.02	0.05	6.17	6.15	-0.02
Group 4						
<i>PS, transverse</i>	4.79	5.39	0.59	12.39	11.56	-0.82
<i>PS, radial</i>	4.91	5.15	0.24	9.22	8.95	-0.27
<i>PS, tangential</i>	5.07	5.31	0.24	9.29	9.02	-0.26
<i>PS, reference</i>	4.86	4.86	0.00	6.07	6.09	0.02
Group 5						
<i>PS, transverse</i>	4.94	5.50	0.56	12.52	11.70	-0.82
<i>PS, radial</i>	4.97	5.14	0.17	9.37	9.10	-0.27
<i>PS, tangential</i>	4.97	5.19	0.22	8.76	8.52	-0.24
<i>PS, reference</i>	4.24	4.27	0.03	5.47	5.45	-0.02
Average						
<i>PS, transverse</i>	4.89	5.53	0.64	12.67	11.73	-0.94
<i>PS, radial</i>	5.00	5.24	0.24	9.33	9.05	-0.29
<i>PS, tangential</i>	5.03	5.26	0.23	8.93	8.66	-0.27
<i>PS, reference</i>	4.74	4.79	0.05	5.91	5.90	-0.01

Appendix 4 (1/3)

Masses, volumes, densities and moisture contents of pine heartwood samples

Table 1 Oven dry masses, volumes and densities of pine heartwood samples of groups 1-5 and the average values.

	m_{od} (g)	V_{od} (cm ³)	ρ_{od} (kg/m ³)
Group 1			
<i>PH, transverse</i>	6.253	11.39	549.0
<i>PH, radial</i>	6.070	11.34	535.3
<i>PH, tangential</i>	5.552	11.49	483.1
<i>PH, reference</i>	5.484	10.45	524.9
Group 2			
<i>PH, transverse</i>	6.269	11.39	550.4
<i>PH, radial</i>	6.557	11.44	573.1
<i>PH, tangential</i>	5.923	11.14	531.7
<i>PH, reference</i>	5.306	11.24	472.1
Group 3			
<i>PH, transverse</i>	6.035	10.89	554.4
<i>PH, radial</i>	5.949	11.44	520.0
<i>PH, tangential</i>	6.063	11.29	537.1
<i>PH, reference</i>	5.829	11.95	487.6
Group 4			
<i>PH, transverse</i>	5.741	11.44	501.8
<i>PH, radial</i>	5.335	11.70	456.2
<i>PH, tangential</i>	5.784	11.29	512.3
<i>PH, reference</i>	6.027	11.24	536.4
Group 5			
<i>PH, transverse</i>	6.054	11.34	533.9
<i>PH, radial</i>	5.336	11.49	464.3
<i>PH, tangential</i>	4.996	11.44	436.7
<i>PH, reference</i>	6.248	11.44	546.1
Average			
<i>PH, transverse</i>	6.070	11.29	537.7
<i>PH, radial</i>	5.849	11.48	509.4
<i>PH, tangential</i>	5.664	11.32	500.3
<i>PH, reference</i>	5.779	11.23	514.7

Appendix 4 (2/3)

Masses, volumes, densities and moisture contents of pine heartwood samples

Table 2 Masses of pine heartwood samples in groups 1-5 and the average values after conditioning in RH 32% without aluminum tape or plastic foil, before the adsorption test, after adsorption test, before desorption test, after desorption test and the mass of the aluminum tape or, in case of reference, plastic foil.

	$m_{RH32\%}$ (g)	$m_{bt,RH32\%}$ (g)	$m_{at,RH80\%}$ (g)	$m_{bt,RH80\%}$ (g)	$m_{at,RH32\%}$ (g)	m_{tape} (g)
Group 1						
<i>PH, transverse</i>	6.548	7.158	7.190	7.603	7.552	0.610
<i>PH, radial</i>	6.362	6.947	6.958	7.139	7.124	0.585
<i>PH, tangential</i>	5.817	6.261	6.271	6.439	6.429	0.444
<i>PH, reference</i>	5.750	6.202	6.206	6.272	6.274	0.452
Group 2						
<i>PH, transverse</i>	6.550	7.034	7.067	7.459	7.414	0.484
<i>PH, radial</i>	6.871	7.366	7.377	7.538	7.525	0.495
<i>PH, tangential</i>	6.209	6.662	6.676	6.867	6.854	0.453
<i>PH, reference</i>	5.556	5.936	5.943	5.989	5.990	0.380
Group 3						
<i>PH, transverse</i>	6.318	6.857	6.887	7.285	7.237	0.539
<i>PH, radial</i>	6.233	6.722	6.732	6.885	6.873	0.489
<i>PH, tangential</i>	6.354	7.059	7.068	7.230	7.215	0.705
<i>PH, reference</i>	6.104	6.457	6.462	6.515	6.514	0.353
Group 4						
<i>PH, transverse</i>	6.008	6.573	6.613	6.989	6.934	0.565
<i>PH, radial</i>	5.582	6.081	6.098	6.262	6.251	0.499
<i>PH, tangential</i>	6.059	6.573	6.585	6.770	6.758	0.514
<i>PH, reference</i>	6.306	6.651	6.656	6.720	6.721	0.345
Group 5						
<i>PH, transverse</i>	6.336	6.830	6.866	7.265	7.216	0.494
<i>PH, radial</i>	5.590	6.081	6.099	6.258	6.249	0.491
<i>PH, tangential</i>	5.230	5.746	5.766	5.960	5.949	0.516
<i>PH, reference</i>	6.532	6.893	6.898	6.967	6.967	0.361
Average						
<i>PH, transverse</i>	6.352	6.890	6.925	7.320	7.271	0.538
<i>PH, radial</i>	6.128	6.639	6.653	6.816	6.804	0.512
<i>PH, tangential</i>	5.934	6.460	6.473	6.653	6.641	0.526
<i>PH, reference</i>	6.050	6.428	6.433	6.493	6.493	0.378

Appendix 4 (3/3)

Masses, volumes, densities and moisture contents of pine heartwood samples

Table 3 Moisture contents of the pine heartwood samples groups1-5 and average values before the adsorption test, after the adsorption test, the change in MC during the adsorption, MC before the desorption test, after the desorption test and the change in MC during the desorption. The equations for the moisture contents are presented in Appendix 1.

	MC _{bt,RH32%} (%)	MC _{at,RH80%} (%)	MC _{ads} (%)	MC _{bt,RH80%} (%)	MC _{at,RH32%} (%)	MC _{des} (%)
Group 1						
<i>PH, transverse</i>	4.72	5.23	0.51	11.83	11.02	-0.82
<i>PH, radial</i>	4.81	4.99	0.18	7.97	7.73	-0.25
<i>PH, tangential</i>	4.77	4.95	0.18	7.98	7.80	-0.18
<i>PH, reference</i>	4.85	4.92	0.07	6.13	6.16	0.04
Group 2						
<i>PH, transverse</i>	4.48	5.01	0.53	11.26	10.54	-0.72
<i>PH, radial</i>	4.79	4.96	0.17	7.41	7.21	-0.20
<i>PH, tangential</i>	4.83	5.07	0.24	8.29	8.07	-0.22
<i>PH, reference</i>	4.71	4.84	0.13	5.71	5.73	0.02
Group 3						
<i>PH, transverse</i>	4.69	5.19	0.50	11.78	10.99	-0.80
<i>PH, radial</i>	4.77	4.94	0.17	7.51	7.31	-0.20
<i>PH, tangential</i>	4.80	4.95	0.15	7.62	7.37	-0.25
<i>PH, reference</i>	4.72	4.80	0.09	5.71	5.70	-0.02
Group 4						
<i>PH, transverse</i>	4.65	5.35	0.70	11.90	10.94	-0.96
<i>PH, radial</i>	4.63	4.95	0.32	8.02	7.82	-0.21
<i>PH, tangential</i>	4.75	4.96	0.21	8.16	7.95	-0.21
<i>PH, reference</i>	4.63	4.71	0.08	5.77	5.79	0.02
Group 5						
<i>PH, transverse</i>	4.66	5.25	0.59	11.84	11.03	-0.81
<i>PH, radial</i>	4.76	5.10	0.34	8.08	7.91	-0.17
<i>PH, tangential</i>	4.68	5.08	0.40	8.97	8.75	-0.22
<i>PH, reference</i>	4.55	4.63	0.08	5.73	5.73	0.00
Average						
<i>PH, transverse</i>	4.64	5.20	0.56	11.72	10.90	-0.82
<i>PH, radial</i>	4.76	4.99	0.23	7.78	7.58	-0.21
<i>PH, tangential</i>	4.77	5.00	0.23	8.18	7.96	-0.22
<i>PH, reference</i>	4.69	4.78	0.09	5.81	5.82	0.01

Appendix 5 (1/3)

Masses, volumes, densities and moisture contents of dry pine heartwood samplesA

Table 1 Oven dry masses, volumes and densities of dry pine heartwood samples of groups 1-5 and the average values.

	m_{od} (g)	V_{od} (cm ³)	ρ_{od} (kg/m ³)
Group 1			
<i>PH_{dry}, transverse</i>	6.038	11.14	542.1
<i>PH_{dry}, radial</i>	5.955	11.14	534.7
<i>PH_{dry}, tangential</i>	6.233	11.74	530.8
<i>PH_{dry}, reference</i>	5.760	10.49	548.9
Group 2			
<i>PH_{dry}, transverse</i>	5.804	10.84	535.6
<i>PH_{dry}, radial</i>	5.611	10.45	537.0
<i>PH_{dry}, tangential</i>	5.848	11.04	529.8
<i>PH_{dry}, reference</i>	5.142	11.59	443.5
Group 3			
<i>PH_{dry}, transverse</i>	5.829	10.94	533.1
<i>PH_{dry}, radial</i>	6.381	11.44	557.8
<i>PH_{dry}, tangential</i>	5.890	11.03	533.8
<i>PH_{dry}, reference</i>	5.026	11.69	429.8
Group 4			
<i>PH_{dry}, transverse</i>	5.871	10.88	539.4
<i>PH_{dry}, radial</i>	5.713	10.98	520.2
<i>PH_{dry}, tangential</i>	5.342	11.14	479.6
<i>PH_{dry}, reference</i>	6.899	11.34	608.4
Group 5			
<i>PH_{dry}, transverse</i>	6.087	11.24	541.6
<i>PH_{dry}, radial</i>	5.648	10.36	545.4
<i>PH_{dry}, tangential</i>	5.396	11.39	473.8
<i>PH_{dry}, reference</i>	6.036	11.03	547.0
Average			
<i>PH_{dry}, transverse</i>	5.926	11.01	538.4
<i>PH_{dry}, radial</i>	5.862	10.87	539.2
<i>PH_{dry}, tangential</i>	5.742	11.27	509.5
<i>PH_{dry}, reference</i>	5.773	11.23	514.1

Appendix 5 (2/3)

Masses, volumes, densities and moisture contents of dry pine heartwood samplesA

Table 2 Masses of dry pine heartwood samples in groups 1-5 and the average values after conditioning in RH 32% without aluminum tape or plastic foil, before the adsorption test, after adsorption test, before desorption test, after desorption test and the mass of the aluminum tape or, in case of reference, plastic foil.

	$m_{bt,RH0\%}$ (g)	$m_{at,RH80\%}$ (g)	$m_{bt,RH80\%}$ (g)	$m_{at,RH32\%}$ (g)	m_{tape} (g)
Group 1					
<i>PH_{dry}, transverse</i>	6.611	6.68	7.322	7.273	0.573
<i>PH_{dry}, radial</i>	6.647	6.67	6.972	6.953	0.692
<i>PH_{dry}, tangential</i>	7.127	7.148	7.442	7.426	0.894
<i>PH_{dry}, reference</i>	6.31	6.316	6.428	6.432	0.550
Group 2					
<i>PH_{dry}, transverse</i>	6.439	6.504	7.121	7.075	0.635
<i>PH_{dry}, radial</i>	6.155	6.177	6.558	6.544	0.544
<i>PH_{dry}, tangential</i>	6.396	6.418	6.883	6.87	0.548
<i>PH_{dry}, reference</i>	5.525	5.529	5.653	5.658	0.383
Group 3					
<i>PH_{dry}, transverse</i>	6.618	6.696	7.313	7.259	0.789
<i>PH_{dry}, radial</i>	7.105	7.126	7.542	7.527	0.724
<i>PH_{dry}, tangential</i>	6.525	6.55	6.865	6.851	0.635
<i>PH_{dry}, reference</i>	5.522	5.527	5.785	5.788	0.496
Group 4					
<i>PH_{dry}, transverse</i>	6.41	6.494	7.105	7.051	0.539
<i>PH_{dry}, radial</i>	6.329	6.349	6.617	6.607	0.616
<i>PH_{dry}, tangential</i>	6.112	6.133	6.447	6.436	0.770
<i>PH_{dry}, reference</i>	7.286	7.292	7.662	7.664	0.387
Group 5					
<i>PH_{dry}, transverse</i>	6.626	6.701	7.349	7.297	0.539
<i>PH_{dry}, radial</i>	6.22	6.249	6.569	6.558	0.572
<i>PH_{dry}, tangential</i>	6.079	6.106	6.448	6.437	0.683
<i>PH_{dry}, reference</i>	6.474	6.479	6.745	6.749	0.438
Average					
<i>PH_{dry}, transverse</i>	6.541	6.615	7.242	7.191	0.615
<i>PH_{dry}, radial</i>	6.491	6.514	6.852	6.838	0.630
<i>PH_{dry}, tangential</i>	6.448	6.471	6.817	6.804	0.706
<i>PH_{dry}, reference</i>	6.223	6.229	6.455	6.458	0.451

Appendix 5 (3/3)

Masses, volumes, densities and moisture contents of dry pine heartwood samples

Table 3 Moisture contents of the dry pine heartwood samples groups1-5 and average values before the adsorption test, after the adsorption test, the change in MC during the adsorption, MC before the desorption test, after the desorption test and the change in MC during the desorption. The equations for the moisture contents are presented in Appendix 1.

	MC _{ads} (%)	MC _{bt,RH80%} (%)	MC _{at,RH32%} (%)	MC _{des} (%)
Group 1				
<i>PH_{dry}, transverse</i>	1.14	11.78	10.96	-0.81
<i>PH_{dry}, radial</i>	0.39	5.46	5.14	-0.32
<i>PH_{dry}, tangential</i>	0.34	5.05	4.80	-0.26
<i>PH_{dry}, reference</i>	0.10	2.05	2.12	0.07
Group 2				
<i>PH_{dry}, transverse</i>	1.12	11.75	10.96	-0.79
<i>PH_{dry}, radial</i>	0.39	7.18	6.93	-0.25
<i>PH_{dry}, tangential</i>	0.38	8.33	8.11	-0.22
<i>PH_{dry}, reference</i>	0.08	2.49	2.59	0.10
Group 3				
<i>PH_{dry}, transverse</i>	1.34	11.92	11.00	-0.93
<i>PH_{dry}, radial</i>	0.33	6.85	6.61	-0.24
<i>PH_{dry}, tangential</i>	0.42	5.77	5.53	-0.24
<i>PH_{dry}, reference</i>	0.10	5.23	5.29	0.06
Group 4				
<i>PH_{dry}, transverse</i>	1.43	11.84	10.92	-0.92
<i>PH_{dry}, radial</i>	0.35	5.04	4.87	-0.18
<i>PH_{dry}, tangential</i>	0.39	6.27	6.07	-0.21
<i>PH_{dry}, reference</i>	0.09	5.45	5.48	0.03
Group 5				
<i>PH_{dry}, transverse</i>	1.23	11.88	11.02	-0.85
<i>PH_{dry}, radial</i>	0.51	6.18	5.98	-0.19
<i>PH_{dry}, tangential</i>	0.50	6.84	6.63	-0.20
<i>PH_{dry}, reference</i>	0.08	4.49	4.56	0.07
Average				
<i>PH_{dry}, transverse</i>	1.25	11.83	10.97	-0.86
<i>PH_{dry}, radial</i>	0.39	6.15	5.91	-0.24
<i>PH_{dry}, tangential</i>	0.40	6.43	6.20	-0.23
<i>PH_{dry}, reference</i>	0.09	4.01	4.07	0.06

Appendix 6 (1/3)

Masses, volumes, densities and moisture contents of birch and concrete samples

Table 1 Oven dry masses, volumes and densities of birch and concrete samples of groups 1-5 and the average values.

	m_{od} (g)	V_{od} (cm ³)	ρ_{od} (kg/m ³)
Group 1			
<i>B, transverse</i>	7.606	11.44	665.0
<i>B, radial</i>	7.613	11.09	686.6
<i>B, tangential</i>	6.734	11.29	596.5
<i>Concrete</i>	18.427	12.00	1535.6
Group 2			
<i>B, transverse</i>	6.902	11.34	608.7
<i>B, radial</i>	7.122	11.34	628.0
<i>B, tangential</i>	6.929	11.39	608.4
<i>Concrete</i>	18.181	12.00	1515.1
Group 3			
<i>B, transverse</i>	7.686	11.39	674.8
<i>B, radial</i>	7.239	11.58	624.9
<i>B, tangential</i>	7.088	11.03	642.4
<i>Concrete</i>	20.821	15.00	1388.1
Group 4			
<i>B, transverse</i>	7.237	11.34	638.5
<i>B, radial</i>	7.514	11.49	654.0
<i>B, tangential</i>	7.733	11.59	667.4
<i>Concrete</i>	17.883	10.00	1788.3
Group 5			
<i>B, transverse</i>	7.107	11.34	626.9
<i>B, radial</i>	7.224	11.54	626.1
<i>B, tangential</i>	6.993	11.39	614.0
<i>Concrete</i>	18.833	12.00	1569.4
Average			
<i>B, transverse</i>	7.308	11.37	642.8
<i>B, radial</i>	7.342	11.41	643.6
<i>B, tangential</i>	7.095	11.34	625.8
<i>Concrete</i>	18.829	12.20	1543.4

Appendix 6 (2/3)

Masses, volumes, densities and moisture contents of birch and concrete samples

Table 2 Masses of birch and concrete samples in groups 1-5 and the average values after conditioning in RH 32% without aluminum tape or plastic foil, before the adsorption test, after adsorption test, before desorption test, after desorption test and the mass of the aluminum tape or, in case of reference, plastic foil.

	$m_{RH32\%}$ (g)	$m_{bt,RH32\%}$ (g)	$m_{at,RH80\%}$ (g)	$m_{bt,RH80\%}$ (g)	$m_{at,RH32\%}$ (g)	m_{tape} (g)
Group 1						
<i>B, transverse</i>	8.014	8.512	8.546	8.784	8.748	0.498
<i>B, radial</i>	8.022	8.523	8.528	8.569	8.561	0.501
<i>B, tangential</i>	7.117	7.614	7.623	7.689	7.674	0.497
<i>Concrete</i>	18.557	19.071	19.080	19.115	19.111	0.514
Group 2						
<i>B, transverse</i>	7.277	7.734	7.767	7.999	7.965	0.457
<i>B, radial</i>	7.509	7.975	7.980	8.020	8.013	0.466
<i>B, tangential</i>	7.318	7.779	7.784	7.835	7.826	0.461
<i>Concrete</i>	18.382	18.827	18.844	18.878	18.870	0.445
Group 3						
<i>B, transverse</i>	8.091	8.654	8.683	8.890	8.866	0.563
<i>B, radial</i>	7.641	8.147	8.160	8.216	8.205	0.506
<i>B, tangential</i>	7.482	8.031	8.036	8.078	8.072	0.549
<i>Concrete</i>	20.965	21.530	21.574	21.544	21.580	0.565
Group 4						
<i>B, transverse</i>	7.621	8.034	8.070	8.282	8.259	0.413
<i>B, radial</i>	7.924	8.413	8.423	8.470	8.462	0.489
<i>B, tangential</i>	8.164	8.602	8.610	8.649	8.641	0.438
<i>Concrete</i>	18.090	18.550	18.556	18.586	18.585	0.460
Group 5						
<i>B, transverse</i>	7.486	7.945	7.978	8.190	8.172	0.459
<i>B, radial</i>	7.626	8.119	8.128	8.172	8.163	0.493
<i>B, tangential</i>	7.390	7.901	7.909	7.965	7.958	0.511
<i>Concrete</i>	18.974	19.552	19.561	19.593	19.593	0.578
Average						
<i>B, transverse</i>	7.698	8.176	8.209	8.429	8.402	0.478
<i>B, radial</i>	7.744	8.235	8.244	8.289	8.281	0.491
<i>B, tangential</i>	7.494	7.985	7.992	8.043	8.034	0.491
<i>Concrete</i>	18.994	19.506	19.517	19.585	19.548	0.512

Appendix 6 (3/3)

Masses, volumes, densities and moisture contents of birch and concrete samples

Table 3 Moisture contents of birch and concrete samples groups1-5 and average values before the adsorption test, after the adsorption test, the change in MC during the adsorption, MC before the desorption test, after the desorption test and the change in MC during the desorption. The equations for the moisture contents are presented in Appendix 1.

	MC _{bt,RH32%} (%)	MC _{at,RH80%} (%)	MC _{ads} (%)	MC _{bt,RH80%} (%)	MC _{at,RH32%} (%)	MC _{des} (%)
Group 1						
<i>B, transverse</i>	5.36	5.81	0.45	8.94	8.47	-0.47
<i>B, radial</i>	5.37	5.44	0.07	5.98	5.87	-0.11
<i>B, tangential</i>	5.69	5.82	0.13	6.80	6.58	-0.22
<i>Concrete</i>	0.71	0.75	0.05	0.94	0.92	-0.02
Group 2						
<i>B, transverse</i>	5.43	5.91	0.48	9.27	8.78	-0.49
<i>B, radial</i>	5.43	5.50	0.07	6.07	5.97	-0.10
<i>B, tangential</i>	5.61	5.69	0.07	6.42	6.29	-0.13
<i>Concrete</i>	1.11	1.20	0.09	1.39	1.34	-0.04
Group 3						
<i>B, transverse</i>	5.27	5.65	0.38	8.34	8.03	-0.31
<i>B, radial</i>	5.55	5.73	0.18	6.51	6.35	-0.15
<i>B, tangential</i>	5.56	5.63	0.07	6.22	6.14	-0.08
<i>Concrete</i>	0.69	0.90	0.21	0.76	0.93	0.17
Group 4						
<i>B, transverse</i>	5.31	5.80	0.50	8.73	8.42	-0.32
<i>B, radial</i>	5.46	5.59	0.13	6.22	6.11	-0.11
<i>B, tangential</i>	5.57	5.68	0.10	6.18	6.08	-0.10
<i>Concrete</i>	1.16	1.19	0.03	1.36	1.35	-0.01
Group 5						
<i>B, transverse</i>	5.33	5.80	0.46	8.78	8.53	-0.25
<i>B, radial</i>	5.56	5.69	0.12	6.30	6.17	-0.12
<i>B, tangential</i>	5.68	5.79	0.11	6.59	6.49	-0.10
<i>Concrete</i>	0.75	0.80	0.05	0.97	0.97	0.00
Average						
<i>B, transverse</i>	5.34	5.79	0.45	8.80	8.44	-0.37
<i>B, radial</i>	5.48	5.59	0.11	6.21	6.09	-0.12
<i>B, tangential</i>	5.62	5.72	0.10	6.44	6.32	-0.13
<i>Concrete</i>	0.88	0.97	0.09	1.08	1.10	0.02

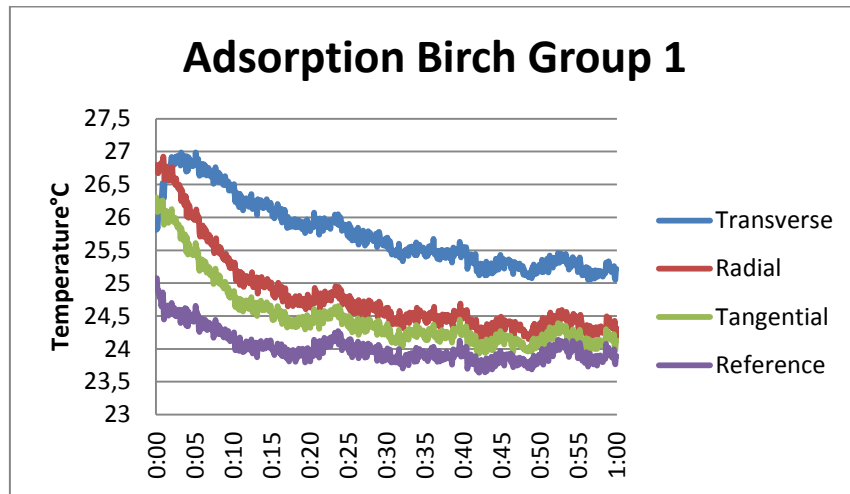


Figure 1 Temperature changes of group 1 birch samples and reference during adsorption from RH 32% to RH 80%.

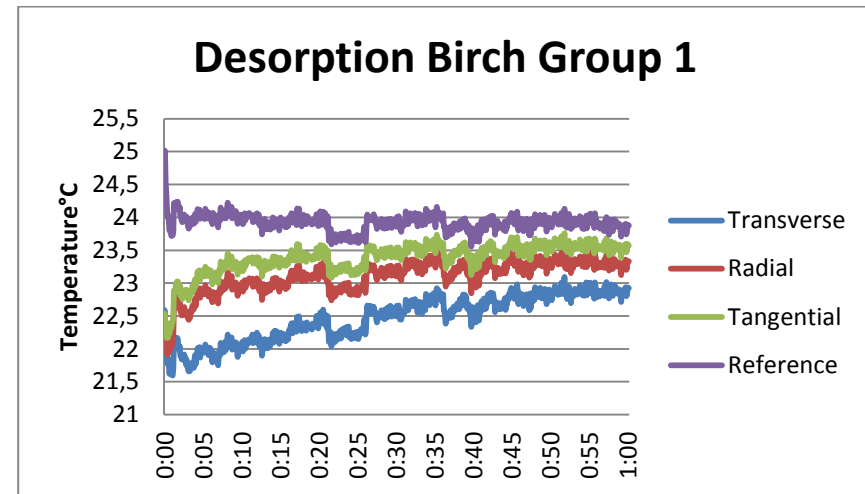


Figure 3 Temperature changes of group 1 birch samples and reference during desorption from RH 80% to RH 32%.

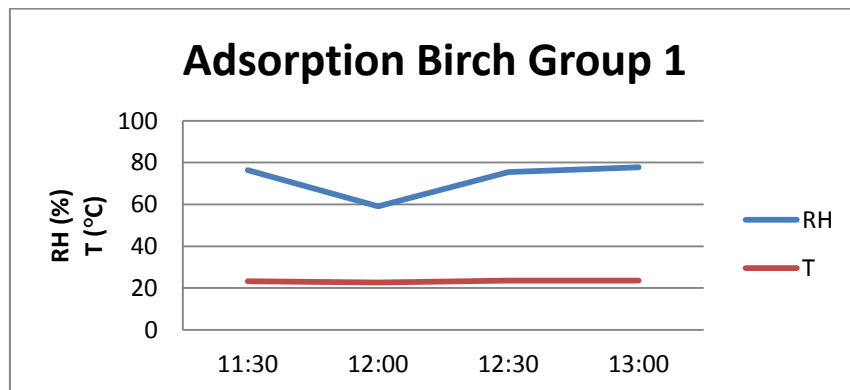


Figure 2 Conditions in climate cabinet during adsorption of the birch samples group 1.

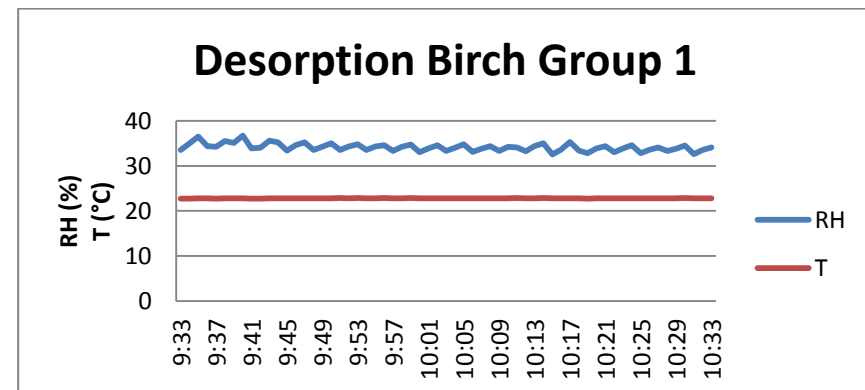


Figure 4 Conditions in climate cabinet during desorption of the birch samples group 1.

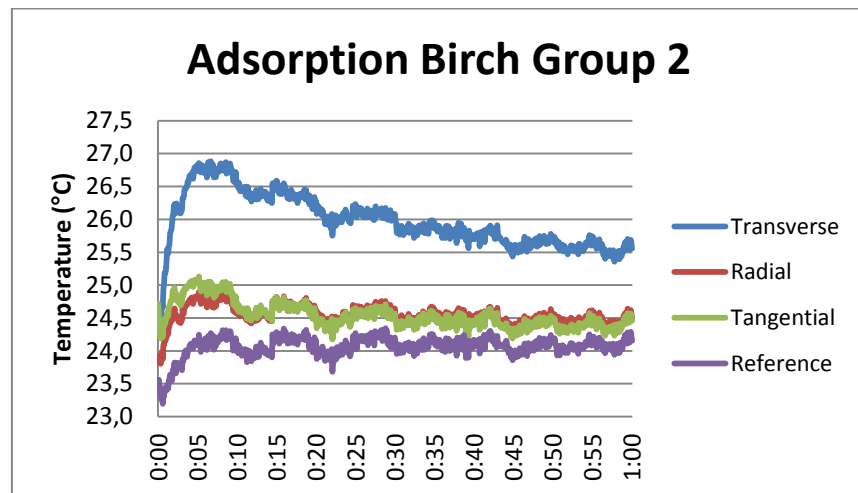


Figure 5 Temperature changes of group 2 birch samples and reference during adsorption from RH 32% to RH 80%.

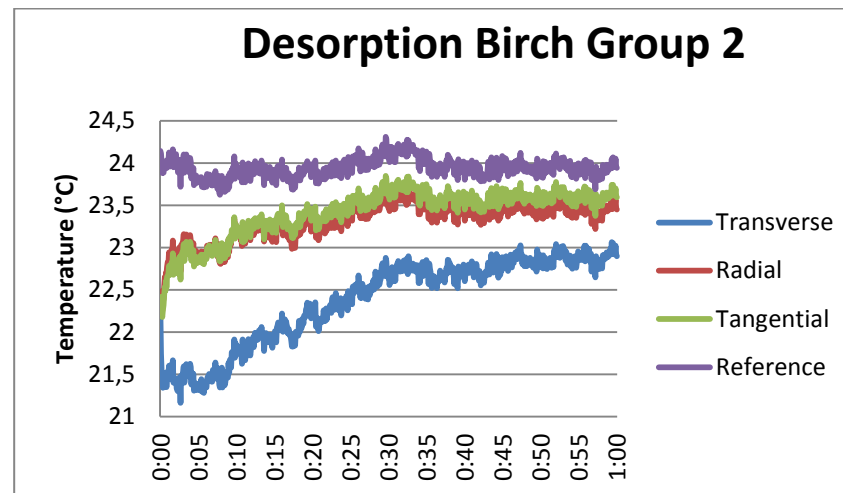


Figure 7 Temperature changes of group 2 birch samples and reference during desorption from RH 80% to RH 32%.

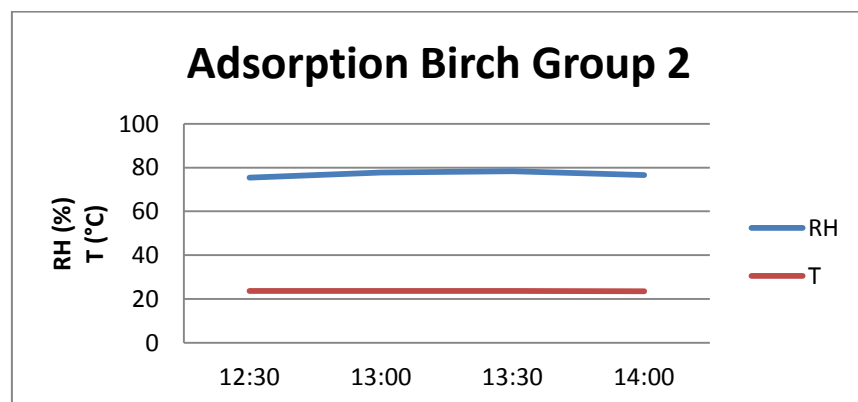


Figure 6 Conditions in climate cabinet during adsorption of the birch samples group 2.

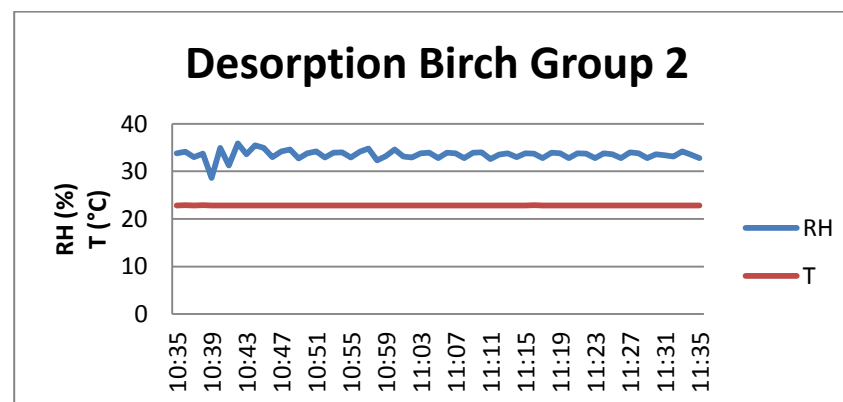


Figure 8 Conditions in climate cabinet during desorption of the birch samples group 2.

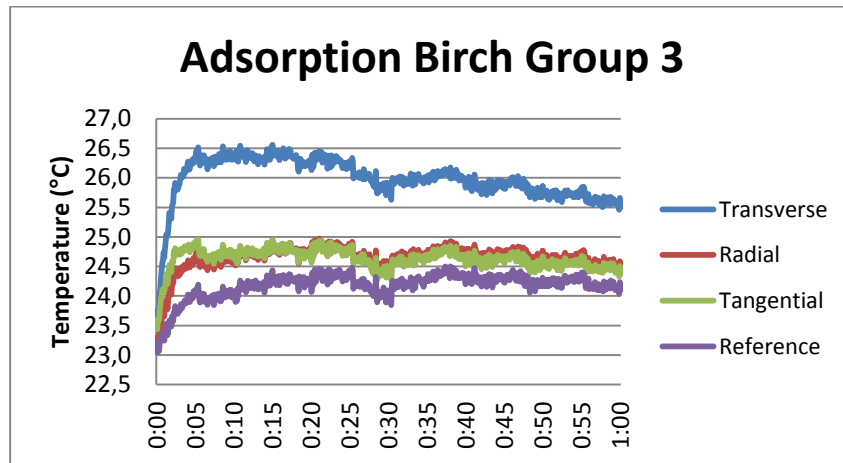


Figure 9 Temperature changes of group 3 birch samples and reference during adsorption from RH 32% to RH 80%.

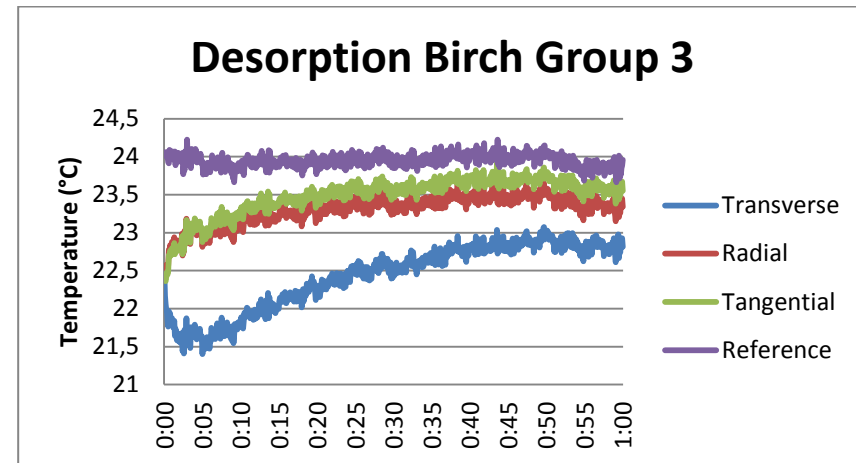


Figure 11 Temperature changes of group 3 birch samples and reference during desorption from RH 80% to RH 32%.

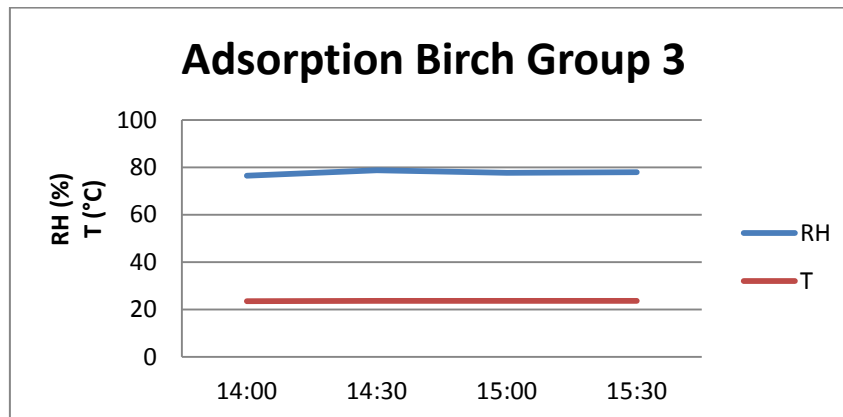


Figure 10 Conditions in climate cabinet during adsorption of the birch samples group 3.

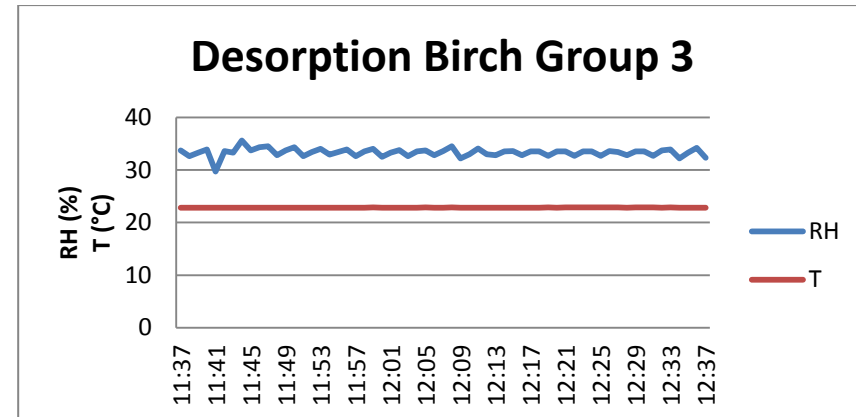


Figure 12 Conditions in climate cabinet during desorption of the birch samples group 3.

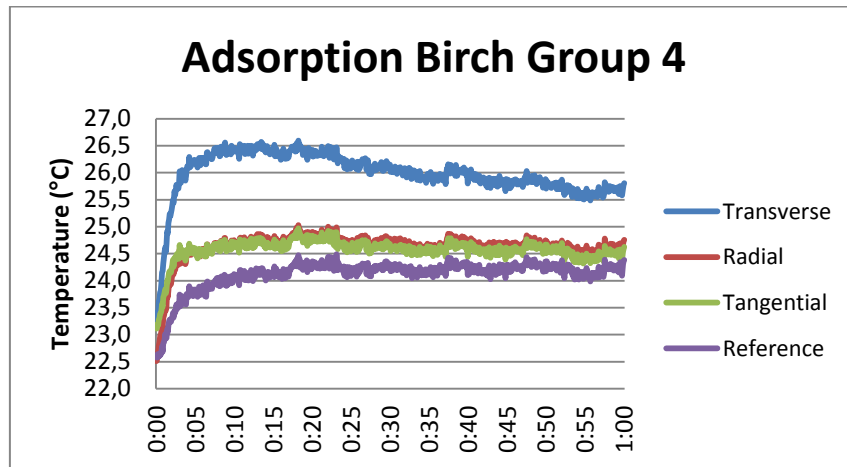


Figure 13 Temperature changes of group 4 birch samples and reference during adsorption from RH 32% to RH 80%.

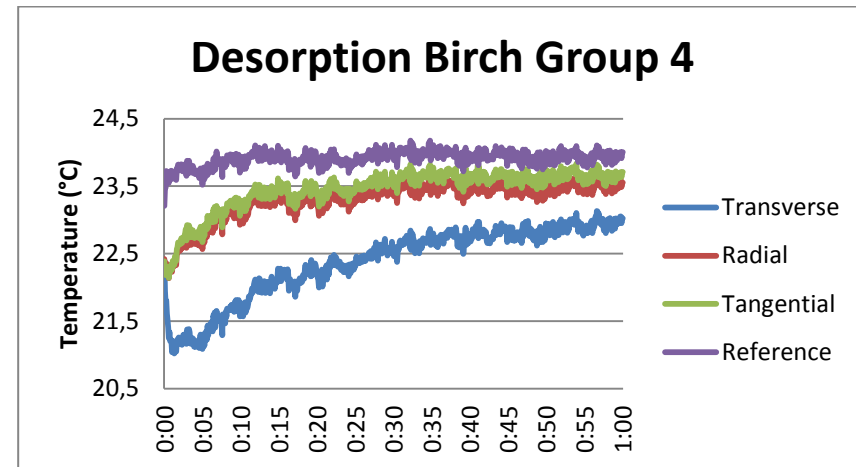


Figure 15 Temperature changes of group 4 birch samples and reference during desorption from RH 80% to RH 32%.

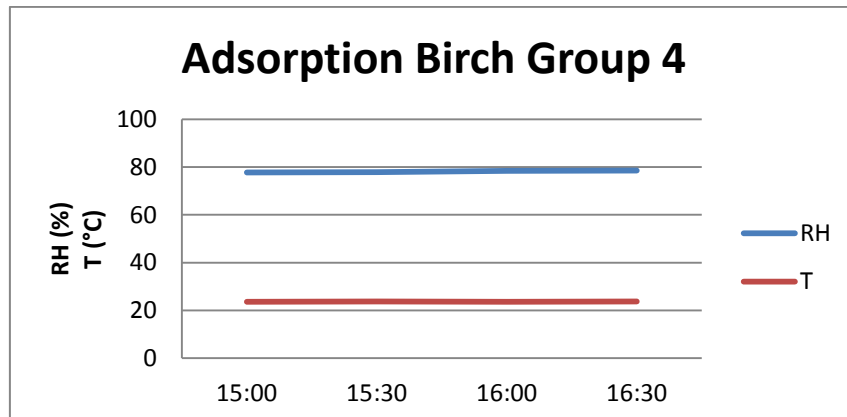


Figure 14 Conditions in climate cabinet during adsorption of the birch samples group 4.

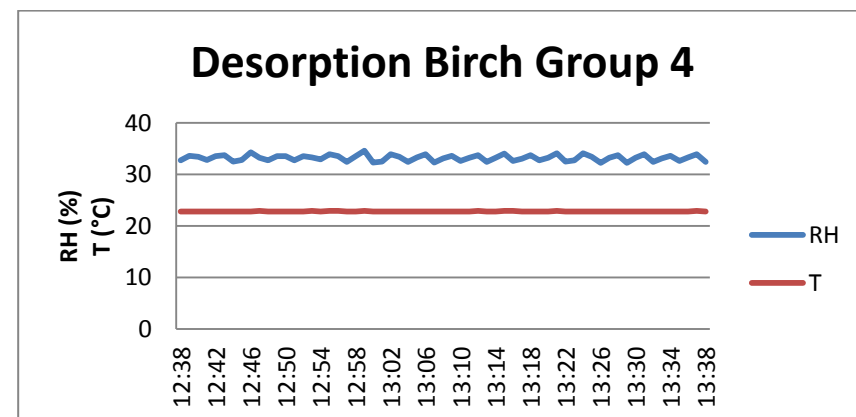


Figure 16 Conditions in climate cabinet during desorption of the birch samples group 4.

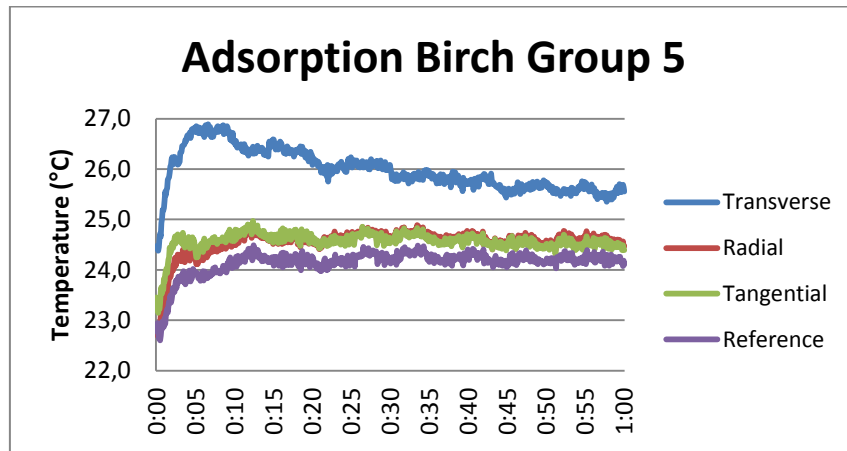


Figure 17 Temperature changes of group 5 birch samples and reference during adsorption from RH 32% to RH 80%.

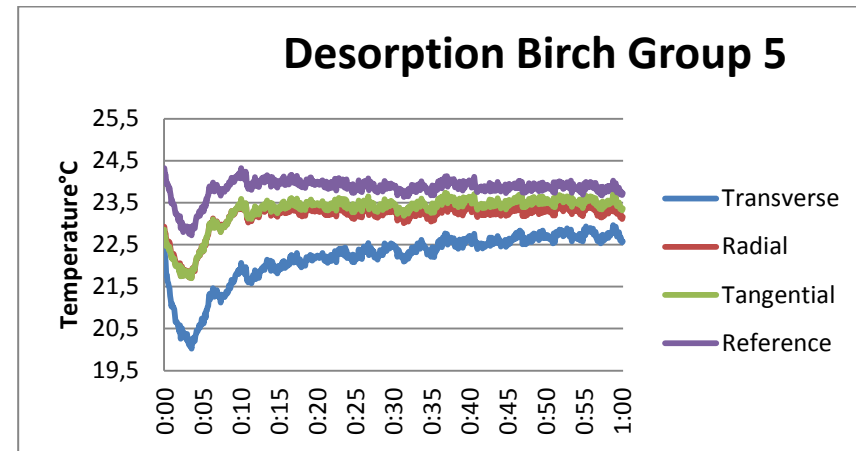


Figure 19 Temperature changes of group 5 birch samples and reference during desorption from RH 80% to RH 32%.

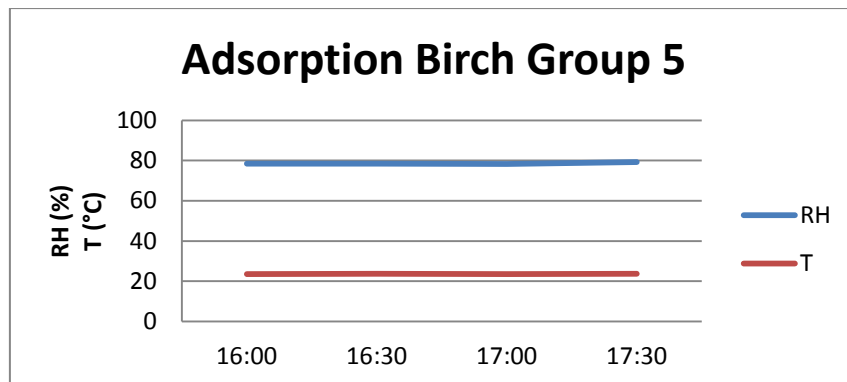


Figure 18 Conditions in climate cabinet during adsorption of the birch samples group 5.

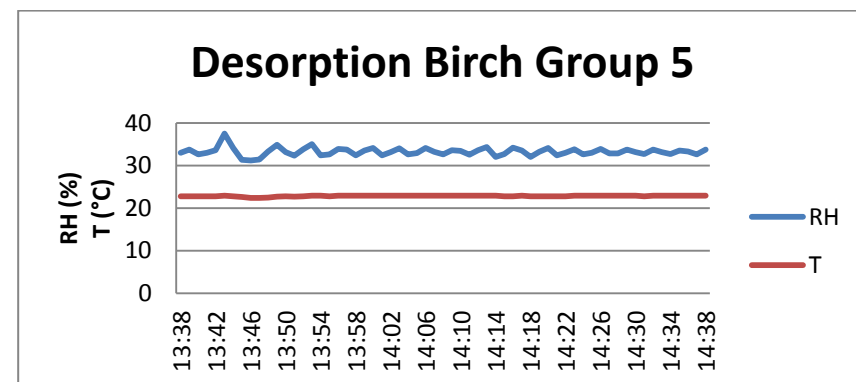


Figure 20 Conditions in climate cabinet during desorption of the birch samples group 5.

Appendix 7 Thermographs, condition graphs and temperature changes of birch samples

Table 1 Maximum temperature rises of all birch samples during adsorption and the time it occurred in, and maximum temperature decrease during desorption, the time it occurred in and the time where the temperature regained the value of initial temperature. The (-) denotes that the temperature did not return to the initial value.

	$\Delta T_{ads,max}$ (°C)	$\Delta t_{ads,max}$ (min)	$\Delta T_{des,max}$ (°C)	$\Delta t_{des,max}$ (min)	$\Delta t_{des,0}$ (min)
Group 1					
<i>B, transverse</i>	1.18	3	-1.00	1	21
<i>B, radial</i>	0.13	1	-0.52	1	1
<i>B, tangential</i>	0	0	-0.31	1	1
<i>B, reference</i>	0	0	-1.31	1	-
Group 2					
<i>B, transverse</i>	2.44	7	-0.92	1	19
<i>B, radial</i>	1.07	9	-0.23	0	1
<i>B, tangential</i>	0.93	5	-0.24	0	1
<i>B, reference</i>	1.12	8	-0.26	1	1
Group 3					
<i>B, transverse</i>	2.86	5	-1.06	3	20
<i>B, radial</i>	1.68	13	-0.03	0	1
<i>B, tangential</i>	1.52	6	-0.06	0	0
<i>B, reference</i>	1.44	25	-0.14	1	1
Group 4					
<i>B, transverse</i>	3.33	18	-1.36	2	19
<i>B, radial</i>	2.52	18	-0.19	1	2
<i>B, tangential</i>	1.80	18	-0.25	1	1
<i>B, reference</i>	1.87	18	-0.26	0	0
Group 5					
<i>B, transverse</i>	3.64	6	-2.56	4	27
<i>B, radial</i>	2.19	12	-1.20	4	6
<i>B, tangential</i>	1.82	12	-1.14	4	6
<i>B, reference</i>	1.90	12	-1.56	4	10
Average	Groups 2, 3, 4 and 5		Groups 2, 3 and 4		
<i>B, transverse</i>	2.94	9	-1.10	5	22
<i>B, radial</i>	1.71	18	-0.09	0	1
<i>B, tangential</i>	1.26	9	-0.14	0	1
<i>B, reference</i>	1.36	15	-0.02	0	0

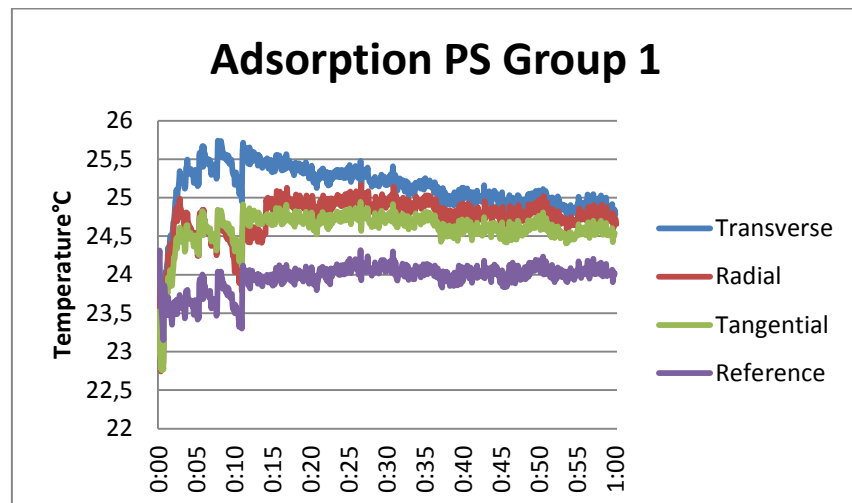


Figure 1 Temperature changes of group 1 pine sapwood samples and reference during adsorption from RH 32% to RH 80%.

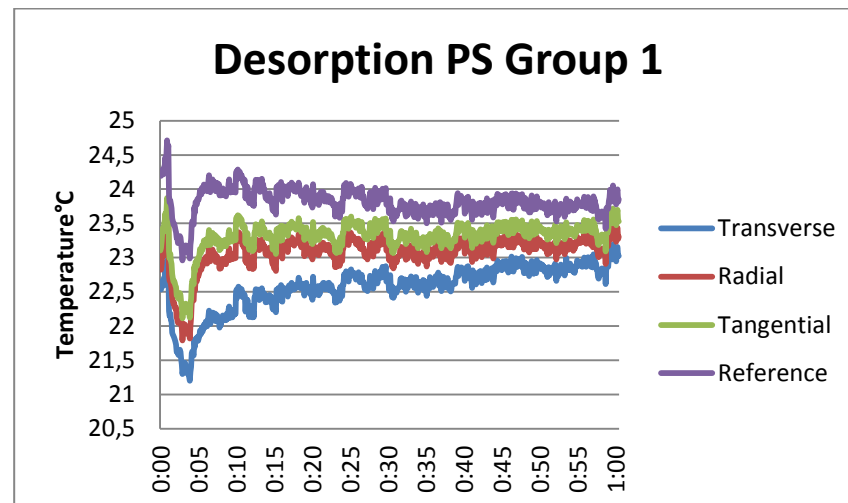


Figure 3 Temperature changes of group 1 pine sapwood samples and reference during desorption from RH 80% to RH 32%.

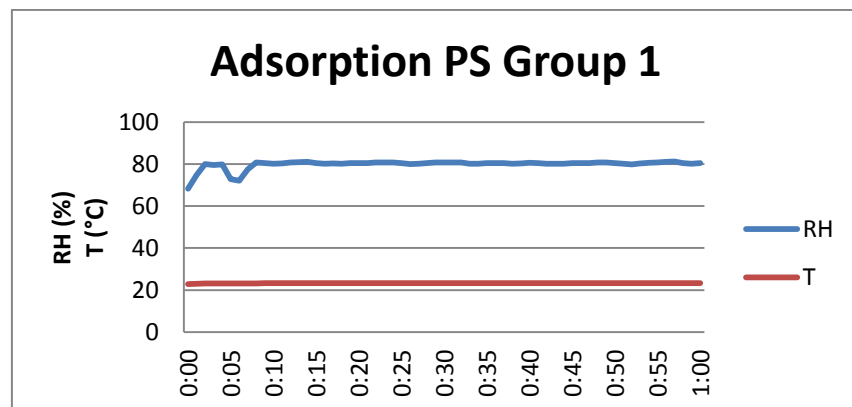


Figure 2 Conditions in climate cabinet during adsorption of the pine sapwood samples group 1.

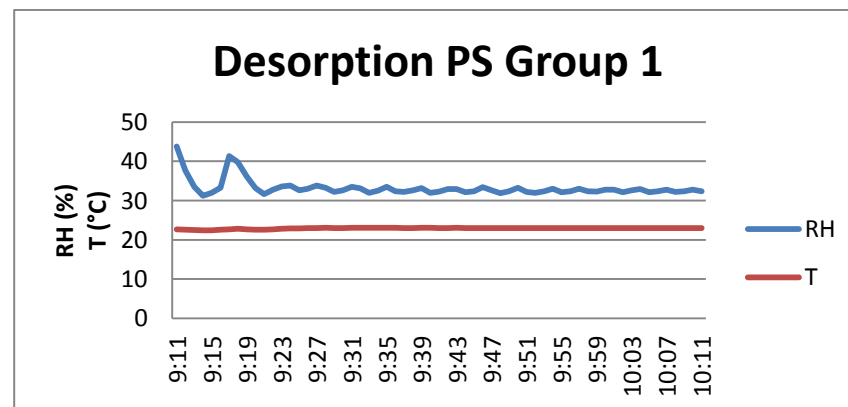


Figure 4 Conditions in climate cabinet during desorption of the pine sapwood samples group 1.

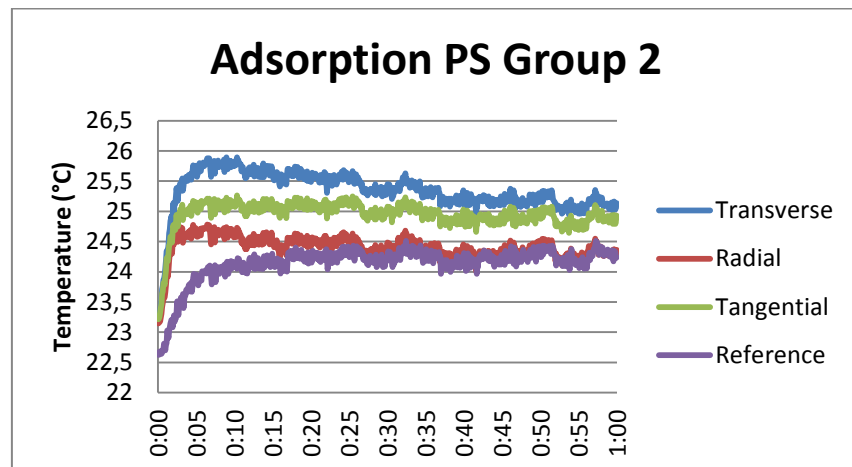


Figure 5 Temperature changes of group 2 pine sapwood samples and reference during adsorption from RH 32% to RH 80%.

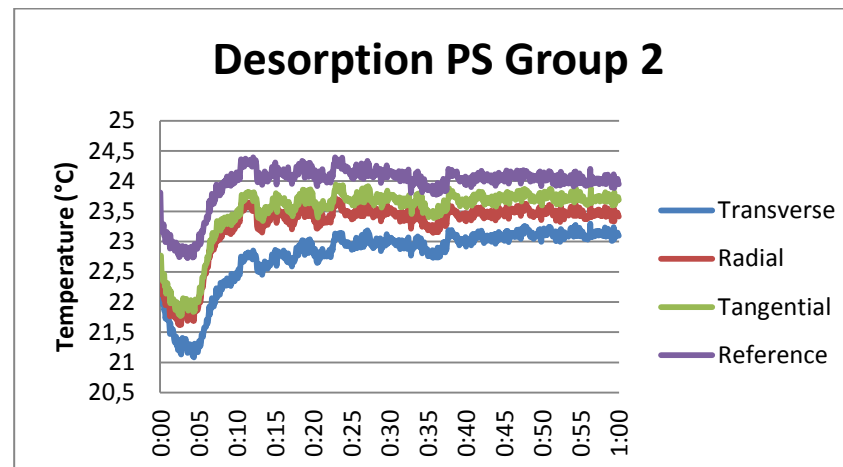


Figure 7 Temperature changes of group 2 pine sapwood samples and reference during desorption from RH 80% to RH 32%.

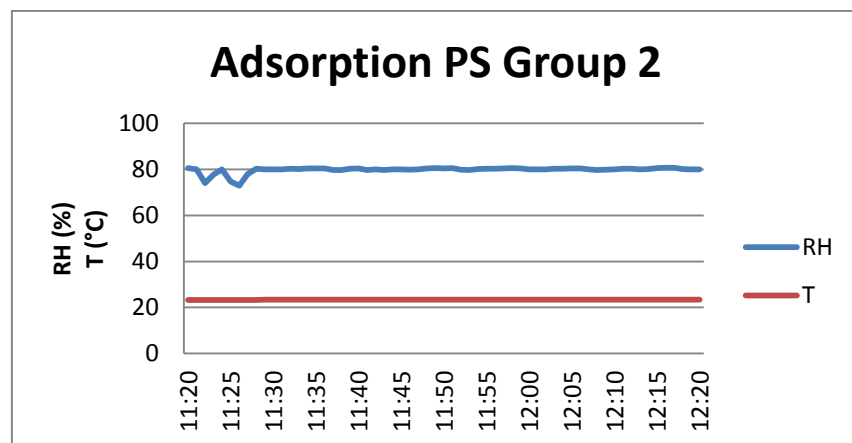


Figure 6 Conditions in climate cabinet during adsorption of the pine sapwood samples group 2.

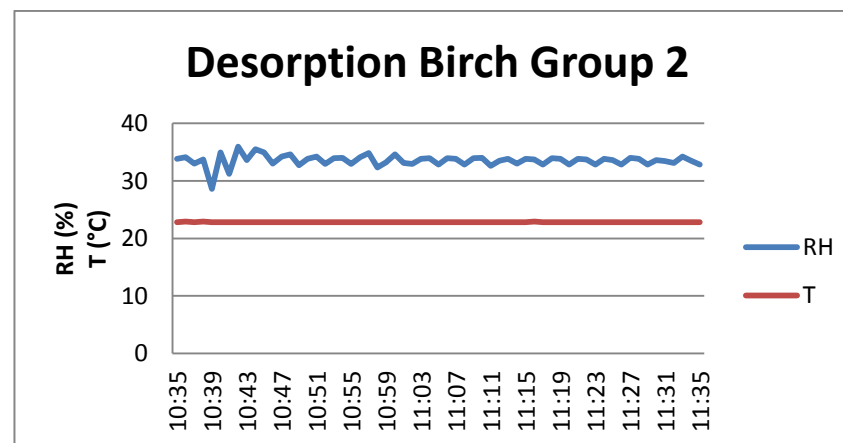


Figure 8 Conditions in climate cabinet during desorption of the pine sapwood samples group 2.

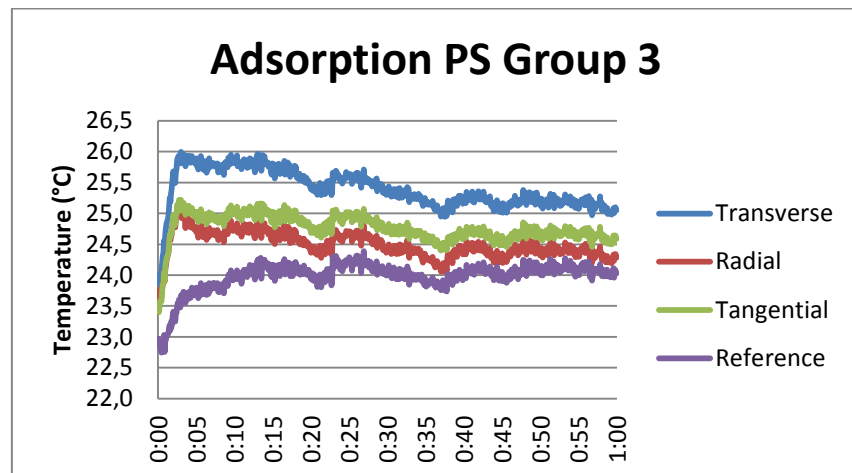


Figure 9 Temperature changes of group 3 pine sapwood samples and reference during adsorption from RH 32% to RH 80%.

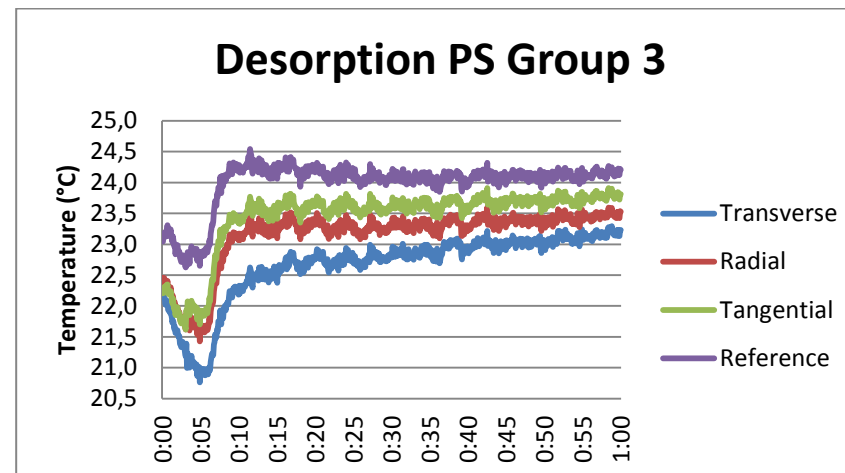


Figure 11 Temperature changes of group 3 pine sapwood samples and reference during desorption from RH 80% to RH 32%.

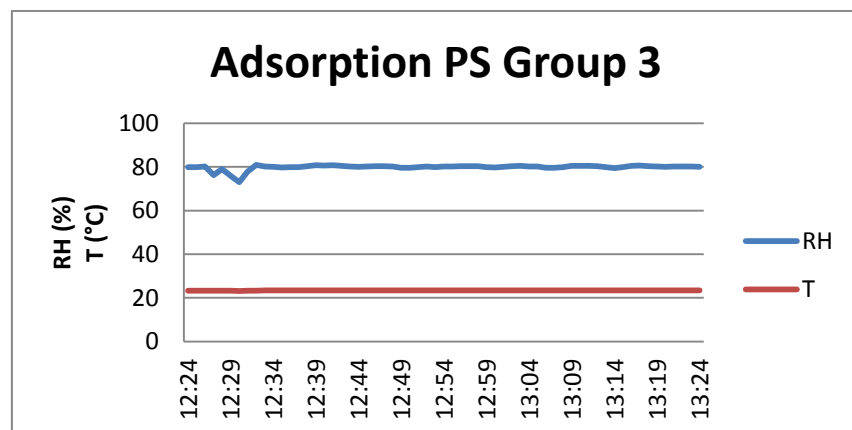


Figure 10 Conditions in climate cabinet during adsorption of the pine sapwood samples group 3.

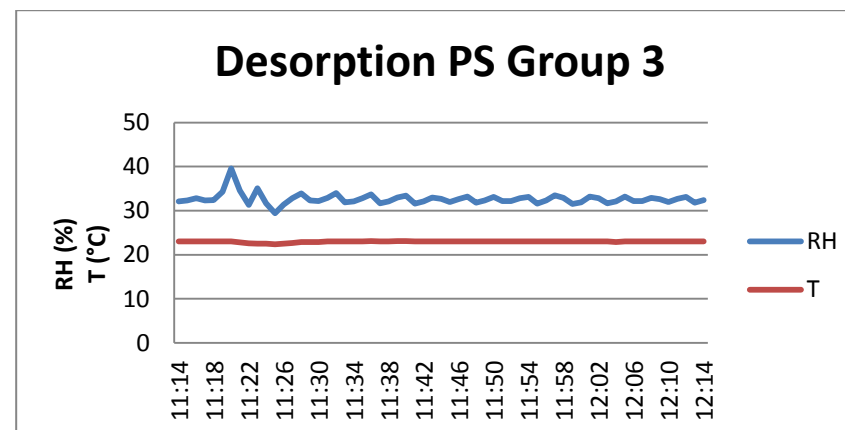


Figure 12 Conditions in climate cabinet during desorption of the pine sapwood samples group 3.

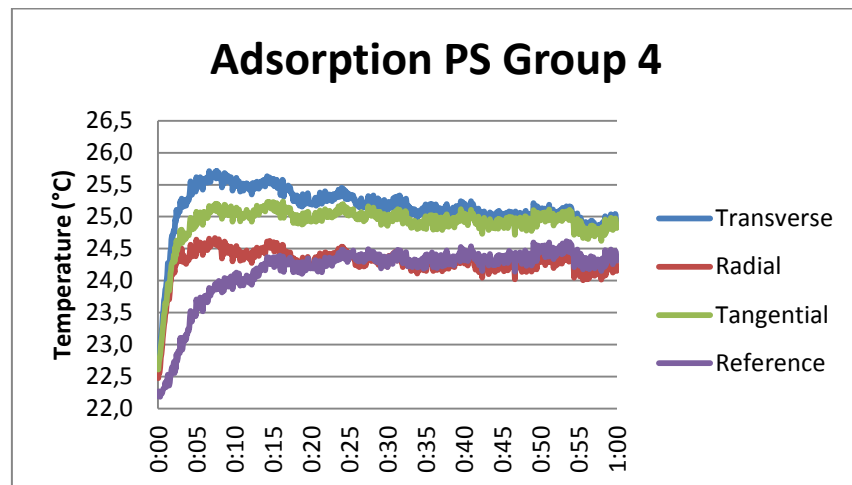


Figure 13 Temperature changes of group 4 pine sapwood samples and reference during adsorption from RH 32% to RH 80%.

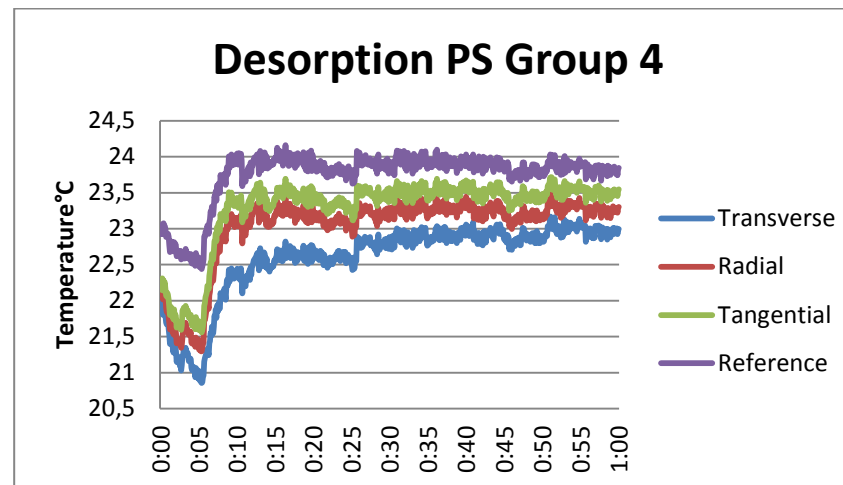


Figure 15 Temperature changes of group 4 pine sapwood samples and reference during desorption from RH 80% to RH 32%.

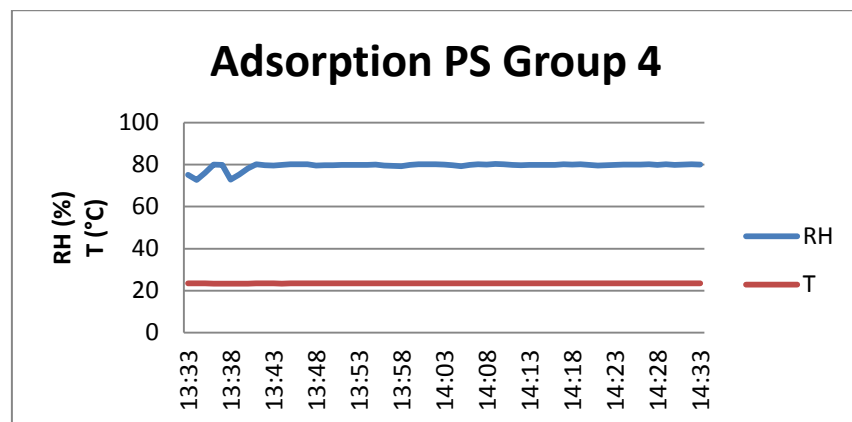


Figure 14 Conditions in climate cabinet during adsorption of the pine sapwood samples group 4.

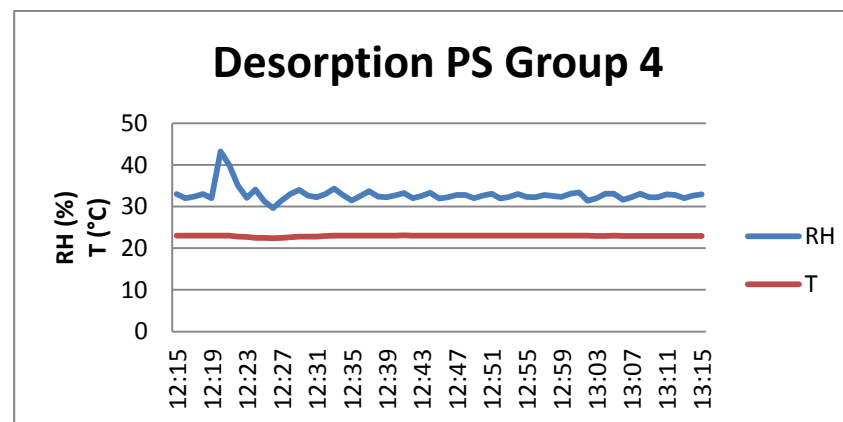


Figure 16 Conditions in climate cabinet during desorption of the pine sapwood samples group 4.

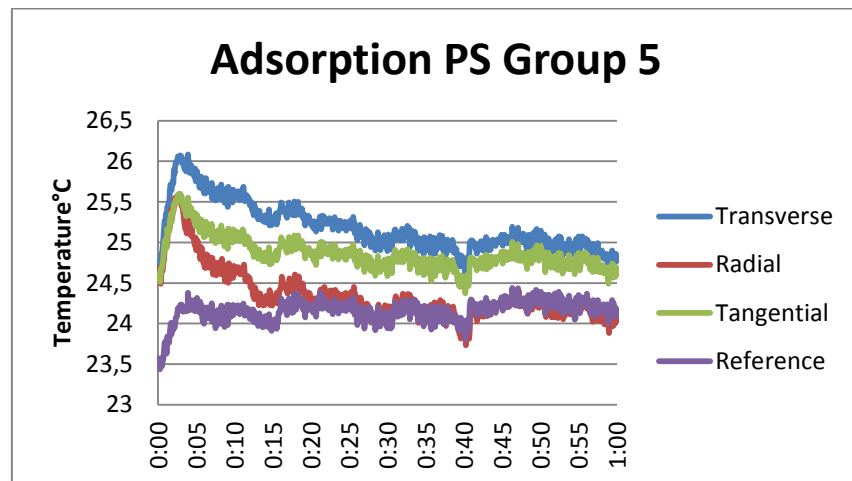


Figure 17 Temperature changes of group 5 pine sapwood samples and reference during adsorption from RH 32% to RH 80%.

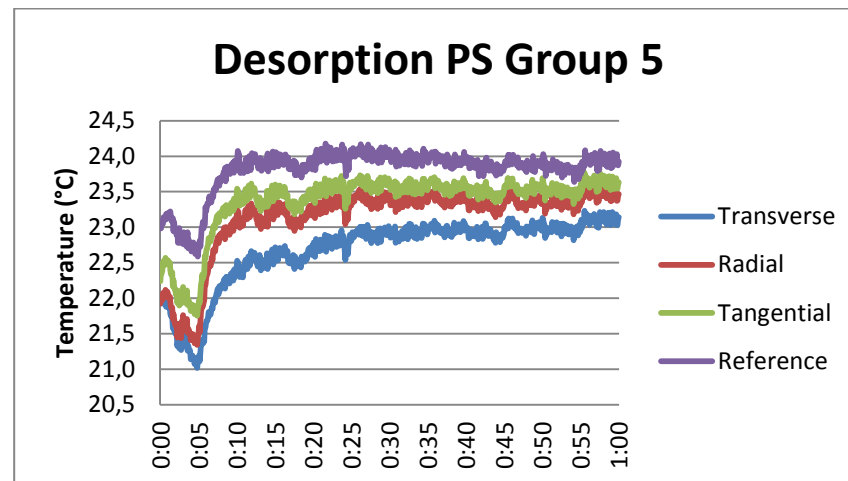


Figure 19 Temperature changes of group 5 pine sapwood samples and reference during desorption from RH 80% to RH 32%.

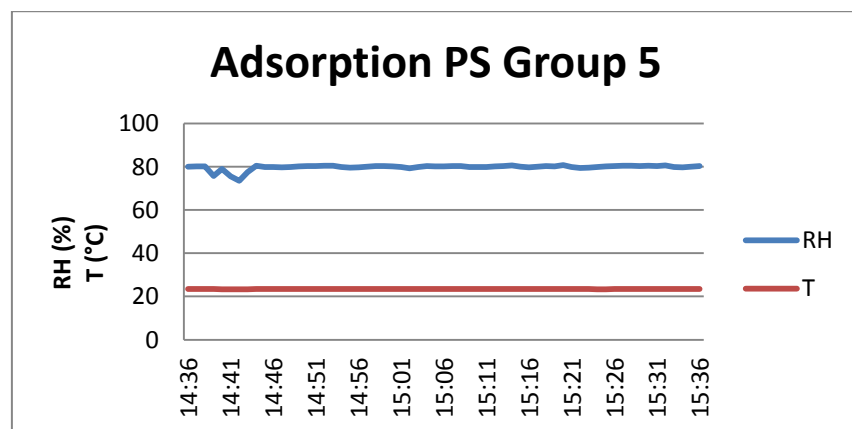


Figure 18 Conditions in climate cabinet during adsorption of the pine sapwood samples group 5.

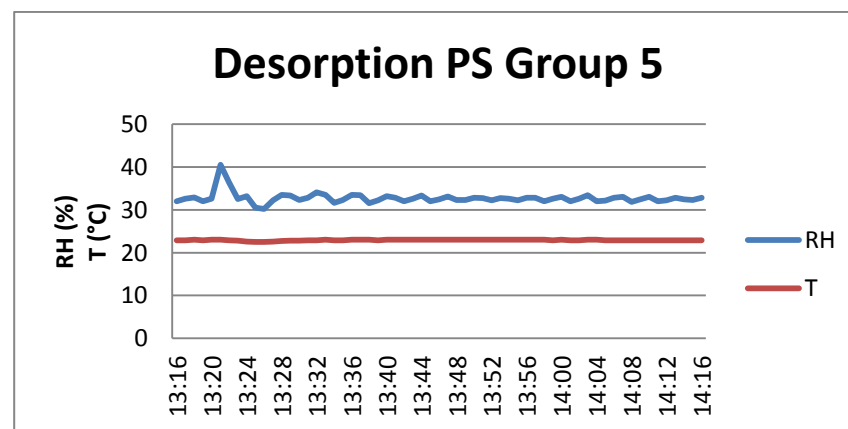


Figure 20 Conditions in climate cabinet during desorption of the pine sapwood samples group 5.

Appendix 8 Thermographs, condition graphs and temperature changes of pine sapwood samples

(6/6)

Table 1 Maximum temperature rises of all pine sapwood samples during adsorption and the time it occurred in, and maximum temperature decrease during desorption, the time it occurred in and the time where the temperature regained the value of initial temperature.

	$\Delta T_{ads,max}$ (°C)	$\Delta t_{ads,max}$ (min)	$\Delta T_{des,max}$ (°C)	$\Delta t_{des,max}$ (min)	$\Delta t_{des,0}$ (min)
Group 1					
<i>PS, transverse</i>	2.83	8	-1.34	3	10
<i>PS, radial</i>	2.21	3	-1.11	3	5
<i>PS, tangential</i>	2.15	11	-0.98	3	5
<i>PS, reference</i>	0.89	11	-1.27	3	10
Group 2					
<i>PS, transverse</i>	2.68	5	-1.37	2	10
<i>PS, radial</i>	1.64	5	-0.82	2	5
<i>PS, tangential</i>	2.05	5	-0.96	2	6
<i>PS, reference</i>	1.89	16	-1.09	3	7
Group 3					
<i>PS, transverse</i>	2.01	3	-1.48	5	9
<i>PS, radial</i>	1.50	3	-1.03	5	7
<i>PS, tangential</i>	1.69	3	-0.62	3	6
<i>PS, reference</i>	1.64	12	-0.42	3	6
Group 4					
<i>PS, transverse</i>	3.04	6	-0.97	5	7
<i>PS, radial</i>	2.10	6	-0.58	4	5
<i>PS, tangential</i>	2.35	6	-0.48	5	5
<i>PS, reference</i>	2.30	15	-0.40	5	6
Group 5					
<i>PS, transverse</i>	1.37	4	-1.08	5	8
<i>PS, radial</i>	1.11	3	-0.77	5	6
<i>PS, tangential</i>	1.08	3	-0.60	5	6
<i>PS, reference</i>	0.94	4	-0.48	5	6
Average	Groups 2, 3 and 4		Groups 2, 3 and 4		
<i>PS, transverse</i>	2.53	7	-1.24	5	8
<i>PS, radial</i>	1.60	3	-0.66	4	6
<i>PS, tangential</i>	1.80	7	-0.55	4	6
<i>PS, reference</i>	1.74	24	-0.56	5	6

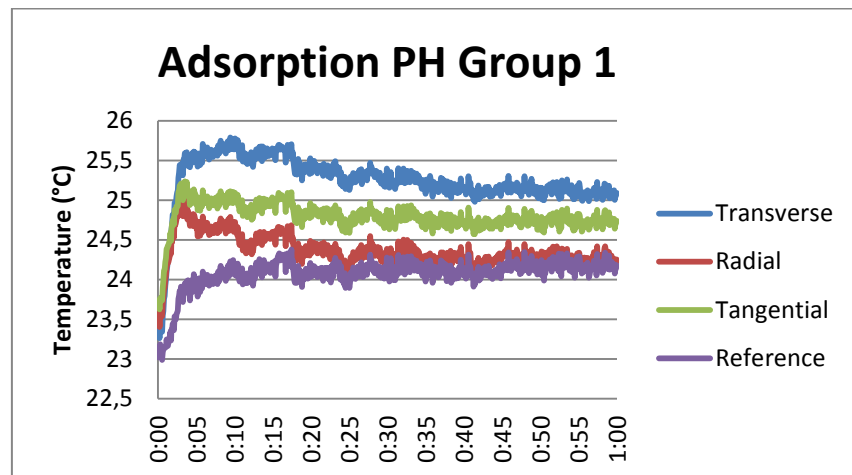


Figure 1 Temperature changes of group 1 pine heartwood samples and reference during adsorption from RH 32% to RH 80%.

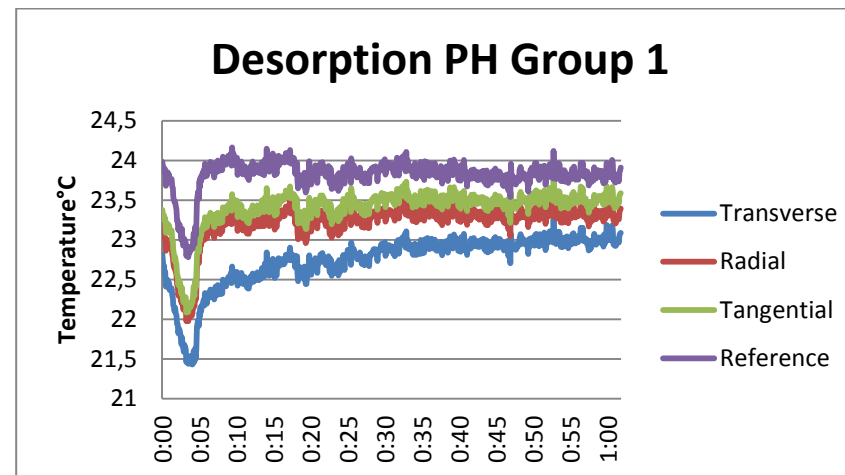


Figure 3 Temperature changes of group 1 pine heartwood samples and reference during desorption from RH 80% to RH 32%.

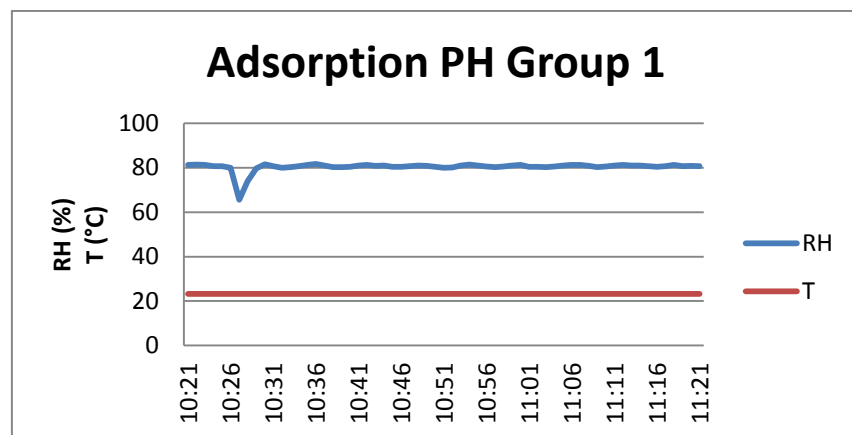


Figure 2 Conditions in climate cabinet during adsorption of the pine heartwood samples group 1.

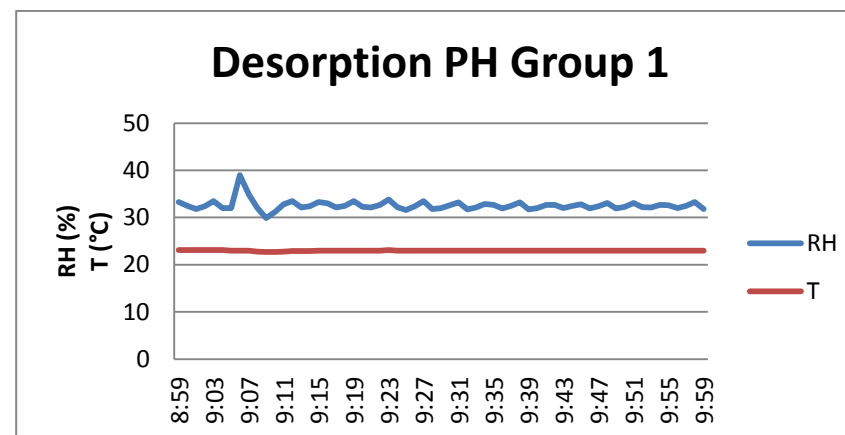


Figure 4 Conditions in climate cabinet during desorption of the pine heartwood samples group 1.

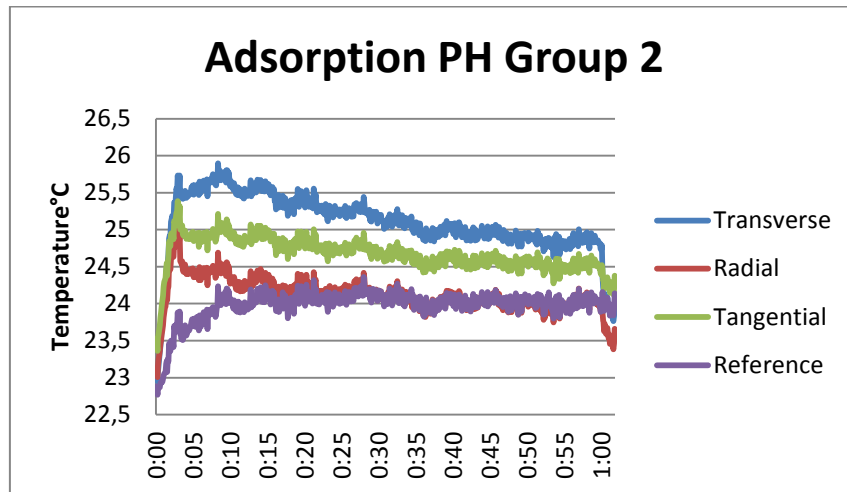


Figure 5 Temperature changes of group 2 pine heartwood samples and reference during adsorption from RH 32% to RH 80%.

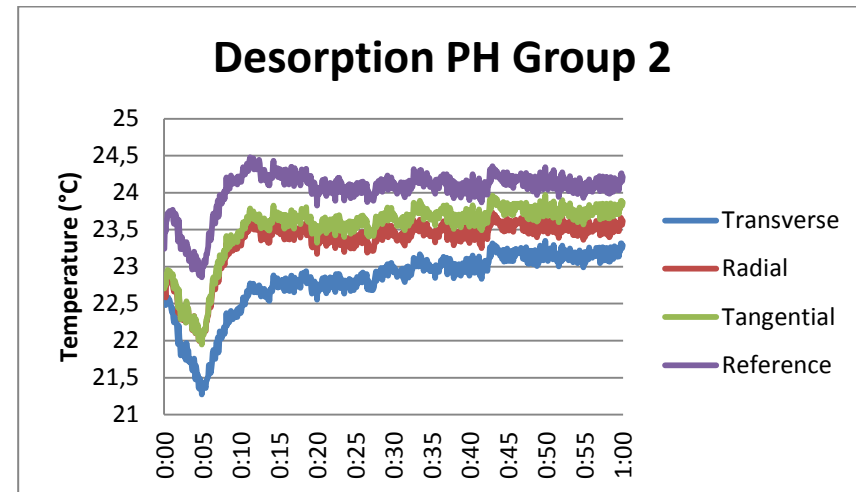


Figure 7 Temperature changes of group 2 pine heartwood samples and reference during desorption from RH 80% to RH 32%.

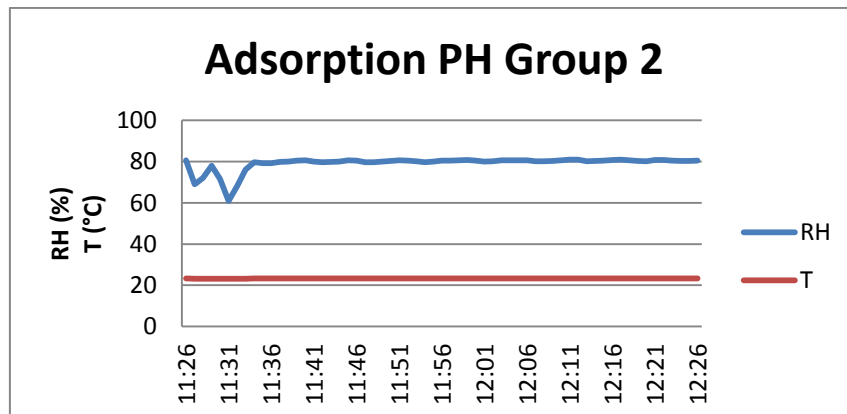


Figure 6 Conditions in climate cabinet during adsorption of the pine heartwood samples group 2.

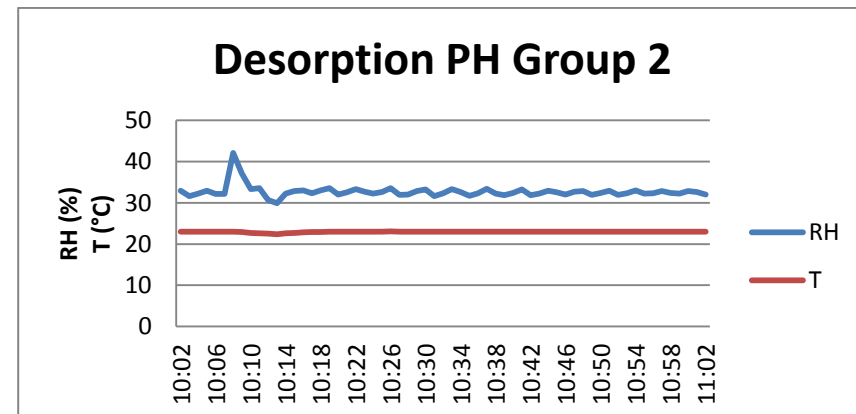


Figure 8 Conditions in climate cabinet during desorption of the pine heartwood samples group 2.

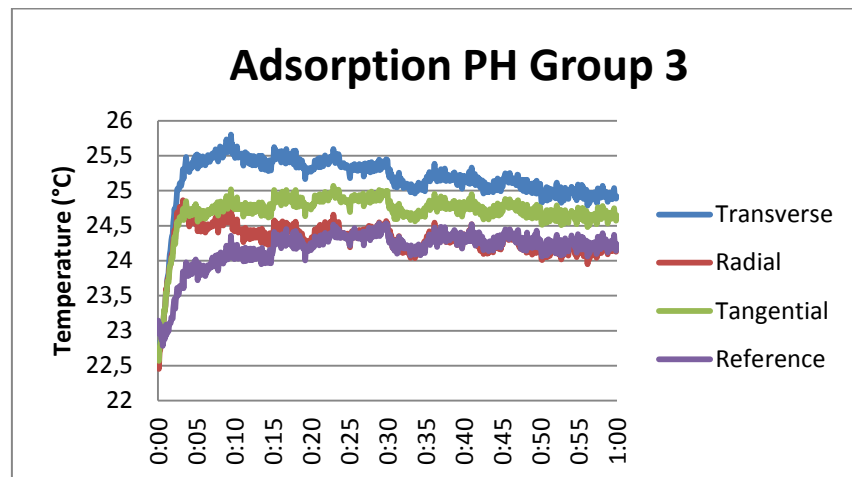


Figure 9 Temperature changes of group 3 pine heartwood samples and reference during adsorption from RH 32% to RH 80%.

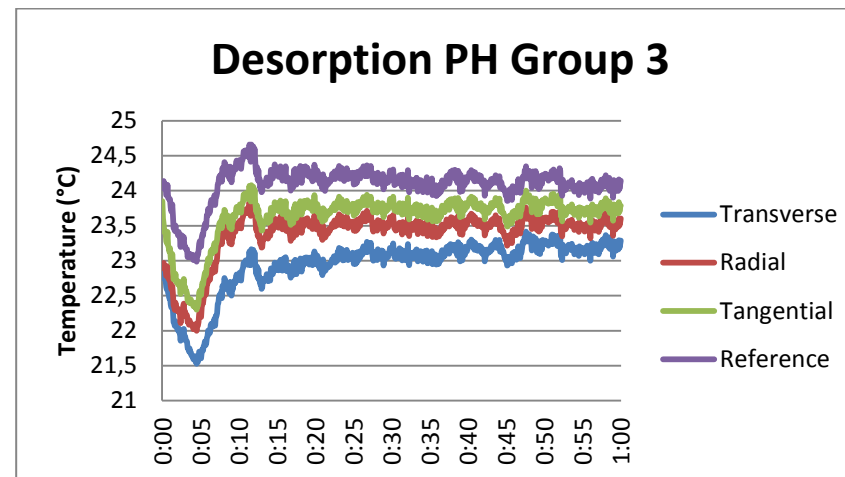


Figure 11 Temperature changes of group 3 pine heartwood samples and reference during desorption from RH 80% to RH 32%.

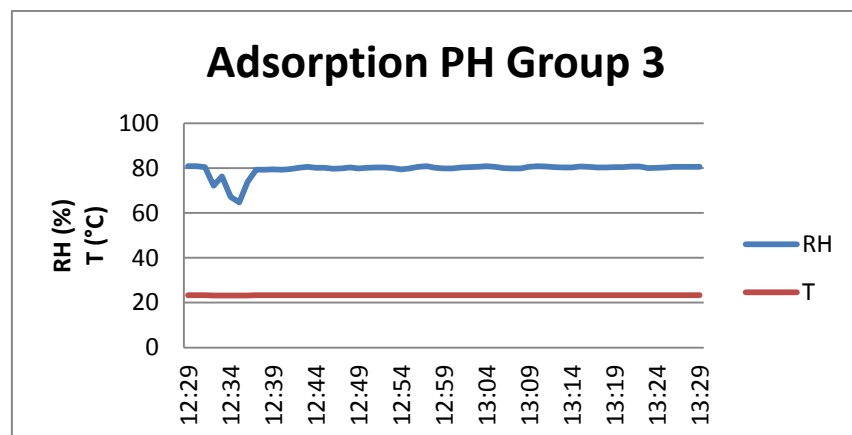


Figure 10 Conditions in climate cabinet during adsorption of the pine heartwood samples group 3.

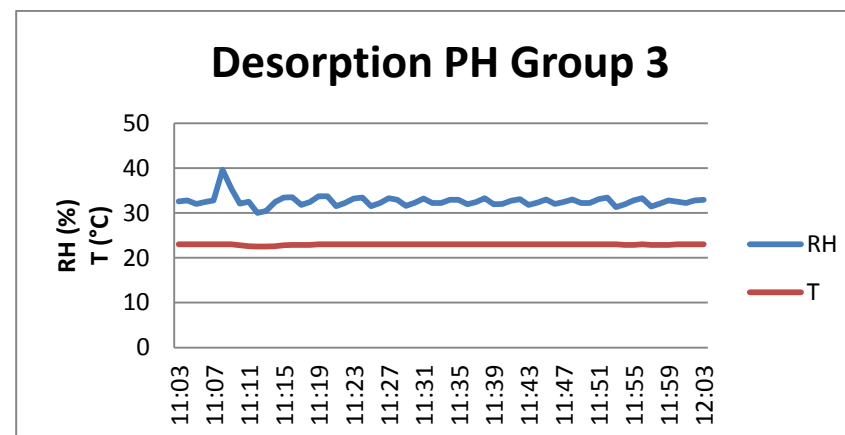


Figure 12 Conditions in climate cabinet during desorption of the pine heartwood samples group 3.

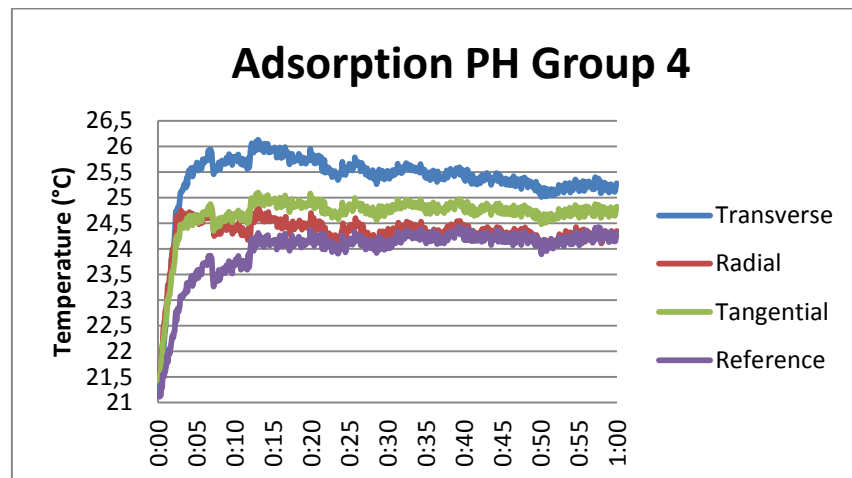


Figure 13 Temperature changes of group 4 pine heartwood samples and reference during adsorption from RH 32% to RH 80%.

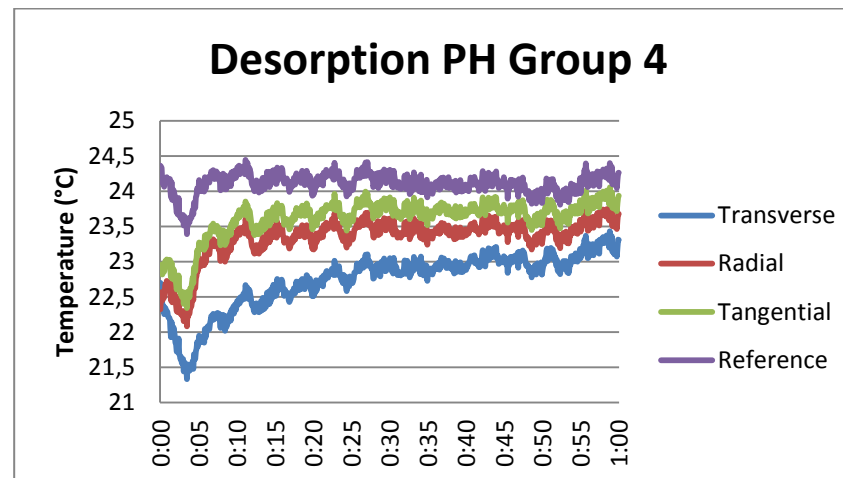


Figure 15 Temperature changes of group 4 pine heartwood samples and reference during desorption from RH 80% to RH 32%.

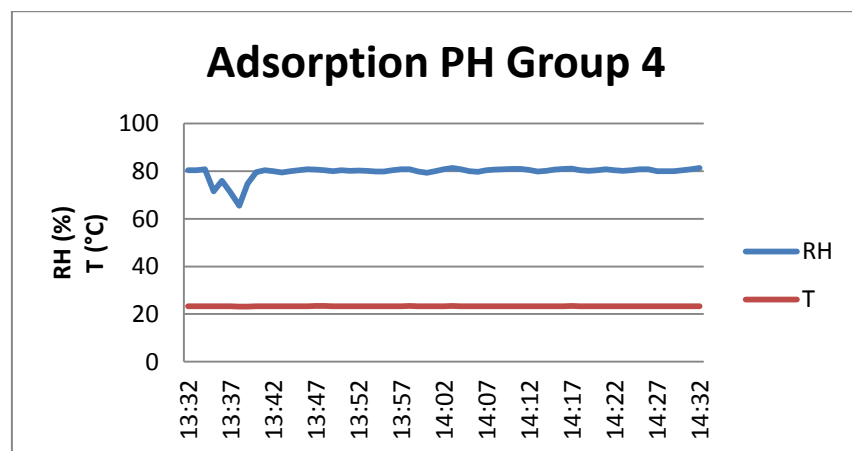


Figure 14 Conditions in climate cabinet during adsorption of the pine heartwood samples group 4.

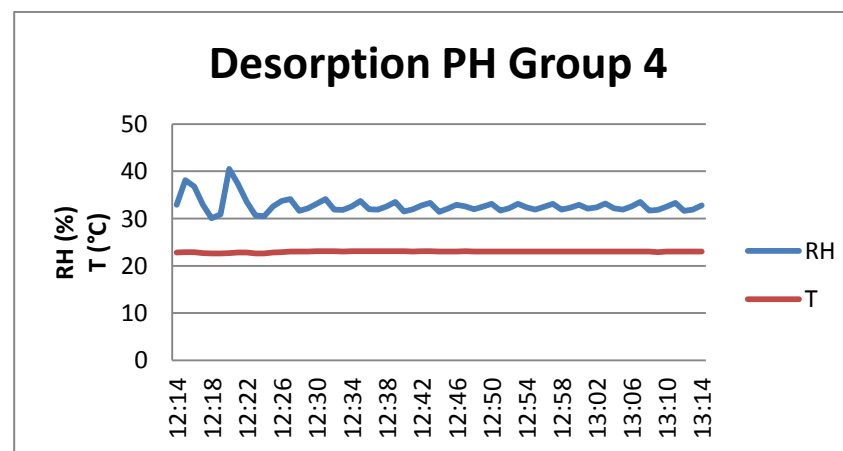


Figure 16 Conditions in climate cabinet during desorption of the pine heartwood samples group 4.

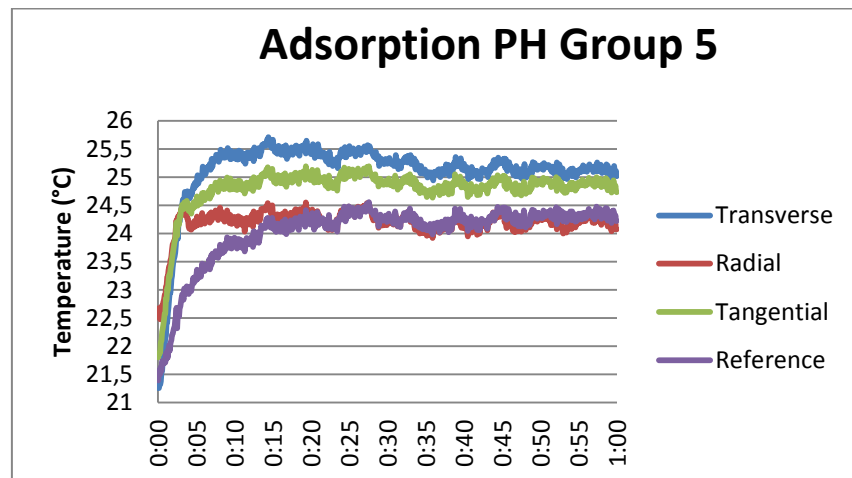


Figure 17 Temperature changes of group 5 pine heartwood samples and reference during adsorption from RH 32% to RH 80%.

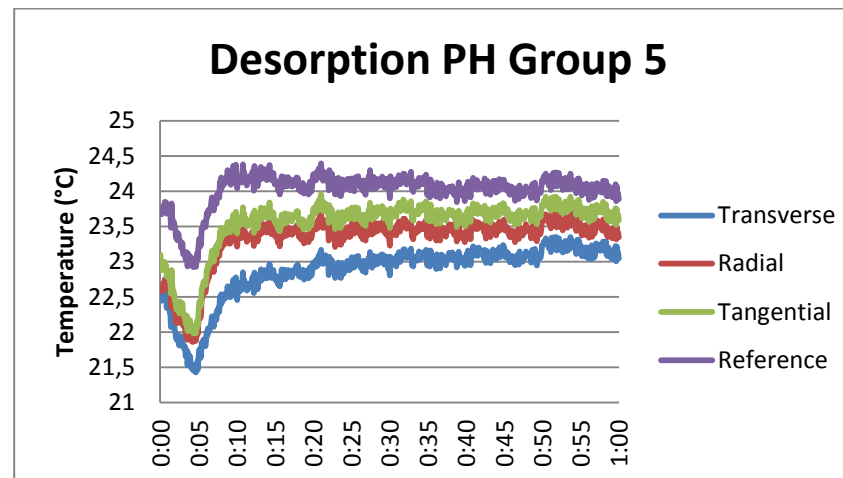


Figure 19 Temperature changes of group 5 pine heartwood samples and reference during desorption from RH 80% to RH 32%.

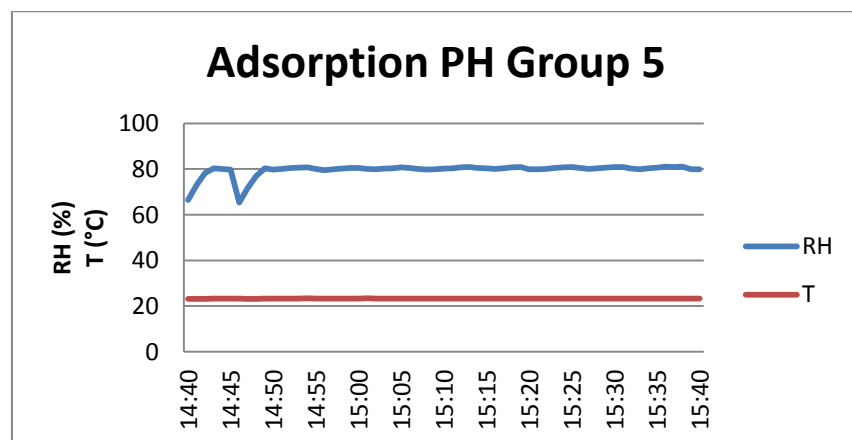


Figure 18 Conditions in climate cabinet during adsorption of the pine heartwood samples group 5.

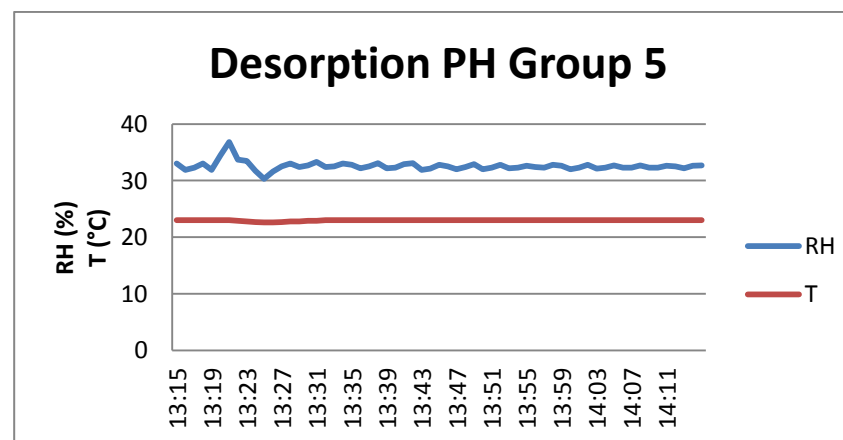


Figure 20 Conditions in climate cabinet during desorption of the pine heartwood samples group 5.

Appendix 9 Thermographs, condition graphs and temperature changes of pine heartwood samples

(6/6)

Table 1 Maximum temperature rises of all pine heartwood samples during adsorption and the time it occurred in, and maximum temperature decrease during desorption, the time it occurred in and the time where the temperature regained the value of initial temperature.

	$\Delta T_{ads,max}$ (°C)	$\Delta t_{ads,max}$ (min)	$\Delta T_{des,max}$ (°C)	$\Delta t_{des,max}$ (min)	$\Delta t_{des,0}$ (min)
Group 1					
<i>PH, transverse</i>	2.22	4	-1.36	3	14
<i>PH, radial</i>	1.35	3	-1.25	3	8
<i>PH, tangential</i>	1.51	4	-1.23	3	8
<i>PH, reference</i>	1.22	10	-1.20	3	7
Group 2					
<i>PH, transverse</i>	2.69	2	-1.24	5	10
<i>PH, radial</i>	1.96	2	-0.71	4	6
<i>PH, tangential</i>	1.86	2	-0.76	4	6
<i>PH, reference</i>	1.01	2	-0.69	4	6
Group 3					
<i>PH, transverse</i>	2.66	4	-1.34	4	10
<i>PH, radial</i>	2.31	3	-0.96	4	6
<i>PH, tangential</i>	2.25	4	-1.55	4	10
<i>PH, reference</i>	1.40	10	-1.03	4	7
Group 4					
<i>PH, transverse</i>	4.63	7	-1.36	3	11
<i>PH, radial</i>	3.06	3	-0.48	3	4
<i>PH, tangential</i>	3.34	7	-0.55	3	4
<i>PH, reference</i>	2.71	7	-0.97	3	10
Group 5					
<i>PH, transverse</i>	4.26	9	-1.12	4	8
<i>PH, radial</i>	1.98	3	-0.76	4	6
<i>PH, tangential</i>	3.17	10	-1.12	4	6
<i>PH, reference</i>	2.88	15	-0.78	4	6
Average	Groups 1, 3, 4 and 5		Groups 2, 3, 4 and 5		
<i>PH, transverse</i>	3.07	9	-1.21	4	10
<i>PH, radial</i>	2.10	3	-0.52	4	6
<i>PH, tangential</i>	2.37	4	-0.86	4	6
<i>PH, reference</i>	2.03	10	-0.66	4	6

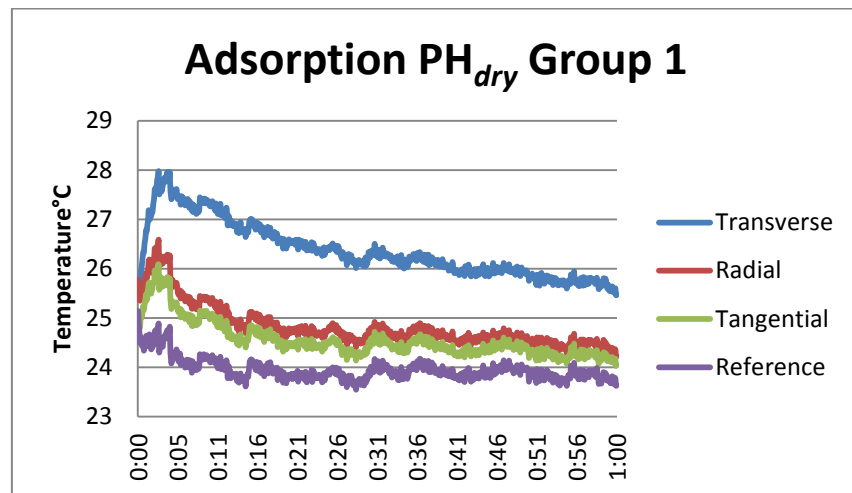


Figure 1 Temperature changes of group 1 dry pine heartwood samples and reference during adsorption from RH 1% to RH 80%.

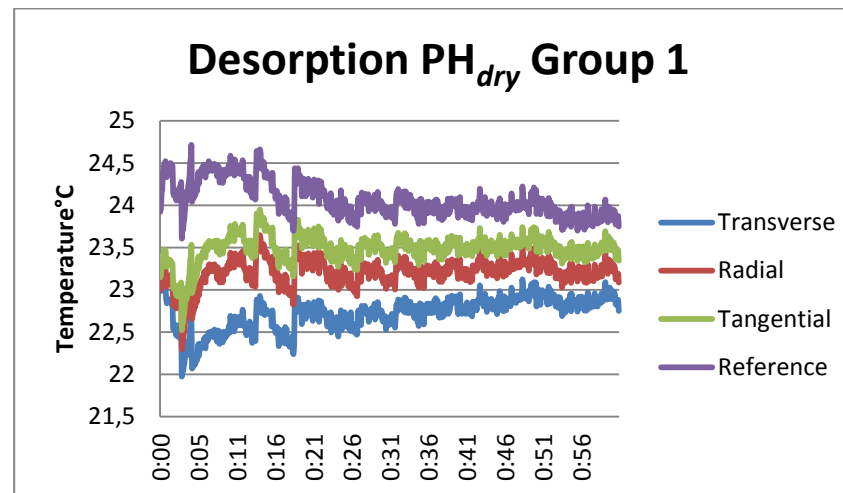


Figure 3 Temperature changes of group 1 dry pine heartwood samples and reference during desorption from RH 80% to RH 32%.

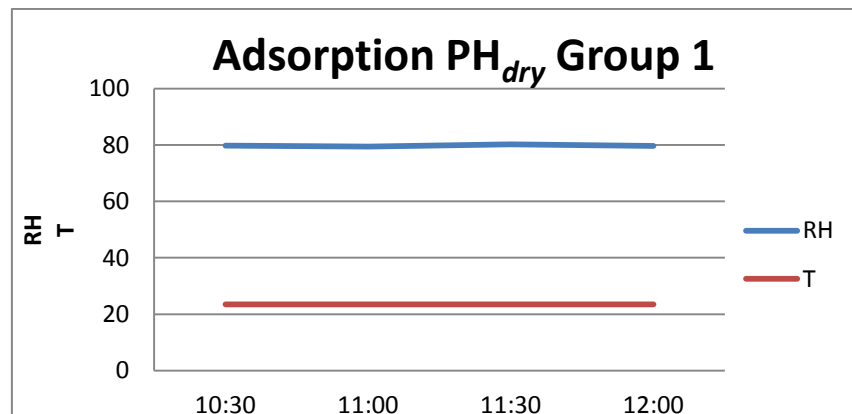


Figure 2 Conditions in climate cabinet during adsorption of the dry pine heartwood samples group 1.

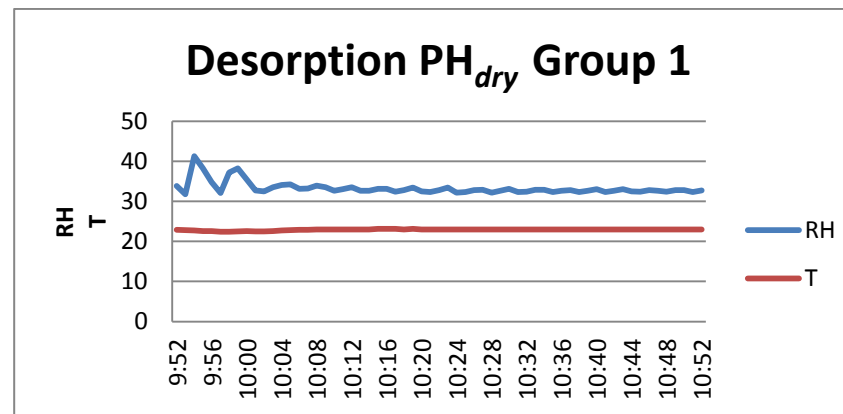


Figure 4 Conditions in climate cabinet during desorption of the dry pine heartwood samples group 1.

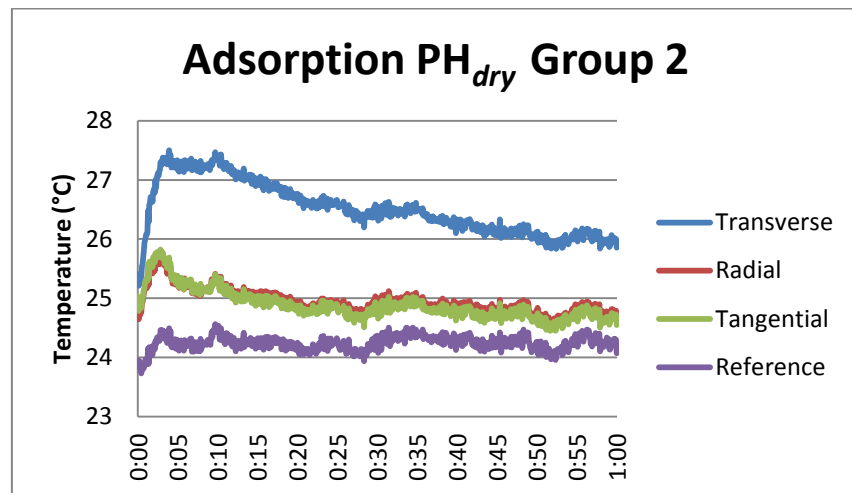


Figure 5 Temperature changes of group 2 dry pine heartwood samples and reference during adsorption from RH 1% to RH 80%.

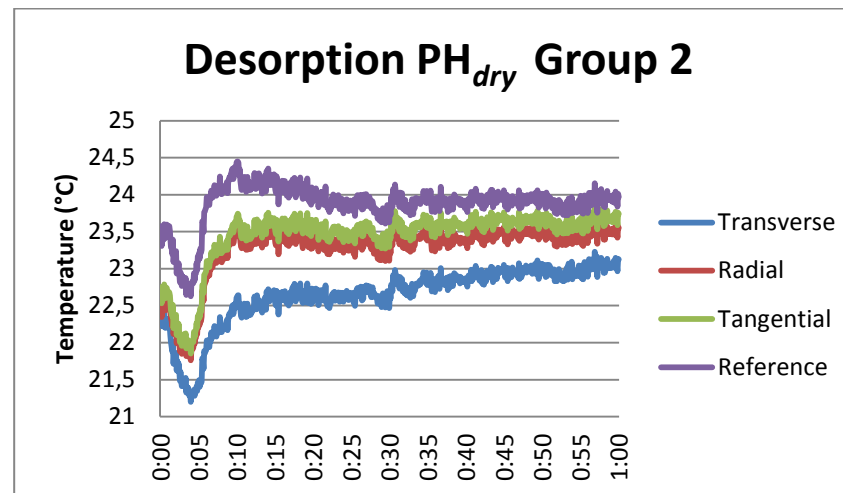


Figure 7 Temperature changes of group 2 dry pine heartwood samples and reference during desorption from RH 80% to RH 32%.

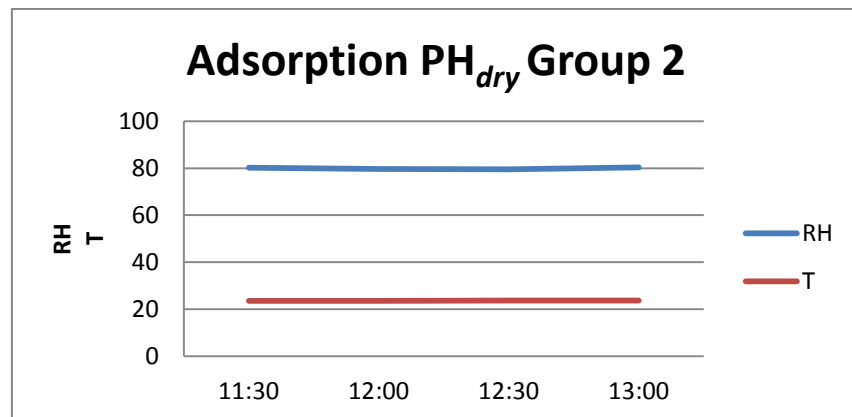


Figure 6 Conditions in climate cabinet during adsorption of the dry pine heartwood samples group 2.

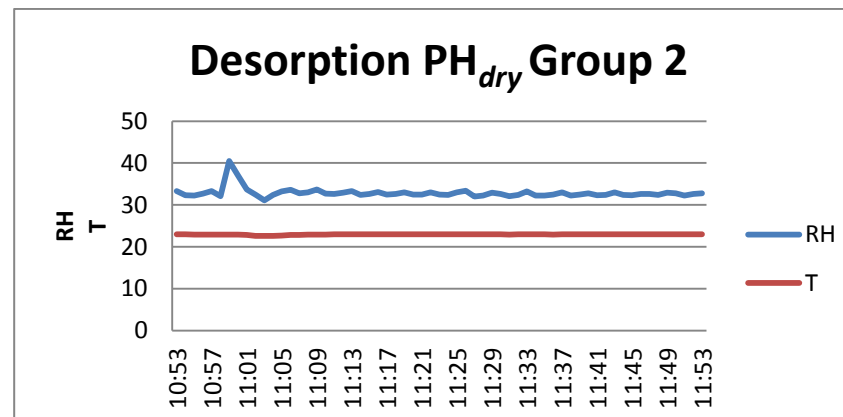


Figure 8 Conditions in climate cabinet during desorption of the dry pine heartwood samples group 2.

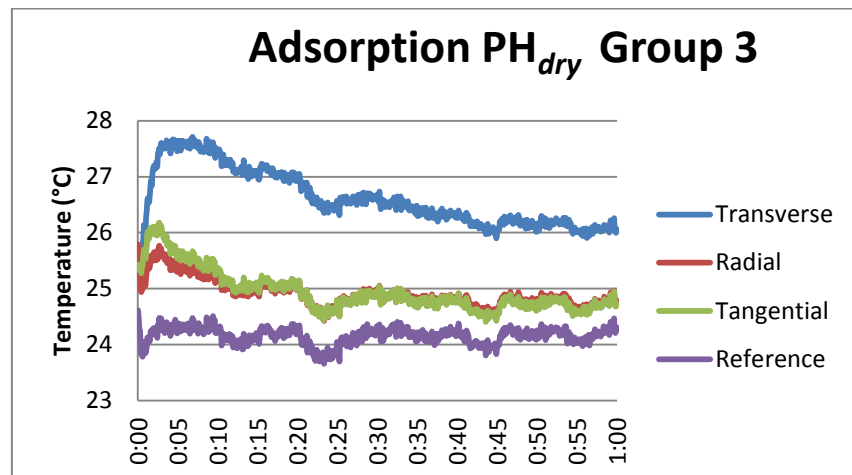


Figure 9 Temperature changes of group 3 dry pine heartwood samples and reference during adsorption from RH 1% to RH 80%.

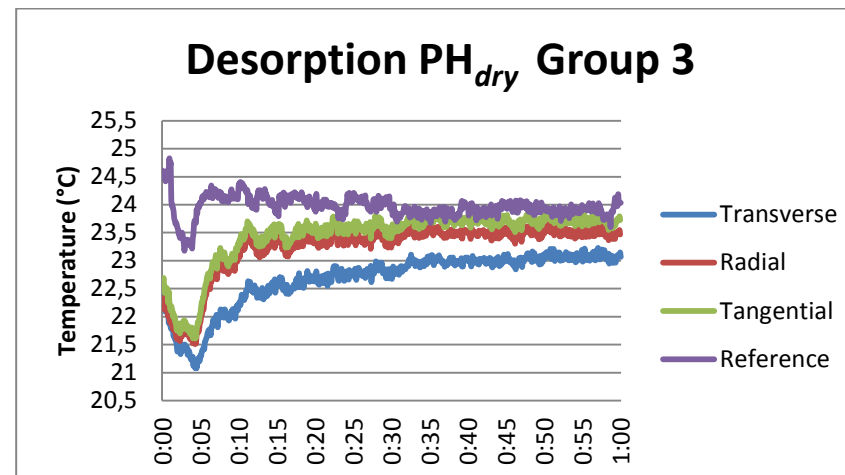


Figure 11 Temperature changes of group 3 dry pine heartwood samples and reference during desorption from RH 80% to RH 32%.

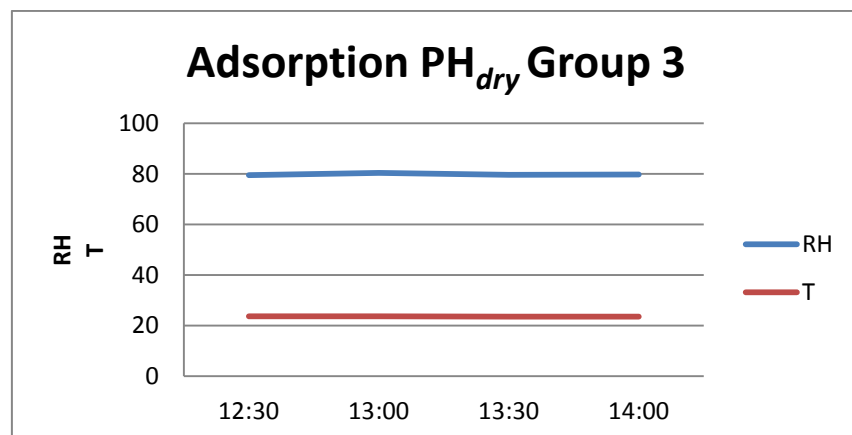


Figure 10 Conditions in climate cabinet during adsorption of the dry pine heartwood samples group 3.

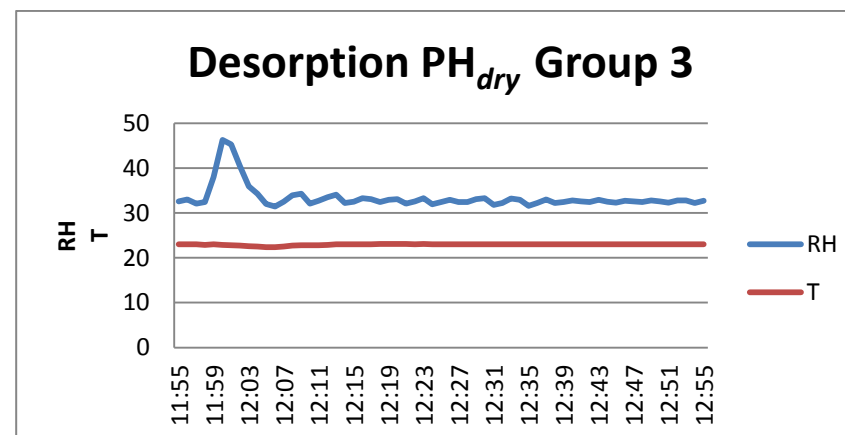


Figure 12 Conditions in climate cabinet during desorption of the dry pine heartwood samples group 3.

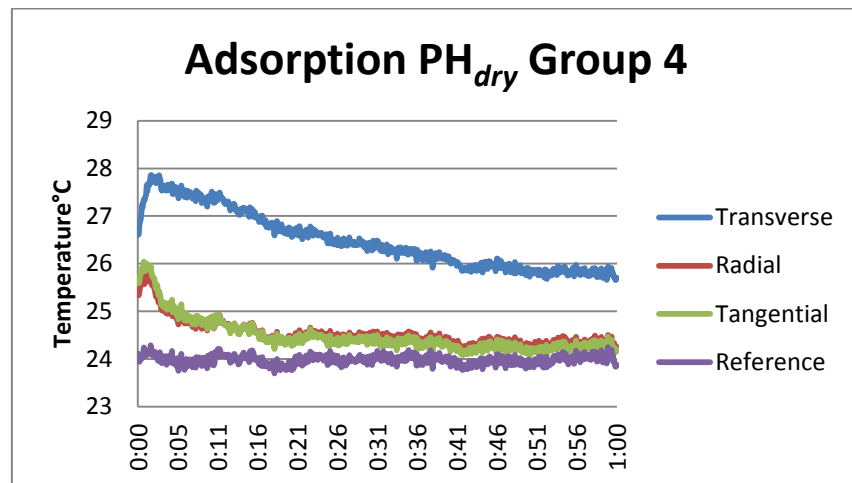


Figure 13 Temperature changes of group 4 dry pine heartwood samples and reference during adsorption from RH 1% to RH 80%.

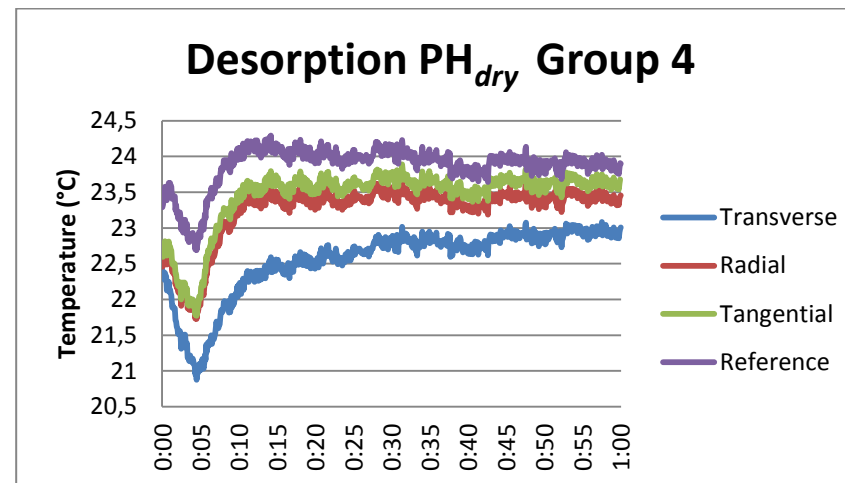


Figure 15 Temperature changes of group 4 dry pine heartwood samples and reference during desorption from RH 80% to RH 32%.

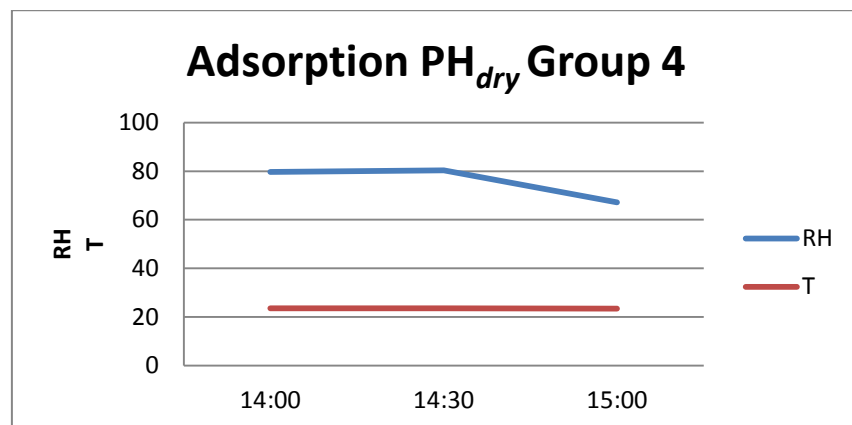


Figure 14 Conditions in climate cabinet during adsorption of the dry pine heartwood samples group 4.

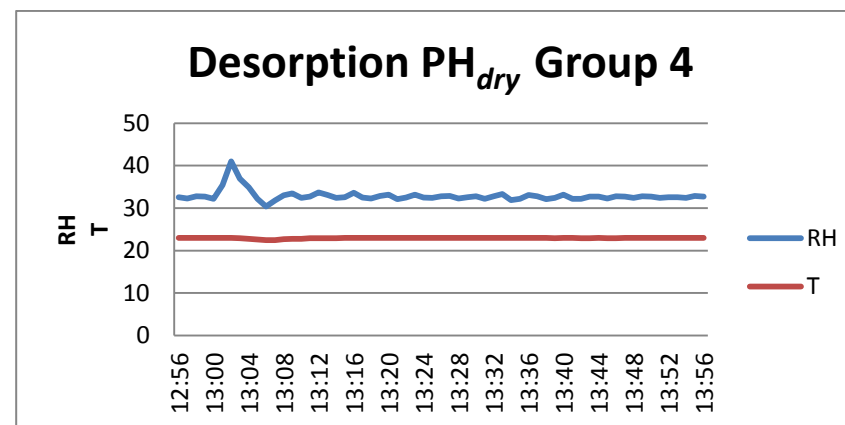


Figure 16 Conditions in climate cabinet during desorption of the dry pine heartwood samples group 4.

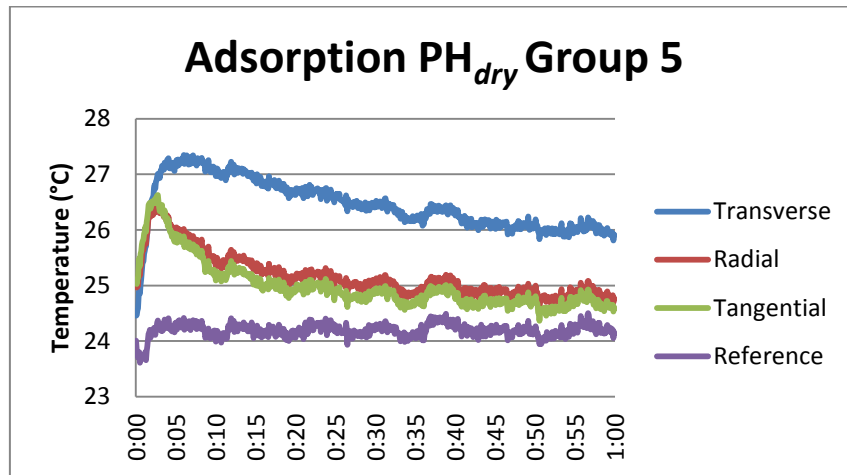


Figure 17 Temperature changes of group 5 dry pine heartwood samples and reference during adsorption from RH 1% to RH 80%.

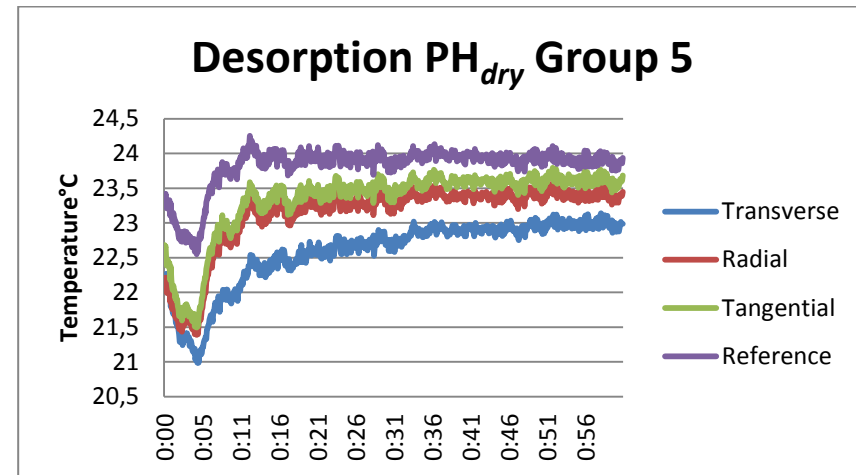


Figure 19 Temperature changes of group 5 dry pine heartwood samples and reference during desorption from RH 80% to RH 32%.

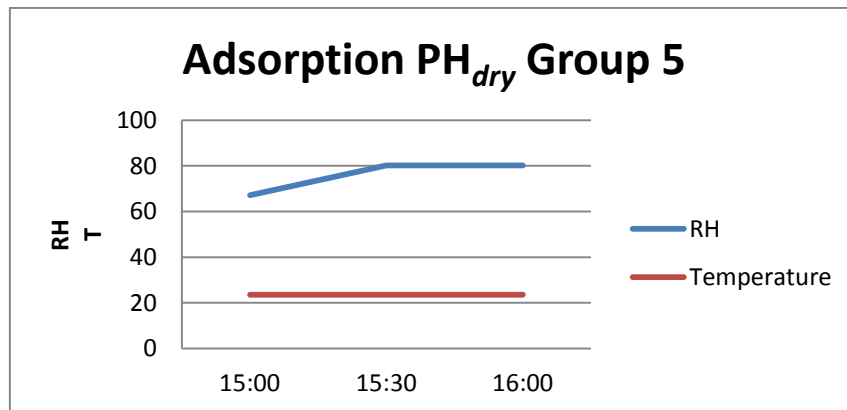


Figure 18 Conditions in climate cabinet during adsorption of the dry pine heartwood samples group 5.

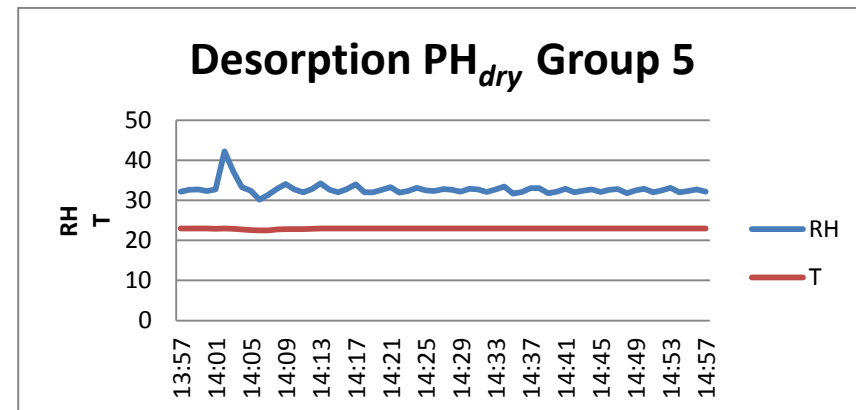


Figure 20 Conditions in climate cabinet during desorption of the dry pine heartwood samples group 5.

Appendix 10 Thermographs, condition graphs and temperature changes of dry pine heartwood samples (6/6)

Table 1 Maximum temperature rises of all dry pine heartwood samples during adsorption and the time it occurred in, and maximum temperature decrease during desorption, the time it occurred in and the time where the temperature regained the value of initial temperature. The (-) denotes that the temperature did not return to the initial value.

	$\Delta T_{ads,max}$ (°C)	$\Delta t_{ads,max}$ (min)	$\Delta T_{des,max}$ (°C)	$\Delta t_{des,max}$ (min)	$\Delta t_{des,0}$ (min)
Group 1					
<i>PH_{dry}, transverse</i>	2.59	3	-1.12	3	-
<i>PH_{dry}, radial</i>	0.81	3	-0.75	3	5
<i>PH_{dry}, tangential</i>	1.06	3	-0.62	3	5
<i>PH_{dry}, reference</i>	0.39	3	-0.32	3	4
Group 2					
<i>PH_{dry}, transverse</i>	2.29	4	-1.21	4	7
<i>PH_{dry}, radial</i>	1.11	3	-0.77	4	5
<i>PH_{dry}, tangential</i>	1.04	3	-0.90	4	5
<i>PH_{dry}, reference</i>	0.70	4	-0.93	3	5
Group 3					
<i>PH_{dry}, transverse</i>	2.29	5	-1.26	4	10
<i>PH_{dry}, radial</i>	0.83	3	-0.66	4	5
<i>PH_{dry}, tangential</i>	0.85	3	-1.05	4	6
<i>PH_{dry}, reference</i>	0.69	3	-1.40	4	-
Group 4					
<i>PH_{dry}, transverse</i>	1.26	2	-1.45	5	11
<i>PH_{dry}, radial</i>	0.33	2	-0.7	4	6
<i>PH_{dry}, tangential</i>	0.38	1	-0.84	4	6
<i>PH_{dry}, reference</i>	0.17	2	-0.6	4	6
Group 5					
<i>PH_{dry}, transverse</i>	2.80	6	-1.26	5	11
<i>PH_{dry}, radial</i>	1.53	3	-0.67	5	6
<i>PH_{dry}, tangential</i>	1.60	3	-1.09	5	7
<i>PH_{dry}, reference</i>	0.81	6	-0.70	5	6
Average	Groups 2, 3 and 5		Groups 2, 3, 4 and 5		
<i>PH_{dry}, transverse</i>	2.31	4	-1.35	4	11
<i>PH_{dry}, radial</i>	0.97	3	-0.58	4	6
<i>PH_{dry}, tangential</i>	1.09	3	-0.84	4	6
<i>PH_{dry}, reference</i>	0.64	3	-0.87	4	6

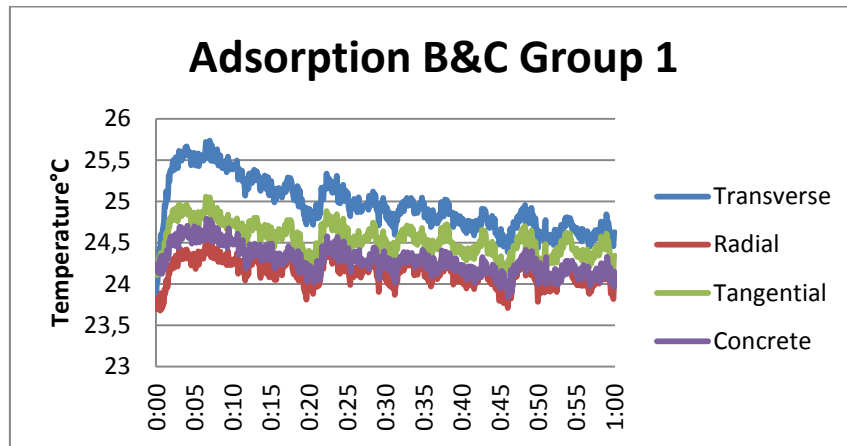


Figure 1 Temperature changes of group 1 birch and concrete samples during adsorption from RH 32% to RH 70%.

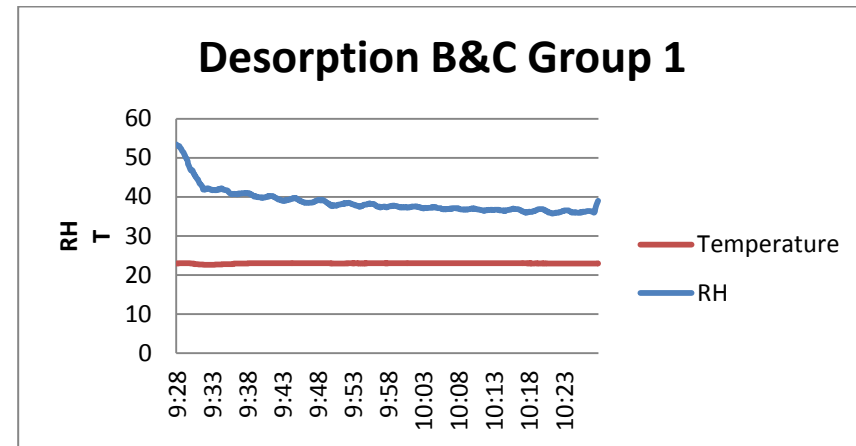


Figure 3 Conditions in climate cabinet during desorption of the birch and concrete samples group 1.

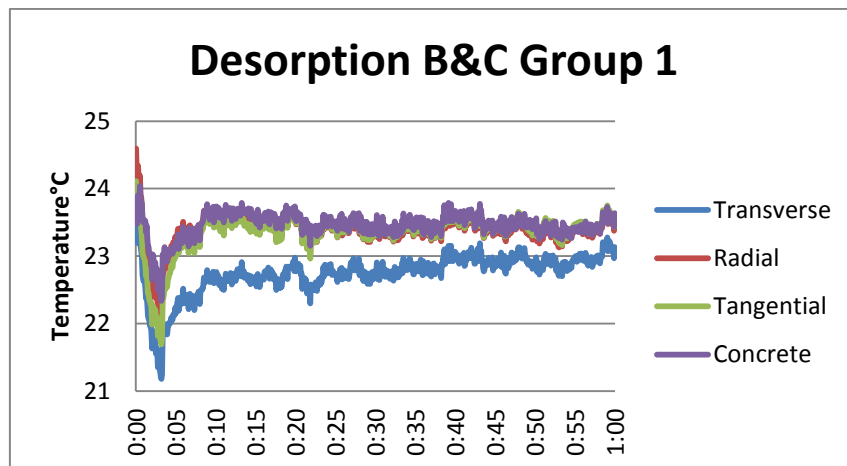


Figure 2 Temperature changes of group 1 birch and concrete samples during desorption from RH 70% to RH 36%.

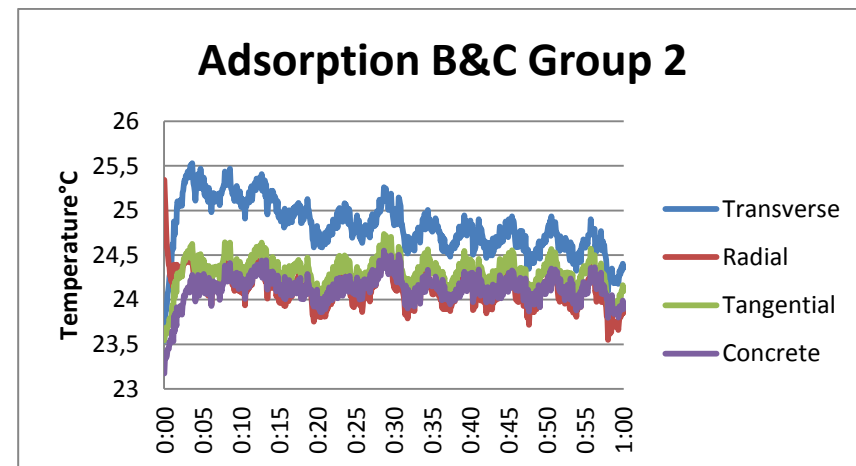


Figure 4 Temperature changes of group 2 birch and concrete samples during adsorption from RH 32% to RH 70%.

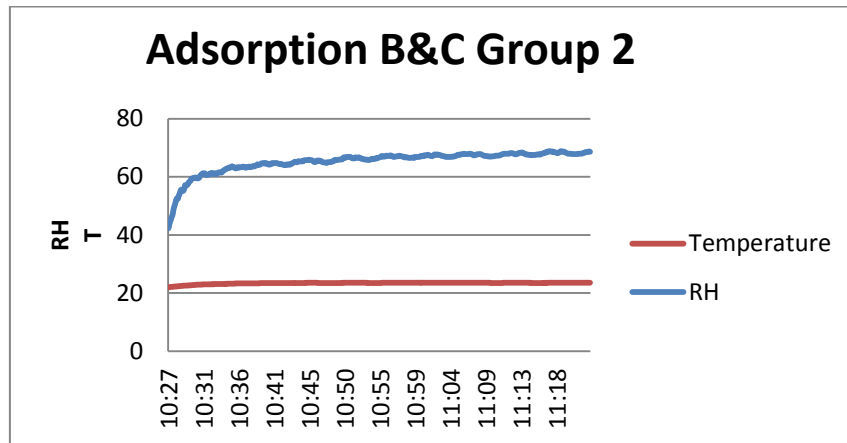


Figure 5 Conditions in climate cabinet during adsorption of the birch and concrete samples group 2.

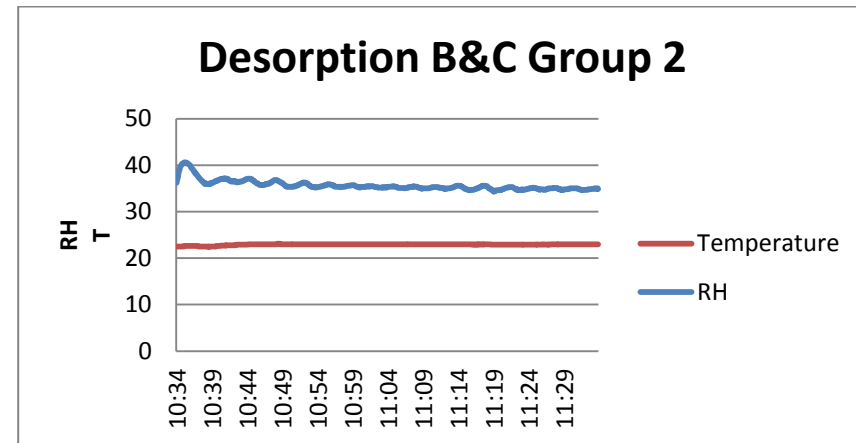


Figure 7 Conditions in climate cabinet during desorption of the birch and concrete samples group 2.

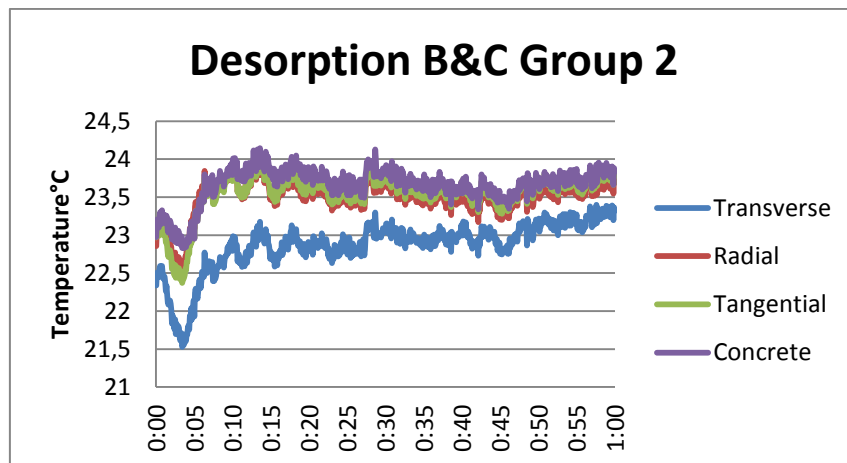


Figure 6 Temperature changes of group 2 birch and concrete samples during desorption from RH 70% to RH 36%.

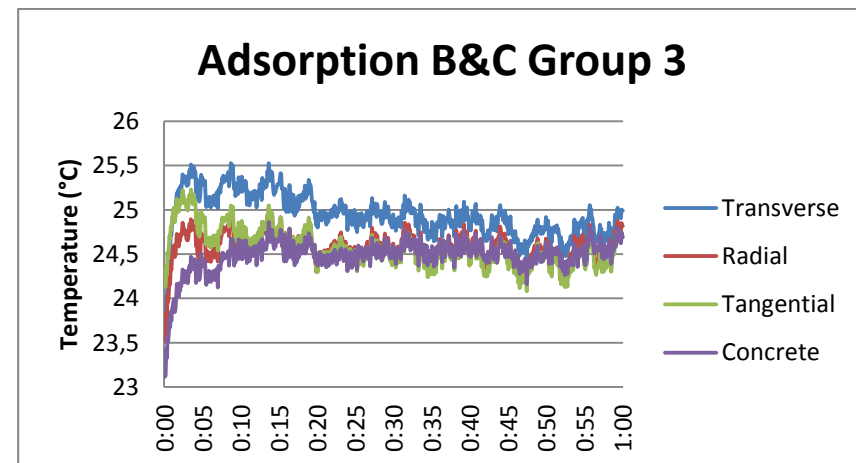


Figure 8 Temperature changes of group 3 birch and concrete samples during adsorption from RH 32% to RH 70%.

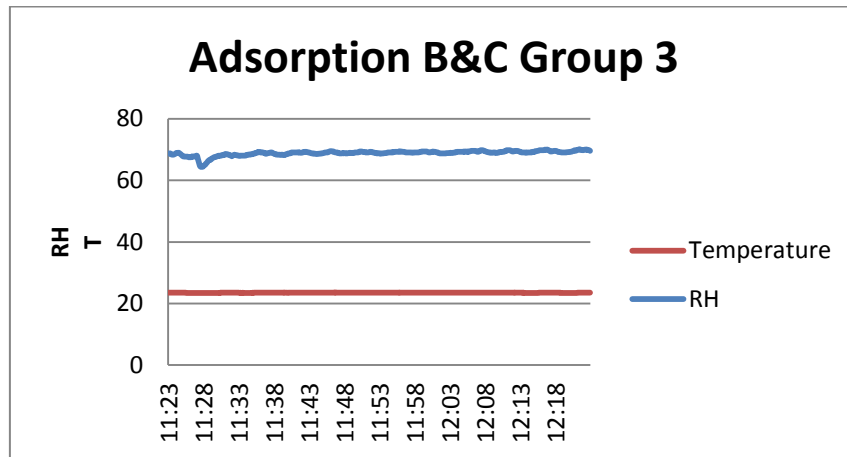


Figure 9 Conditions in climate cabinet during adsorption of the birch and concrete samples group 3.

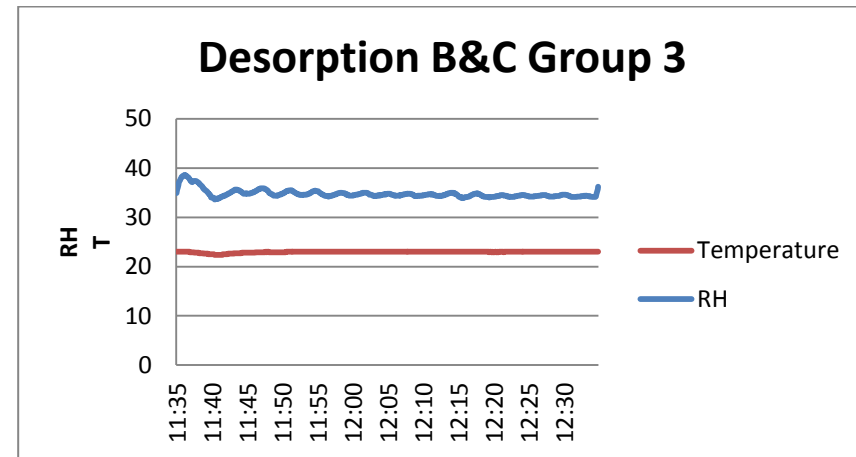


Figure 11 Conditions in climate cabinet during desorption of the birch and concrete samples group 3.

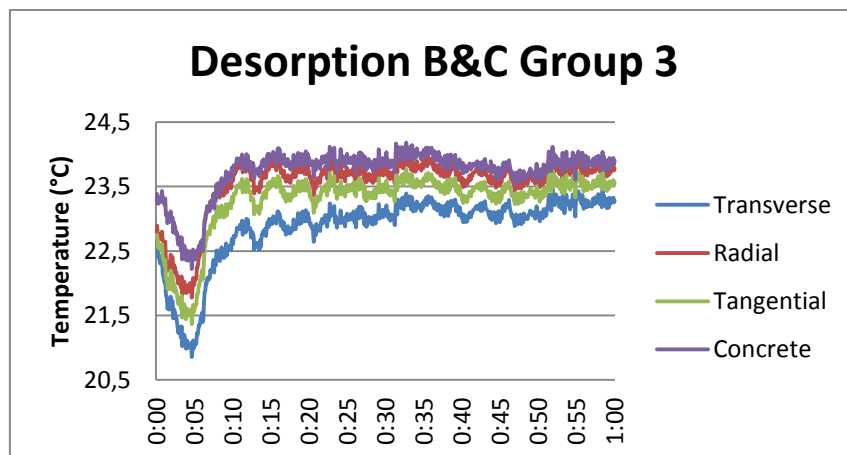


Figure 10 Temperature changes of group 3 birch and concrete samples during desorption from RH 70% to RH 36%.

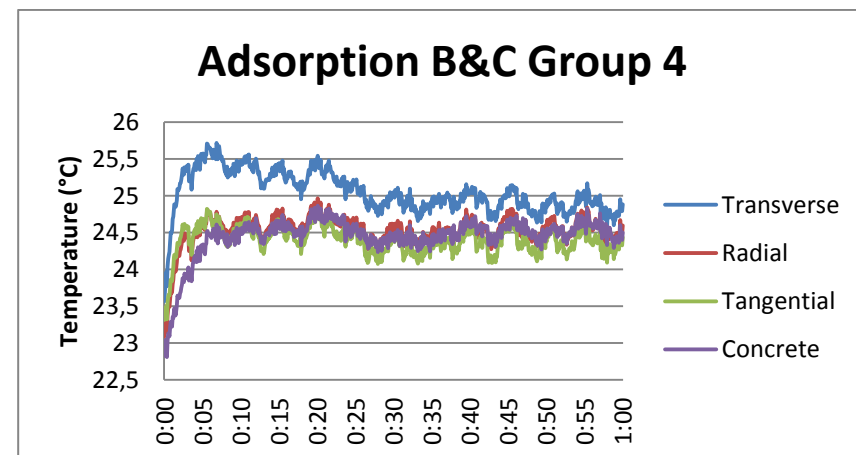


Figure 12 Temperature changes of group 4 birch and concrete samples during adsorption from RH 32% to RH 70%.

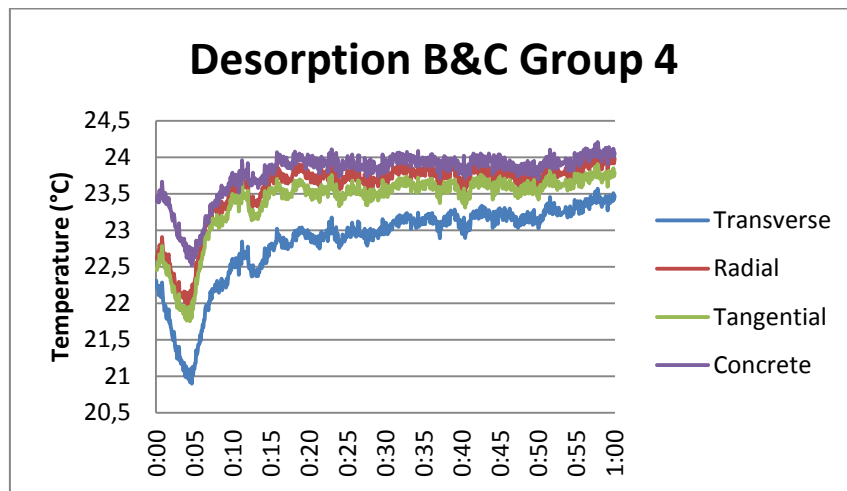


Figure 13 Temperature changes of group 4 birch and concrete samples during desorption from RH 70% to RH 36%.

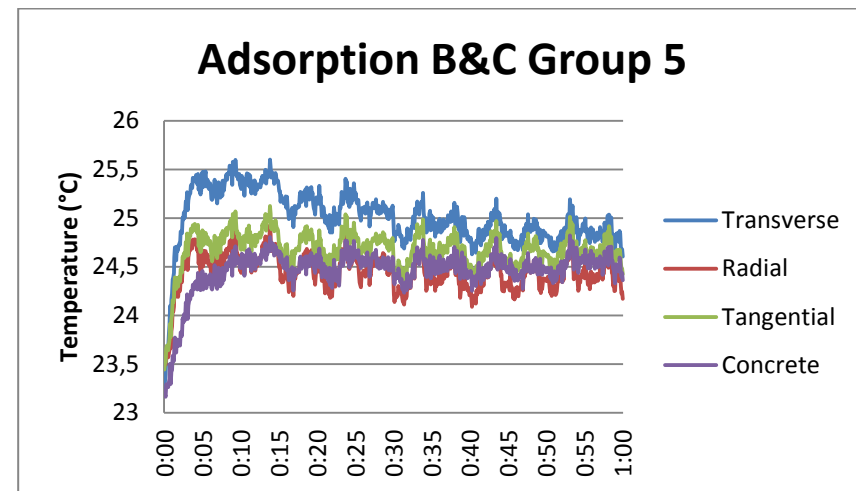


Figure 15 Temperature changes of group 5 birch and concrete samples during adsorption from RH 32% to RH 70%.

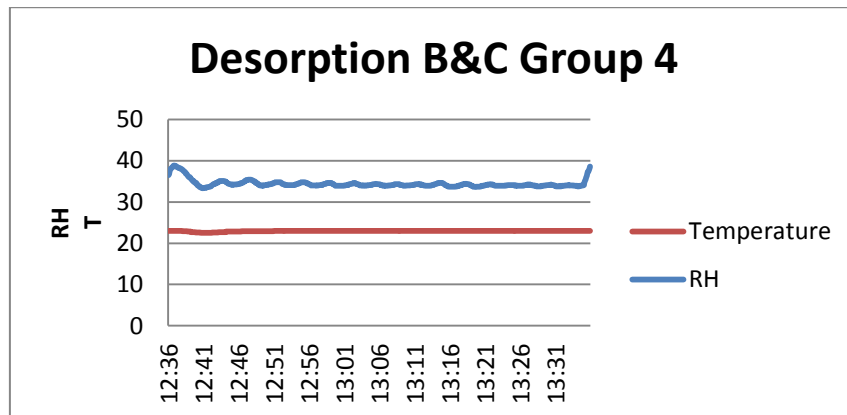


Figure 14 Conditions in climate cabinet during desorption of the birch and concrete samples group 4.

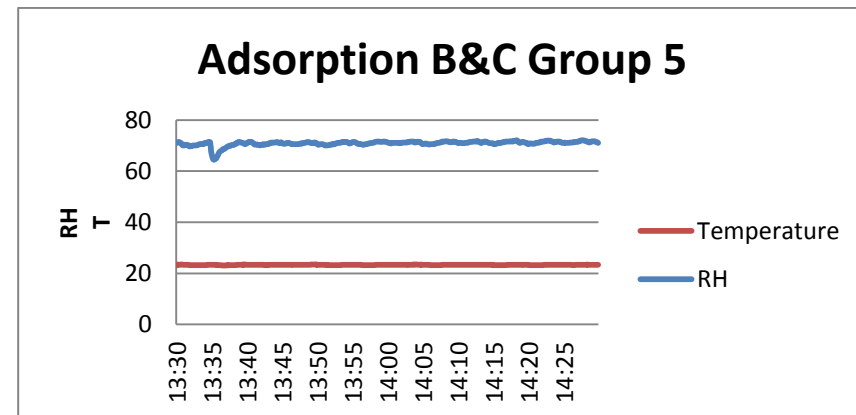


Figure 16 Conditions in climate cabinet during adsorption of the birch and concrete samples group 5.

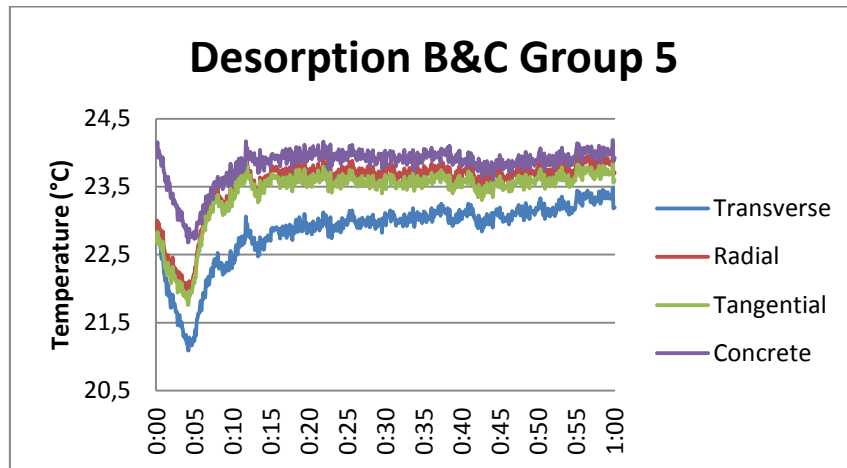


Figure 17 Temperature changes of group 5 birch and concrete samples during desorption from RH 70% to RH 36%.

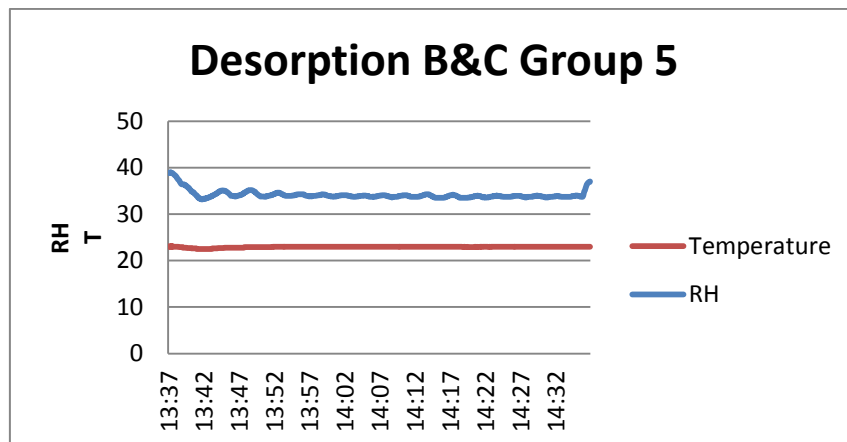


Figure 18 Conditions in climate cabinet during desorption of the birch and concrete samples group 5.

Appendix 11 Thermographs, condition graphs and temperature changes of birch and concrete samples (6/6)

Table 1 Maximum temperature rises of all birch and concrete samples during adsorption and the time it occurred in, and maximum temperature decrease during desorption, the time it occurred in and the time where the temperature regained the value of initial temperature. The (-) denotes that the temperature did not return to the initial value.

	$\Delta T_{ads,max}$ (°C)	$\Delta t_{ads,max}$ (min)	$\Delta T_{des,max}$ (°C)	$\Delta t_{des,max}$ (min)	$\Delta t_{des,0}$ (min)
Group 1					
<i>B, transverse</i>	1.74	3	-2.47	3	-
<i>B, radial</i>	0.85	3	-2.47	3	-
<i>B, tangential</i>	0.73	3	-2.33	3	-
<i>Concrete</i>	0.48	4	-1.22	3	9
Group 2					
<i>B, transverse</i>	1.99	3	-0.77	2	6
<i>B, radial</i>	1.23	3	-0.27	2	4
<i>B, tangential</i>	1.08	3	-0.54	2	5
<i>Concrete</i>	1.1	5	-0.13	2	5
Group 3					
<i>B, transverse</i>	1.91	4	-1.82	5	10
<i>B, radial</i>	1.38	4	-1.01	5	6
<i>B, tangential</i>	1.09	4	-1.34	5	7
<i>Concrete</i>	1.73	14	-1.06	5	7
Group 4					
<i>B, transverse</i>	2.15	7	-1.41	5	9
<i>B, radial</i>	1.48	4	-0.66	4	6
<i>B, tangential</i>	1.27	3	-0.71	4	6
<i>Concrete</i>	1.80	11	-0.92	5	8
Group 5					
<i>B, transverse</i>	2.32	9	-1.92	5	12
<i>B, radial</i>	1.28	4	-0.94	4	6
<i>B, tangential</i>	1.40	4	-0.93	4	6
<i>Concrete</i>	1.52	10	-1.37	5	8
Average	Groups 3, 4 and 5		Groups 3, 4 and 5		
<i>B, transverse</i>	1.98	5	-1.69	5	11
<i>B, radial</i>	1.33	4	-0.84	4	6
<i>B, tangential</i>	1.16	4	-0.92	4	6
<i>Concrete</i>	1.67	15	-1.11	5	9